1973

Finite element analysis of elastic-plastic plates and eccentrically stiffened plates, February 1973.

Anton W. Wegmüller

Celal N. Kostem

LEHIGH UNIVERSITY

OFFICE
OF
RESEARCH

FINITE ELEMENT ANALYSIS OF ELASTIC-PLASTIC PLATES AND ECCENTRICALLY STIFFENED PLATES

BY
ANTON W. WEGMULLER
CELAL N. KOSTEM

FRITZ ENGINEERING LABORATORY REPORT NO. 378A.4

FINITE ELEMENT ANALYSIS OF ELASTIC-PLASTIC PLATES AND ECCENTRICALLY STIFFENED PLATES

by

Anton W. Wegmuller

Celal N. Kostem

This work was conducted as a part of the project Overloading Behavior of Beam-Slab Highway Bridges, sponsored by the National Science Foundation.

Fritz Engineering Laboratory
Department of Civil Engineering
Lehigh University
Bethlehem, Pennsylvania

February, 1973

Fritz Engineering Laboratory Report No. 378A.4

TABLE OF CONTENTS

ABSTRACT

This report deals with the analysis of plates and eccentrically stiffened plates in the elastic-plastic range using the finite element stiffness approach. The analysis is based on the classical theory of thin plates exhibiting small deformations.

A general procedure for the analysis of elastic-plastic plates is presented. A description of the mathematical model, consisting of a plate subdivided into a finite number of layers is given and the associated incremental elastic-plastic solution technique is outlined. A few example solutions show the accuracy and the versatility of the proposed tangent stiffness approach.

A general procedure for the elastic-plastic analysis of eccentrically stiffened plate structures is developed. The layered plate model used in the elastic-plastic analysis of plates is supplemented by a similar layered beam element for this analysis and the associated step-by-step iteration technique, used to solve the linearized governing equations, is described.

1. INTRODUCTION

Plates of various shapes are commonly used as structural systems or structural components. Most frequently, plates form part of floor systems in buildings or bridges and are often used in connection with beams and columns. Generally, there is ample room for a variation in geometry, thickness and loading, as illustrated in Fig. 1 and hence, the analysis of such complex structures often presents considerable difficulties (Refs. 30 and 31).

An elastic analysis cannot predict the response of a structure stressed beyond the elastic limit load and up to its failure load. An analysis of the post-elastic range is needed to predict eventual damages and to determine the deformations occurring during the application of overloads (Ref. 30). No damage is desired to occur under working loads but at the same time it is required that a structure should be able to withstand a certain overload. The strength of a structure of the type considered in this investigation is needed to ascertain that failure should not occur under working load and hence to design a structure with an adequate factor of safety. An attempt to analyze complex shaped plate structures in the post-elastic range as well as to predict the failure load is developed in Chapter 2.

Most engineering materials, such as steel, aluminum and, if properly designed, reinforced concrete, are ductile and can withstand strains much greater than the strain associated with the

elastic limit state. As the structure is loaded beyond this state, plastic straining occurs causing a redistribution of stress in a redundant structure. The ductility in redundant structures permits a redistribution of stresses beyond the elastic limit allowing a structure to carry considerable additional loads. Thus, it is felt today that a design should also consider the post-elastic behavior of a structure and its ultimate strength. The post-elastic response of a structure is of interest because it enables the designer to judge the effects of overloads which might be applied to a structure. The knowledge of the load carrying capacity or ultimate strength of a structure is twofold: (1) it allows the determination of the factor of safety of a structure against failure, and (2) the stress resultants resisted by the structural components at ultimate stage are required to properly dimension each structural part.

The goal of the reported study is the development of an approach which will allow the tracing of the entire load-deformation behavior of complex shaped stiffened plate structures, as well as to find the ultimate load-carrying capacity of such structures. Its application to the inelastic analysis of beam-slab type bridges will allow the study of the behavior of such bridges in the post-elastic range as well as at failure. It is obvious that, due to the current trend of increasing vehicular weight limits, the behavior of bridges above the elastic limit stage must be known in order to judge the effects of overloading.

Current permit regulations are not based on a rational structural analysis of the bridge superstructure under the load level in question. Also, there is no existing rational method to judge the effects of overloading of bridge superstructures. The continuous load-deformation behavior of a stiffened plate structure stressed beyond its elastic limit is needed to judge the effects of overloading. At this point it would be appropriate to note that the concept of Ultimate Strength Design, as outlined in the ACI Building Code (Ref. 1), does not account for a redistribution of stresses due to redundancy of the structure. Recognizing that this redistribution actually plays an important role in highly redundant structures, it is felt that modern bridge design philosophy should reflect the inelastic behavior.

The analysis of the complete load-deformation behavior of complex shaped plates is mathematically difficult to accomplish. The inclusion of the non-linear material behavior in plate analysis results in partial differential equations which are not amenable to analytic solution but for some very simple structures. As a consequence, simplified methods designed to compute the ultimate strength of structures have been developed by a number of investigators (Refs. 6, 11, 22). These methods are based on the theorems of limit analysis and allow the establishment of bounds on the collapse load. However, the prediction of the elastic-plastic behavior of complex shaped plates cannot be accomplished using these methods.

Virtually no work has been done in the elastic-plastic analysis of eccentrically stiffened plate structures. A general method capable of analyzing such inelastic structures is presented in Chapter 3.

Within the framework of this report, the numerical technique by which the elastic-plastic response of complex shaped stiffened plates can be obtained, is described (Ref. 30). The application of the developed technique to beam-slab type highway bridge superstructures of arbitrary material behavior is the subject of future research (Refs. 15 - 19).

2. ANALYSIS OF ELASTIC-PLASTIC PLATES

2.1 Introduction

It is generally accepted that a structure is capable of redistributing high local stresses and, if properly dimensioned, is able to withstand loads significantly higher than the elastic limit load.

A general method of analysis based on the finite element displacement concept and capable of predicting the entire load-deformation behavior of complex shaped transversely loaded plates is presented. A description of the layered model used in the present analysis is given which significantly simplifies the mathematical description of the elastic-plastic behavior of a plate element. Elastic and plastic stress-strain relations are derived, and yield conditions and a flow rule are discussed.

The applied incremental elastic-plastic solution procedure is based on the tangent stiffness concept. The assembly of the system tangent stiffness matrix and the iterative solution technique are described. Loading and unloading of a layer are discussed, as well as the yield surface correction used in the analysis.

Finally, a number of example solutions are presented demonstrating the power and versatility of the proposed approach. Convergence and accuracy of the presented approach are shown.

2.2 Existing Methods of Analysis

2.2.1 Upper and Lower Bound Approaches

The theory of plastic analysis has developed from two directions: (1) the classical approach known as limit analysis and, (2) the yield line theory. Tresca, Von Mises, Prager and Hodge (Ref. 11) have pioneered the classical point of view, whereas Bach (Ref. 5) and Johansen (Ref. 13) developed the yield line theory. These methods allow the structural analyst to establish bounds on the collapse load. However, none can be applied to study the entire load-deflection behavior of complex shaped plate structures. Many investigators have dealt with the plastic analysis of structures composed of beam, plate or shell components. Most of the investigations have been concerned with the determination of the collapse load using the two fundamental theorems of limit analysis. These theorems were proved for elastic perfectly-plastic material by Drucker, Prager and Greenberg (Ref. 8).

Most of the approximate solutions for the collapse load are based on the upper bound approach. The limit load is computed on the basis of an assumed plastic velocity field, and the rate of internal plastic work is equated to the rate of external work. Upper bound solutions for a variety of plate problems are known and compiled in Refs. 28 and 34. Since the assumed collapse mechanism is chosen on a trial basis in such a way as to seek a minimum for the upper bound values obtained, this method is tedious. In addition, without the availability of at least one lower bound

solution, a designer cannot predict the accuracy of the best upper bound value. The application of this approach to structures combined of beams and plates is cumbersome since the true collapse pattern is difficult to establish. Furthermore, in this approach the material is assumed to be elastic-perfectly plastic, and the strain hardening effect is neglected. The yield line theory is based on the work of Bach (Ref. 5) and Johansen (Ref. 13). This theory is extensively used in the design of reinforced concrete slabs. Sawzuk and Jaeger (Ref. 28) summarize this theory and give a comprehensive bibliography of literature in this area. This method is subject to the same restrictions as discussed above.

Lower bound solutions are based on the lower bound theorems of limit analysis. In this approach the load is computed on the basis of an assumed equilibrium state of stress distribution which nowhere violates the yield condition. Very little work has been done in finding lower bound solutions needed to test the accuracy of upper bounds. Hodge (Ref. 11) gives a summary of the limit analysis theory pertaining to rectangular and circular plates. Shull and Hu (Ref. 29) utilized Tresca's yield criterion to arrive at lower bounds for uniformly loaded, simply supported rectangular plates. No exact solution is yet available for this relatively simple plate problem. Koopman and Lance (Ref. 14) introduced the concept of linear programming to arrive at lower bounds of the collapse load of plates made of perfectly-plastic material. A similar approach was pioneered by Wolfensberger

(Ref. 33) for reinforced concrete plates by linearizing the yield condition and using finite difference approximations.

In summary, although limit analysis techniques provide valuable information concerning the collapse mechanism and the collapse load, they cannot be used to predict the response of complex shaped plates in the post-elastic range.

2.2.2 Finite Difference Methods

Approximate solutions using the finite difference approach were obtained by Bhaumik and Hanley (Ref. 7) for the case of uniformly loaded rectangular plates. However, for this investigation it was assumed that at any mesh point of the plate the entire thickness is either fully elastic or fully plastic. This assumption facilitates the solution of a plate bending problem; however, for some structural materials the approximation of the moment-curvature relationship by two straight lines is unrealistic. In addition, finite difference approaches are not well-suited for automatic computation, and are greatly complicated if in-plane behavior is to be considered.

2.2.3 Discrete and Finite Element Methods

Among the methods that have been used successfully in the determination of approximate solutions to continuum problems are approaches in which the continuum is represented by a lumped parameter model. A model capable of treating flexural problems in plates was developed by Ang and Lopez (Ref. 20). This discrete

flexural model, in which the stiffness of the actual plate is lumped into a system of bars and springs, has been applied to small and large deformation plate problems. The field equations are derived in incremental form, leading to a linearization of the problem in the case of the small deflection analysis, and are shown to be the finite difference equivalent of the corresponding equations of the continuous plate. The inelastic analysis is greatly simplified in this approach by assuming that the plate can be represented by a sandwich plate consisting of two layers of an elastic perfectly-plastic material, and of a shear core between these two layers. Due to the tedious way of satisfying the boundary conditions, this method is not ideally suited for the development of a fully automated approach.

To date, finite element methods for the inelastic analysis of structures have been primarily developed for the analysis and design of aircraft structures. A review of the current state of the art of finite element analysis applied to inelastic problems is given by Armen, et al. (Ref. 3). It appears that most of the work has been done for plane stress or plane strain problems associated with either the Von Mises or the Tresca yield condition. Little work has been done in the inelastic analysis of plates and shells. To date, two different approaches have emerged. In the first approach, the accumulated plastic strains are treated as initial strains, and applied as forces to the structure. A solution is then obtained by using an appropriate convergent iterative

technique. This approach is referred to as the initial strain or initial stiffness approach, and was the earliest approach to plasticity analysis in the context of the finite element methods. The alternative approach requires the modification of the system stiffness matrix for each step, taking into account plastification when and wherever occurring, and resolving the final system of equilibrium equations at each step of an iteration. This approach is referred to as the tangent stiffness approach. Pope (Ref. 24) describes the application of the tangent stiffness approach for the analysis of plane elastic-plastic problems. In another recent paper, Anand, et al. (Ref. 2) describe a finite element stiffness approach to elastic-plastic plane stress problems based on Tresca's yield criterion.

Armen and Pifko (Ref. 4) used the initial stiffness approach in the analysis of beams, plates and shells. These authors point out the difficulties encountered in depicting the progressive yielding through the thickness of plates and shells subjected to bending, and base their analysis on an assumed variation in plastic strain from the surfaces of the element to an elastic-plastic boundary within the element. Popov, et al. (Ref. 25) divide the thickness of the plate into layers in their solution of elastic-plastic circular plate problems. Whang (Ref. 32) describes both the initial and the tangent stiffness approach in the solution of orthotropic plane stress, plate and shell problems, and presents elastic-plastic solutions for plates, using the initial stiffness

approach. Surveys and summaries of recent progress in the application of finite element techniques applied to materially and geometrically nonlinear problems have been given by Armen, et al. (Ref. 4) and Oden (Ref. 23).

2.3 A Finite Element Stiffness Approach Using a Layered Model

2.3.1 Description of the Layered Model

In this section a finite element displacement approach is described which allows the establishment of the entire load-formation behavior of arbitrarily shaped and loaded plates. Since the process and the extend of plastification are difficult to describe, a solution is accomplished by dividing each finite plate element into a number of layers in order to study its elastic-plastic behavior. The procedure is based on linear geometry; hence, it is applicable to problems where the structure experiences significant plasticity before the deformations become excessive. First, the in-plane deformations are neglected, but the model will allow in-plane behavior to be included, as will be shown in Chapter 3.

The method is based on the tangent stiffness concept. The load is applied in incremental form, and the method requires a modification of the element stiffness matrices at each incremental load step. The incremental approach allows the study of the entire load-deformation behavior of a plate structure. The method is outlined here for isotropic elastic linearly strain hardening material. However, it can easily be extended to arbitrary stress-strain

relationships, or orthotropic material, if the associated constitutive relations are known (Refs. 15 - 19).

The process and the extent of plastification is difficult to describe in an arbitrarily shaped and supported plate. At loads higher than the elastic limit load, plastification begins and spreads in the plane of the plate, as well as through its thickness. In the present approach, a finite plate element is subdivided into a number of layers, as shown in Fig. 2. It is assumed here that the elastic-plastic behavior of a finite plate element can adequately be described by this layered model. Since the thickness of the plate can be subdivided into any desired number of layers, the approach should in the limit be able to represent the behavior of the actual plate. Each layer is assumed to be in a state of plane stress, and the state of stress at the centroid of a layer is taken as representative for the entire layer. The effect of this assumption can be studied by observing the convergence of solutions for different mesh sizes. Any even number of layers can be chosen in the present approach. Increasing the number of layers reduces the error introduced in the approximation of the real problem. Any layer is considered to be either elastic or elastic-plastic according to a criterion to be specified. In the case of transversely loaded plates, neglecting in-plane behavior, the strain distribution is symmetric with respect to the neutral axis of the plate, and only the layers lying on one-half of the finite plate element need be considered. It should be emphasized

that with this model the method is not restricted to a particular stress-strain relation. However, for demonstration purposes, the problems solved in this chapter are confined to materials exhibiting isotropic elastic perfectly-plastic behavior.

It is assumed that Kirchhoff's assumptions are satisfied by the model. In addition, compatibility of strain between any two layers is assumed. For the present investigation, all layers are assumed to be of the same thickness; however, differently thick layers could easily be incorporated. It is again assumed that the transverse shear stresses need not be considered. The four nodal points of a finite plate element are defined again at the middle plane of the plate, and internal stress resultants are defined at the centroid of a plate element. As seen from Fig. 2, the strains at any distance z_k from the middle plane of the plate to the centroid of layer k are given by:

$$\begin{Bmatrix} \epsilon_x^k \\ \epsilon_y^k \\ \gamma_{xy}^k \end{Bmatrix} = z_k \begin{bmatrix} 1 & 0 & 0 \\ 0 & 1 & 0 \\ 0 & 0 & 1 \end{bmatrix} \begin{Bmatrix} \phi_x \\ \phi_y \\ \phi_{xy} \end{Bmatrix} \qquad (2.1\,a)$$

or

$$\{\epsilon^k\} = [H^k] \{\phi\} \qquad (2.1\,b)$$

Having found the displacement field by the finite element displacement approach, which will be described in more detail in Section 2.4, the curvatures which are defined at the centroid of a finite

plate element, and the strains and stresses for each layer can be determined. The stress resultants per unit width of plate, defined at the centroid of a plate element, are then found by summing up the contributions of each of the layers:

$$M_x = \sum_{k=1}^{\ell} \sigma_x^k \; z_k \; t_k \qquad (2.2\,a)$$

$$M_y = \sum_{k=1}^{\ell} \sigma_y^k \; z_k \; t_k \qquad (2.2\,b)$$

$$M_{xy} = \sum_{k=1}^{\ell} \tau_{xy}^k \; z_k \; t_k \qquad (2.2\,c)$$

where ℓ is the number of layers and t_k the thickness of layer k, as shown in Fig. 2. Eqs. 2.1 and 2.2 can immediately be cast into an incremental form, and are used in this form in the proposed incremental approach. It should be mentioned that the number of degrees of freedom in the described approach will not be increased by increasing the number of layers, and is dependent only on the mesh size used and the number of degrees of freedom involved per nodal point of the selected finite plate element.

2.3.2 Loading and Elastic Stress-Strain Relations of a Layer

Each layer is assumed to be in a state of plane stress. The stresses acting in a layer are shown in Fig. 3. Each layer is loaded according to a loading program which can vary widely

for practical examples. The loading path, indicated by an arrow in Fig. 3, is described by successive values of the elements of the stress vector $\{\sigma\}$, which is defined as:

$$\{\sigma\}^T = < \sigma_x \quad \sigma_y \quad \tau_{xy} > \tag{2.3}$$

Since the proposed approach is formulated in incremental form, and makes use of plastic stress-strain relations derived from the flow theory, which are themselves incremental, no restrictions must be placed on the loading path. Unloading may or may not occur, and can be accounted for as will be described in Section 2.4.3. An approach based on the deformation theory would not be valid for other than monotonically increasing stresses, and would not allow unloading to occur.

In any elastic-plastic layer the total strains are composed of an elastic, recoverable part of strains and a plastic, irretrievable part of strains. Therefore, in incremental form one can write:

$$\{\dot{\epsilon}\} = \{\dot{\epsilon}^e\} + \{\dot{\epsilon}^p\} \tag{2.4}$$

where the individual strain rate vectors are defined as:

$$\{\dot{\epsilon}\}^T = < \dot{\epsilon}_x \quad \dot{\epsilon}_y \quad \dot{\gamma}_{xy} > \tag{2.5 a}$$

$$\{\dot{\epsilon}^e\}^T = < \dot{\epsilon}^e_x \quad \dot{\epsilon}^e_y \quad \dot{\gamma}^e_{xy} > \tag{2.5 b}$$

$$\{\dot{\epsilon}^p\}^T = < \dot{\epsilon}^p_x \quad \dot{\epsilon}^p_y \quad \dot{\gamma}^p_{xy} > \tag{2.5 c}$$

Elastic strain increments are related to the stress increments by Hooke's law, which in incremental form can be written as:

$$\{\dot{\sigma}\} = [D] \quad \{\dot{\epsilon}^e\} \tag{2.6}$$

where [D] is the stress matrix as defined earlier, and for an isotropic material, is given by:

$$[D] = \frac{E}{1-\nu^2} \begin{bmatrix} 1 & \nu & 0 \\ \nu & 1 & 0 \\ 0 & 0 & \frac{1-\nu}{2} \end{bmatrix} \tag{2.7}$$

2.3.3 Yield Condition and Flow Rule for a Layer

No universal laws governing the plastic behavior of materials have yet been developed. Thus, a choice must be made, among the several existing plasticity theories, of one that successfully combines mathematical simplicity with good representation of the experimentally observed material behavior. A review of currently available plasticity theories is given in Ref. 21. One of the advantages of the finite element approach is that this method is capable of treating complex stress-strain relationships, including strain hardening of the material. The method is able to treat most engineering materials as long as the fundamental laws governing the plastic behavior of a material are known. The present approach is based on isotropic elastic-linearly strain hardening material. In addition, isotropic strain hardening is assumed, hence

simplifying the problem considerably. This theory assumes that during plastic flow the yield surface expands uniformly about the origin of the stress space. Since it is not the purpose of this investigation to develop new concepts in plasticity, no discussion pertaining to the validity of the basic equations is given. As postulated by Ziegler (Ref. 35), the plastic behavior of a material can be described by specifying the following relationships:

1. An initial yield condition defining the elastic limit of a material.

2. A flow rule relating the plastic strain increments to the stresses and stress increments.

3. A hardening rule, used to establish conditions for subsequent yielding from a plastic state of stress.

It can be shown that the points where initial yielding occurs form a space surface which is closed, convex and of the form

$$f^* (\sigma_{ij}) = f^* (\sigma_x, \sigma_y, \tau_{xy}) = 0 \qquad (2.8)$$

where σ_{ij} is the stress tensor describing the state of stress at the centroid of a layer. As shown in Fig. 3, all stress points lying inside the initial yield surface and producing no permanent strains in the virgin material are characterized by

$$f^* (\sigma_{ij}) < 0 \qquad (2.9)$$

and constitute the initial elastic range. A number of yield criteria are currently being used in the elastic-plastic analysis of structures. The most common ones are shown in Fig. 4 and are discussed for the case of plane stress.

Tresca's yield condition is depicted in Fig. 4 a and can be represented by

$$\max \left(|\sigma_1| ; |\sigma_2| ; |\sigma_1 - \sigma_2| \right) = \bar{\sigma} \qquad (2.10)$$

where σ_1 and σ_2 are the principal stresses in the layer and $\bar{\sigma}$ is the current yield stress in simple tension.

Von Mises' yield condition, as shown in Fig. 4 b, is often used since it describes the initial yield surface as a smooth surface in the stress space,and is representable in simple mathematical form. This yield condition is given by

$$J_2 - \frac{1}{3} \bar{\sigma}^2 = \frac{1}{2} S_{ij} S_{ij} - \frac{1}{3} \bar{\sigma}^2 = 0 \qquad (2.11)$$

where: J_2 = Second invariant of the stress deviator tensor

and S_{ij} = Stress deviator tensor defined as

$$S_{ij} = \sigma_{ij} - \frac{1}{3} \sigma_{kk} \qquad (2.12)$$

in which σ_{kk} is the sum of the principal normal stress components.

Johansen's yield condition is a special case of the maximum stress theory introduced by Rankine. This yield condition is

depicted in Fig. 4c and is the basis of Johansen's approach to the yield line theory.

Although the presently discribed approach could be easily extended to any one of the shown yield conditions, and to other yield conditions as well, Von Mises yield condition is chosen for all investigations described in this report. In Cartesian coordinates, this condition is given by:

$$\sigma_x^2 + \sigma_y^2 - \sigma_x\sigma_y + 3\tau_{xy}^2 - \bar{\sigma}^2 = 0 \qquad (2.13)$$

For an isotropic strain hardening material, the subsequent yield surface can be represented by:

$$f\ (\sigma_{ij},\ m) = 0 \qquad (2.14)$$

where m is a measure of the degree of strain hardening of the material. It is assumed that the concept of effective stress can be used to describe the beginning of yielding in a strain hardening material which is subjected to a biaxial state of stress. The basis of this concept is the equivalent stress versus total strain curve (as shown in Fig. 5), which is assumed to be identical with the stress-strain relationship found from a simple tension test. The use of this approach allows the establishment of the conditions for subsequent yielding from a plastic state of stress and is given by:

$$\bar{\sigma} = m\ \sigma_o \qquad (2.15)$$

where σ_o is the initial effective stress and $\bar{\sigma}$ is the current effective or equivalent stress and is taken directly from the stress-strain relationship found in a simple tension test. Eq. 2.16 can then be written as follows for the case of a Von Mises' material:

$$f\ (\sigma_{ij},\ m) = \frac{1}{2} S_{ij}\ S_{ij} - \frac{1}{3} \bar{\sigma}^2 = 0 \qquad (2.16)$$

This equation represents the loading function, indicating further plastic straining if the equation is satisfied identically ($f = 0$), and elastic behavior if $f < 0$. Eq. 2.16 indicates that the effective stress is related to the stress components as follows:

$$\bar{\sigma} = (\sigma_x^2 + \sigma_y^2 - \sigma_x\sigma_y + 3\tau_{xy}^2)^{1/2} \qquad (2.17)$$

Furthermore, $\bar{\sigma}$ is dependent on the amount of plastic deformation that has taken place, as shown in Fig. 5. In incremental form this relationship is of the form:

$$\dot{\bar{\sigma}} = E_p\ \dot{\bar{\epsilon}}^p \qquad (2.18)$$

where E_p is the slope of the equivalent stress versus equivalent plastic strain curve. An expression for the effective plastic strain rate can be derived as a function of the increments of the plastic strain components; thus:

$$\dot{\bar{\epsilon}}^p = \left(\frac{2}{3}\ \dot{\epsilon}^p_{ij}\ \dot{\epsilon}^p_{ij} \right)^{1/2} \qquad (2.19)$$

The effective plastic strain $\bar{\epsilon}^p$ is found as the integral of Eq. 2.19, taken along the loading path so that all of the increments of plastic strain are included.

The yield condition and the loading function serve to establish criteria for yielding from elastic or plastic states of stress, respectively. The remaining problem is to establish relations for predicting the increments in the plastic strain components knowing what the increments in stress and the total stresses are. In order to arrive at plastic strain increments, it is assumed for the purpose of this work that the Prandtl-Reuss flow rule (Ref. 21), which is often used in connection with the Von Mises yield condition, is applicable. This constitutive relation, often termed flow rule, is based on Drucker's postulate for strain hardening material (Ref. 9), and can be written as:

$$\dot{\epsilon}^p_{ij} = \lambda \frac{\partial f}{\partial \sigma_{ij}} = \lambda \frac{\partial f}{\partial S_{ij}} = \lambda S_{ij} \qquad (2.20)$$

where λ is a positive scalar quantity, which can be found from a knowledge of the mechanical behavior of the material. Eq. 2.20 states that the increments of plastic strain depend on the current values of the deviatoric stress components and not on the stress increments to reach this state. Furthermore, it can be shown that the plastic strain increment vector is normal to the yield surface, as indicated in Fig. 3. To determine the unknown multiplier λ, use is made of the Von Mises' yield condition given by Eq. 2.16, and of the consistency equation:

$$\dot{f} = S_{ij}\,\dot{S}_{ij} - \frac{2}{3}\,\bar{\sigma}\,\dot{\bar{\sigma}} = 0 \qquad (2.21)$$

which expresses that the stress increment vector can only be tangential to the yield surface. As shown in Ref. 21, for example, λ is given by

$$\lambda = \frac{3}{2}\,\frac{\dot{\bar{\epsilon}}^p}{\bar{\sigma}} \qquad (2.22)$$

Combining Eq. 2.20 and Eq. 2.22 and using the strain hardening law, given by Eq. 2.18, leads to:

$$\dot{\epsilon}^p_{ij} = \frac{3}{2}\,\frac{S_{ij}\,\dot{\bar{\sigma}}}{\bar{\sigma}\;E_p} \qquad (2.23\,a)$$

or written explicitely in terms of stress components in the Cartesian stress space:

$$\{\dot{\epsilon}^p\} = \begin{bmatrix} \dot{\epsilon}^p_x \\ \dot{\epsilon}^p_y \\ \dot{\gamma}^p_{xy} \end{bmatrix} = \frac{\dot{\bar{\sigma}}}{\bar{\sigma}\;E_p} \begin{bmatrix} \sigma_x - \sigma_y/2 \\ \sigma_y - \sigma_x/2 \\ 3\tau_{xy} \end{bmatrix} \qquad (2.23\,b)$$

Eq. 2.23 establishes the relationships for predicting the increments in the plastic strain components in terms of the current state of stress, the anticipated increments in effective stress, and E_p, the slope of the effective stress versus effective plastic strain curve as shown in Fig. 5.

2.3.4 Elastic-Plastic Stress Matrix for a Layer

For the purpose of deriving the element stiffness matrices used in the finite element displacement approach, which due to the nonlinear nature of the problem, is to be formulated in incremental form, the relationship is sought between the increments in stress and the increments in total strain. A step-by-step method is suited to follow the process of plastification in a structure for which the entire load-deformation history is desired. Having presented the fundamental constitutive relations in the previous section, the elastic-plastic stress matrix needed to generate the element stiffness matrices must now be derived. In order to be able to treat the limiting case of perfect plasticity, as well as the case of work hardening material, with the same general procedure, the following formulation, as described by Felippa (Ref. 10), is adapted. Starting with Eq. 2.17, one finds by implicit differentation:

$$2\bar{\sigma}\dot{\bar{\sigma}} = 2\sigma_x\dot{\sigma}_x - \sigma_y\dot{\sigma}_x + 2\sigma_y\dot{\sigma}_y - \sigma_x\dot{\sigma}_y + 6\tau_{xy}\dot{\tau}_{xy} \qquad (2.24)$$

The rate of effective stress, which is a scalar quantity, is derived from this expression, and can be written as follows:

$$\dot{\bar{\sigma}} = [A]^T \{\dot{\sigma}\} \qquad (2.25)$$

where the vector of stress rates is defined as:

$$\{\dot{\sigma}\}^T = < \dot{\sigma}_x \quad \dot{\sigma}_y \quad \dot{\tau}_{xy} > \qquad (2.26)$$

and [A] is a matrix connecting the rate of effective stress to the rates of total stress, given by:

$$[A] = \begin{bmatrix} (\sigma_x - \sigma_y/2)/\bar{\sigma} \\ (\sigma_y - \sigma_x/2)/\bar{\sigma} \\ 3\tau_{xy}/\bar{\sigma} \end{bmatrix} \tag{2.27}$$

Using Hooke's law, given by Eq. 2.6, and making use of the fact that elastic and plastic strain components can be separated, the vector of stress rates can be written as:

$$\{\dot{\sigma}\} = [D] \left\{ \{\dot{\epsilon}\} - \{\dot{\epsilon}^p\} \right\} \tag{2.28 a}$$

which, when using the constitutive equation 2.23 b, leads to:

$$\{\dot{\sigma}\} = [D] \left\{ \{\dot{\epsilon}\} - [A]\ \dot{\bar{\epsilon}}^p \right\} \tag{2.28 b}$$

Therefore, the rate of effective stress, as given by Eq. 2.25, can be written as:

$$\dot{\bar{\sigma}} = [A]^T \{\dot{\sigma}\} = [A]^T [D] \left\{ \{\dot{\epsilon}\} - [A]\ \dot{\bar{\epsilon}}^p \right\} \tag{2.29}$$

Making use of Eq. 2.18, the rate of incremental effective plastic strain can be found from the above expression as follows:

$$\dot{\bar{\epsilon}}^p = \frac{[A]^T [D] \{\dot{\epsilon}\}}{E_p + [A]^T [D] [A]} \tag{2.30}$$

Substituting Eq. 2.30 for $\dot{\bar{\epsilon}}^p$ in Eq. 2.29 leads to the desired

relationship between the increments of stress and the rates of total strain:

$$\{\dot{\sigma}\} = \left[[D] - \frac{[D]\,[A]\,[A]^T\,[D]}{E_p + [A]^T\,[D]\,[A]} \right] \{\dot{\epsilon}\} \qquad (2.31\,a)$$

which can be written simply as:

$$\{\dot{\sigma}\} = [D_e]\,\{\dot{\epsilon}\} \qquad (2.31\,b)$$

The matrix $[D_e]$, defined as:

$$[D_e] = \left[[D] - \frac{[D]\,[A]\,[A]^T\,[D]}{E_p + [A]^T\,[D]\,[A]} \right] \qquad (2.32)$$

provides for the new relationship between the increments of stress and the increments of total strain. Matrix $[D_e]$ is called the elastic-plastic stress matrix, and is applicable to any layer which is stressed into the plastic range. Using this approach, the degenerate case of perfect plasticity ($E_p = 0$) can be handled with ease. This is in contrast to the initial stiffness approach, which breaks down for this special but frequently occurring case. Furthermore, it should be observed that matrix $[D_e]$ is now fully populated, and must be evaluated for each layer separately. Its elements take on new values for each cycle of iteration. The above derived elastic-plastic stress matrix is the key to the derivation of the element stiffness matrices used in the proposed incremental finite element tangent stiffness approach.

2.4 Incremental Elastic-Plastic Solution Procedure

2.4.1 Assembly of the System Tangent Stiffness Matrix

The essential elements needed in the formulation of the proposed elastic-plastic finite element solution have been derived in Section 2.3. In view of a future extension of this approach to include non-linearity due to geometry, an incremental type formulation is desired in which solutions are obtained by solving a sequence of linear problems associated with an incremental application of the loading. A step-by-step procedure in connection with a small incremental loading is needed for this elastic-plastic analysis, since the relationship between stresses and strains and hence the systems stiffness matrix is nonlinear.

In this step-by-step analysis, the effect of the non-linear material behavior of a structure subjected to the load vector $\{F\}$ is approximated by the sum of a series of linear structures, each subjected to the load increment $\{\dot{F}\}$ and assuming that the deformations during each load increment are essentially linear. In the tangent stiffness approach, taken here as the basis for this inelastic analysis, the systems stiffness matrix $[K]$ of the entire structure at any stage of loading is a function of the existing values of stresses in the structure, and thus needs to be modified for each load increment. For each step, this effective, or often called instantaneous stiffness matrix $[K_e]$, must be assembled for the entire structure taking into account plastification in the plate structure. To simplify this task,

each finite plate element is further subdivided into a number of layers, as discussed in Section 2.3. The stiffness contribution of each layer is then computed separately since the stiffness of any layer depends on the current state of stress; i.e. on the extent of plastification in a layer. The incremental displacement vector $\{\dot{\delta}\}$ resulting from the applied load increment $\{\dot{F}\}$ is then obtained by solving the basic stiffness relationship, which can be written in incremental form as:

$$\{\dot{F}\} = [K_e] \{\dot{\delta}\} \tag{2.33}$$

in which $[K_e]$ is the tangent stiffness matrix for the entire structure, the coefficients of which are recomputed for each load increment by using appropriate incremental stress-strain relations.

As given in Appendix III of Ref. 31 (and Ref. 30), the stiffness matrix for a homogeneous anisotropic rectangular plate element, as originally described by Adini, Clough and Melosh, was rederived in suitable form for the purpose of the present analysis. Three degrees of freedom per nodal point were introduced for this element; namely the lateral deflection w and the two slopes of the deflected plate surface θ_x and θ_y. Taking any layer K of the layered plate model for the inelastic analysis of plates, as shown in Fig. 2, the stiffness contribution for this layer can immediately be derived from the expression for the stiffness matrix given in Refs. 30 and 31.

$$[K]^k = \frac{1}{12}\left[(z_k^a)^3 - (z_k^i)^3 \right] [C^{-1}]^T \Big[D_{11}[K_1] + D_{12}[K_2] + D_{13}[K_3] + D_{22}[K_4] + D_{23}[K_5] + D_{33}[K_6] \Big] [C^{-1}] \qquad (2.34)$$

in which $[K_i]$, where $i = 1, \ldots 6$ are component stiffness matrices and $[C]$ is a transformation matrix as given in Ref. 31.

The process of assembling the systems stiffness matrix follows exactly the procedure outlined in Section 2.3 of Ref. 31, except that instead of treating a finite plate element at a time, a layer at a time must be considered. Depending on whether a layer is found to be elastic or plastic, appropriate stress-strain relationships, here formulated in incremental form as given by Eq. 2.6 or Eq. 2.31, must be used. The coefficients D_{ij} of the stress matrix for an elastic layer are always constant and given by Eq. 2.7, whereas the coefficients D_{ij} for a plastic layer take on different values for subsequent states of plastification and must be evaluated for each cycle of iteration. These coefficients depend on the current state of stress σ_{ij} in a layer as well as on its effective stress $\bar{\sigma}$ given by Eq. 2.17, and the strain hardening parameter E_p.

Explicitely, these coefficients can be evaluated using Eq. 2.32 since at the start of an iteration cycle the current state of stress in a layer and all other needed quantities are known. The procedure for evaluating the stiffness of a plastic layer is as follows:

1. Evaluate the coefficients of matrix [A].

2. Evaluate the coefficients of matrix $[D_e]$.

3. Find the stiffness contribution of the layer in consideration by evaluating Eq. 2.34 and add it to the already accumulated stiffness.

The total stiffness of a finite plate element must be assembled by considering each layer separately and summing up all stiffness contributions. In the case of transversely loaded plates neglecting in-plane deformation, a pair of layers lying symmetric with respect to the middle plane of the plate can be treated at a time. Performing this process for all layers and considering all plate elements leads to the instantaneous or tangent systems stiffness matrix for the entire structure. As this is true for all presently known approaches capable of handling inelastic problems, the availability of a high-speed digital computer is essential for a successful implementation of this approach.

2.4.2 The Iterative Solution Technique

The iterative solution technique used for the solution of inelastic plate problems is summarized graphically by the flowchart shown in Fig. 6. A unit load is applied first to the initially assumed stress-free structure and the associated elastic stress distribution is obtained. The applied loads are then scaled up so as to cause initial yielding in the most stressed layer. This is done by comparing for each layer the effective stress representing the elastic limit of the material in

consideration. Since in the elastic range, and assuming first order theory, stresses and deformations are directly proportional to the applied load, the values of these field quantities can be equally found by scaling up the appropriate values found for the applied unit load.

The structure ceases to behave linearly elastic for loads higher than the elastic limit load. Thus, an incremental procedure must be used to find its response in the non-linear range. Since the final state of stress is not known in advance for each applied load increment added to the accumulated load, an iterative solution is needed to find the new equilibrium configuration corresponding to the applied load increment. Starting out with known values of all involved field quantities at the elastic limit load level, an increment of load $\{\dot{F}\}$ is applied to the structure first. To arrive at the new equilibrium configuration corresponding to this load increment an iterative procedure is started, described here for the i-th cycle of iteration.

For this i-th cycle of the current iteration, the following quantities are known specifically for each layer: First, $\{\sigma\}^{i-1}$, the accumulated stresses as computed at the end of the (i-1)-th cycle are known and hence, $\bar{\sigma}^{i-1}$, the total effective stress can be found. In addition, the maximum effective stress $\bar{\sigma}_{max}^{i-1}$ recorded during the entire loading history is stored. The iteration proceeds as described by the following steps:

1. Assume all layers to be in the same state of stress as

found in the previous cycle; or, if the iteration is started, as found in the last cycle of the previous load increment.

2. For any plastic layer, compute the coefficients of matrix [A]. This step is omitted if a layer is found to be elastic.

3. Compute the coefficients of matrix $[D_e]$ for any plastic layer. For elastic layers use matrix [D], the elements of which always remain constant.

4. Compute the stiffness contribution of this layer as outlined in Section 2.4.1.

5. Add the stiffness contributions of all layers appropriately and establish in this fashion the systems tangent stiffness matrix $[K_e]$ for the entire structure.

6. Solve the system of incremental equilibrium equations $\{\dot{F}\} = [K_e]\ \{\dot{\delta}\}$ for the unknown incremental nodal displacement vector $\{\dot{\delta}\}^i$.

7. Compute the rates of curvature $\{\dot{\phi}\}^i$ at the centroid of each plate element using the curvature-displacement relations as given in Appendix III of Ref. 31.

8. Compute the total strain rates $\{\dot{\epsilon}\}^i$ at the centroid of each layer using the strain-curvature relations.

9. Find the stress rates $\{\dot{\sigma}\}^i$ at the centroid of each layer

using the incremental stress-strain relations given by Eq. 2.31 b for a plastic layer, or by Eq. 2.6 for a layer found to be elastic, respectively.

10. Find the total stresses $\{\sigma\}^i$ at the centroid of each layer by adding the stress increments to the previously accumulated stresses; i.e. $\{\sigma\}^i = \{\sigma\} + \{\dot{\sigma}\}^i$.

11. Check whether layers which were originally elastic are still elastic. Also check the computed effective stress $\bar{\sigma}^i$ against the assumed effective stress $\bar{\sigma}^{i-1}$ for all plastic layers. If $\bar{\sigma}^i$ is within a specified tolerance of $\bar{\sigma}^{i-1}$, then the iteration is terminated and the next load increment is applied to the structure. If $\bar{\sigma}^i$ is not within a tolerance of $\bar{\sigma}^{i-1}$, then the newly computed values for stresses $\{\sigma\}^i$ and effective stress $\bar{\sigma}^i$ are used as new initial guesses for cycle (i + 1). Steps 1 through 11 are then repeated until either $\bar{\sigma}$ is found within a certain tolerance or a specified number of cycles is exhausted. Accumulated values for all needed field quantities can then be computed and printed out if desired.

The analysis proceeds exactly in the same way for the next load increment. Basically, arbitrary values for $\{\dot{F}\}$ could be assigned; however, the present investigation was restricted to the case of proportional loading. It should be mentioned here that

the effect of different values of $\{\dot{F}\}$ on the convergence and accuracy of the involved field quantities can be studied easily by specifying different values for the incremental load and observing the convergence behavior. The effect of the chosen tolerance for the effective stress in a layer can be studied similarly as will be discussed in the presentation of the numerical examples.

2.4.3 Unloading and Neutral Loading of a Layer

By definition, a layer is termed elastic if its effective stress $\bar{\sigma}$ computed at the centroid of the layer is less than the current yield stress of the material. A plastic layer is characterized by the fact that its effective stress is equal to the current effective stress of the material. For such a layer the total strain is composed of an elastic and a plastic part. In the preceeding section it was assumed that those layers which were assumed plastic are being stressed further into the plastic range as the applied loads increase. This assumption must be checked in the analysis by computing the effective stress corresponding to the total stresses in each layer and comparing it to its previous value. If the computed value for the effective stress in the i-th cycle is found to be greater than the stored value, found in cycle (i-1), then the layer in consideration is being further loaded plastically.

On the other hand, if the newly computed value for the effective stress is less than the previously found value, elastic

unloading has taken place. When this occurs, the elastic stress-strain relations must be used and the analysis proceeds as outlined above. It should be mentioned that unloading can occur even though the externally applied loads are monotonically increasing. During unloading the stress path moves inside the current yield surface. Mathematically speaking, unloading from a plastic state which is characterized by Eq. 2.16, occurs if

$$\dot{f} = S_{ij} \dot{S}_{ij} - \frac{2}{3} \bar{\sigma} \dot{\bar{\sigma}} < 0 \qquad (2.35)$$

As this is usually done, it is assumed that elastic straining does not change the yield surface and subsequent loading follows the unloading path as indicated in Fig. 5.

Neutral loading is defined as loading from one plastic state to another plastic state in such a way as to cause no plastic straining. In this case the stress path is moving tangential to the yield surface and in the analysis the elastic or elastic-plastic stress-strain relations can be used.

2.4.4 Yield Surface Correction

In the iterative procedure as described in Section 2.4.2 it is advantageous to find improved values for the state of stress in a layer before entering the next cycle of a given iteration. Convergence is then obtained faster resulting in considerable savings in computer time. Depending on the type of material used, different approaches can be taken to improve the initial guesses

for stresses and for the effective stress. Although the outlined tangent stiffness approach is valid for the more general case of elastic-linearly strain hardening material, the problems treated in this chapter and chosen for the purpose of demonstrating the application of this method are confined to materials exhibiting elastic perfectly-plastic material behavior.

The method of arriving at new improved guesses for stresses in a layer, outlined in this section, is limited to materials exhibiting elastic perfectly-plastic material behavior. A similar approach could be taken for the more general case of linearly-strain hardening material. As mentioned earlier, the incremental stress vector as shown in Fig. 7 is restricted to lie in the tangential plane to the current yield surface which, in the case of a perfectly-plastic material, is always identical with the initial yield surface. However, for any finite increment of load the stress rate vector will be of finite length and hence cannot remain on the yield surface. The state of stress must therefore be corrected in order to conform with the assumptions associated with perfectly-plastic material. This can be done by adding a correction vector to the incremental stress vector as shown in Fig. 7. This yield surface correction is best done in the deviatoric stress space and the following quantities are to be defined for this derivation:

$\{S'\} = (S'_x, S'_y, S'_{xy})$ = The uncorrected deviatoric stress vector

$\{S\} = (S_x, S_y, S_{xy})$ = The corrected deviatoric stress vector

$\{CB\}$ = The correction vector defined by

$$\{S\} = \{S'\} + \{CB\} \tag{2.36}$$

J'_2 = The second invariant of the deviatoric stresses computed from uncorrected stresses

J_2 = The second invariant of the deviatoric stresses computed from corrected stresses

These two quantities can be evaluated if the respective stresses are known; they are related by

$$J'_2 = J_2 + \xi^2 \tag{2.37}$$

where ξ^2 is defined as the error in J'_2. The correction vector is defined to be normal to the yield surface in the deviatoric stress space and is of unknown length c. It follows from the requirement of normality:

$$\{CB\} = c \frac{\text{grad}J_2}{|\text{grad}J_2|} = c \frac{\nabla J_2}{|\nabla J_2|} \tag{2.38}$$

For perfectly-plastic Von Mises' material, J_2 is given by:

$$J_2 = \frac{1}{2} S_{ij} S_{ij} = \frac{1}{3} \sigma_o^2 = k^2 \tag{2.39}$$

where k is the yield stress in pure shear. Proceeding now with the evaluation of the length of the gradient vector to the yield surface, one finds:

$$|\nabla J_2| = \sqrt{2J_2} = \sqrt{2k^2} \tag{2.40}$$

Substituting Eq. 2.38 and Eq. 2.40 into Eq. 2.36, and observing that $\nabla J_2 = \{S\}$ leads to

$$\{S'\} = \left[1 - \frac{c}{\sqrt{2k^2}}\right] \{S\} \tag{2.41}$$

Since J_2 and J_2' are quadratic functions of the deviatoric stresses it follows directly:

$$J_2' = \left[1 - \frac{c}{\sqrt{2k^2}}\right]^2 J_2 \tag{2.42}$$

Substituting Eq. 2.37 and Eq. 2.39 into Eq. 2.42 yields:

$$c = k\sqrt{2}\left[1 \pm \sqrt{1 + \xi^2/k^2}\right] \tag{2.43}$$

Linearizing the expression for the square root in Eq. 2.43, leads finally to:

$$\{S'\} = \left(1 + \frac{\xi^2}{2k^2}\right) \{S\} \tag{2.44}$$

Introducing now:

$$\delta = \frac{\xi^2}{2k^2} \tag{2.45}$$

the corrected deviatoric stress vector is found to be

$$\{S\} = \frac{\{S'\}}{1 + \delta} \tag{2.46}$$

and hence, the corrected stresses are given by:

$$\sigma_{ij} = \frac{\sigma'_{ij}}{1 + \delta} \tag{2.47}$$

The stresses computed in each plastic layer are to be corrected according to Eq. 2.47 before entering into the next cycle of the iteration. Finally, the evaluation of δ, given by Eq. 2.45, leads to:

$$\delta = \frac{1}{2}\left[\frac{\bar{\sigma}^2}{\sigma_o^2} - 1\right] \tag{2.48}$$

2.5 Numerical Results

The following examples have been selected to illustrate the application of the proposed finite element tangent stiffness approach for solving inelastic plate problems. A general computer program has been written for the implementation of this approach. This program allows the tracing of the entire load-deformation behavior of arbitrarily shaped and loaded plates. The approach was outlined in the previous sections of this chapter for the case of isotropic elastic, linearly-strain hardening material. An extension to include orthotropic material behavior can be easily made if the associated constitutive relations are known.

The validity of the proposed method is demonstrated on a few example solutions giving an indication of the reliability of the approach. To simplify comparisons with analytic solutions, the material was restricted to behave elastic perfectly-plastic ($E_p = 0$) and Von Mises' yield criterion in connection with the Prandtl-Reuss' flow rule were used in the solution of all example problems. However, other types of yield conditions could easily be incorporated as well in the present approach.

For the purpose of this investigation all example structures are thought to be made of structural steel with the following numerical values for the material behavior assumed in the analysis:

$$E = 30{,}000 \text{ ksi} \qquad E_p = 0$$

$$\sigma_o = 36 \text{ ksi} \qquad \nu = 0.30$$

The results are presented in non-dimensional form in terms of

$\bar{p} = p/p_y$ = Actual load divided by p_y, where

p_y = The load level at which yielding is initiated

δ_y = The deflection of a point representative for the behavior of the structure at first yielding

M_p = Moment capacity per unit width of plate

All other assumptions made concerning discretization and the geometry of the example structures chosen are listed in the

accompanying figures presented for each problem. The general computer program developed to implement the proposed approach yields the incremental and accumulated values of all involved field quantities; thus it allows the study of the complete elastic-plastic behavior of complex shaped plates.

2.5.1 Simply Supported and Clamped Plate Strip

The proposed method of analysis was first applied to a few simple problems for which the exact solution can be found from the theorems of limit analysis. Fig. 8 shows the load-deflection behavior of a simply supported and uniformly loaded plate strip of unit width. Sixteen elements were used in the idealization of a half-span of the plate strip. Results are plotted for different numbers of layers: k = 6, 8 and 10. It is recognized that an increase in numbers of layers used for the discretization of the plate elements leads to a better approximation of the collapse load. In addition, closer results would be obtained for a finer discretization of the plate strip. For the same example, the propagation of the elastic-plastic boundary for k = 10 (k = number of layers) is depicted in Fig. 9. The elastic-plastic boundary is in general a space surface and difficult to determine analytically. The error introduced in the present approach will be reduced if a finer mesh is used and the number of layers is increased at the locations of greater rate of change of curvature in the plate strip. It is worth noting here, that for the continuous

plate strip, collapse would occur as soon as the center section is fully plastic. In the finite element analysis, however, collapse does not occur until the two innermost layers closest to the center-line of the plate strip yield. In the numerical analysis, this state is indicated by a sudden, rapid increase in deflection. Mathematically speaking, the system stiffness matrix has become singular.

Similarly, the load-deflection behavior of a clamped plate strip of unit width is shown in Fig. 10. As predicted by simple plastic beam theory, this structure can withstand substantial additional loads after first yielding has taken place. The analysis was again performed for different numbers of layers; i.e. for k = 6, 8 and 10 and the respective response is plotted in the same figure. Closer results would again be obtained if a finer mesh size were used. The propagation of the elastic-plastic boundary and the extent of plastification is shown in Fig. 11. The structure becomes unstable as soon as the two innermost layers closest to the center-line of the plate strip exhibit plastic behavior. Fig. 12 is drawn to demonstrate the redistribution of plate moments M_x and M_y along the length of the clamped plate strip. The variation of all other stress and deformation components could be studied in a similar way. It should be noted that the theorems of limit analysis can be used to compute the exact collapse load for these two introductory examples. However, the calculation of the exact collapse load is possible in but a few simple cases.

4.5.2 Simply Supported Square Plate

The behavior of plates of various shapes subject to various boundary conditions and loading is of special interest to the designer and is considered a difficult problem if the elastic-plastic response of such structures is sought. The response of a few typical plate structures stressed into the inelastic range will be presented next in order to demonstrate the versatility of the proposed finite element approach. The load-deflection behavior of the center point of a simply supported and uniformly loaded square plate is illustrated in Fig. 13, along with the best upper and lower bound found in the literature. Sixteen rectangular plate elements were used for the discretization of one quadrant of the plate and six layers were chosen for each finite plate element. It is recognized from this figure that, despite the relatively rough mesh chosen, an already satisfactory solution is obtained. The propagation of yielded regions for different load levels is shown in Fig. 14. Plastification begins at the corners of the square plate and slowly spreads toward the center of the plate. The progression of yielding is in agreement with the solution given by Ang and Lopez (Ref. 20), which is based on a discrete element approach, as discussed in Section 2.2. However, the load-deflection curve found in the present approach is considerably different from the curve obtained by the cited authors due to their assumption of a two layer sandwich-type plate model used in their work.

As this is usually done, the collapse load of this structure is defined as the value of the load at which the pattern of fully plastic elements is such that the structure becomes a mechanism. It is seen from Fig. 13 that substantial deformations must take place before this stage is reached and a small deflection analysis is in fact not capable of predicting the correct collapse load for certain types of structures. Nevertheless, a value of $0.982\ (24\ M_p/L^2)$, where L is the span of the square plate, is estimated for the present example and this value can now be compared with available solutions. This comparison is made in Table 1, where the estimated limit load is compared with available upper and lower bound, finite difference and finite element solutions. An improved solution would be obtained for a finer mesh.

2.5.3 Clamped Square Plate

The elastic-plastic behavior of a uniformly loaded square plate is shown in Fig. 15 along with the best known upper and lower bound solution found in the literature. It is seen that the assumed discretization of sixteen elements per quarter of the plate leads to a slightly higher collapse load than predicted by the best known upper-bound solution. This is due to the fact that the chosen rough discretization cannot properly account for the high stress gradients occurring in the vicinity of the clamped edges. Performing the analysis with the next finer mesh, which

contains thirty-six elements per quadrant of the plate, leads to an improved result as seen from this figure. Fig. 16 depicts the sequence of yielding and the extent of plastification for the same problem. A comparison of this sequence of yielding, which agrees again with the one given by Lopez and Ang (Ref. 20), with the propagation of yielded regions of the simply supported plate reveals some interesting differences. Fig. 17 shows the redistribution of deflections as a result of the plastic flow. In Table 2, a comparison is made between the estimated limit load for this problem and the values found from different other approaches.

2.5.4 Square Plate with Three Edges Simply Supported and One Edge Free

The load-deflection behavior of a uniformly loaded square plate with three simply supported edges and one free edge is shown in Fig. 18 Due to symmetry in loading and geometry only one-half of the plate needs to be analyzed. The curve shown in Fig. 18 applies to the mid-point P of the free edge. No lower bound solution is known for this problem and it cannot be said with assurance how close the given upper bound solution found by Hodge (Ref. 12) is to the true solution. Fig. 19 depicts the propagation of yielded regions for increasing load and Fig. 20 demonstrates how the plate moments are redistributed as a result of plastic flow.

2.5.5 Plate Supported by Rows of Equidistant Columns (Flat Slab)

The load-deflection behavior of the center of a uniformly loaded square plate supported by rows of equidistant columns is illustrated in Fig. 21, along with a lower bound solution found by Wolfensberger (Ref. 33) and an upper bound solution given in (Ref. 34). Attention should be focused to the large additional strength that can be carried by this structure beyond first yielding. The sequence of yielding for this structure is shown in Fig. 22.

2.6 Convergence and Accuracy of Solutions

The presented examples show the validity of the proposed numerical technique from which approximate solutions to complex elastic-plastic plate problems can be obtained. No formal proof of the correctness of the solution method was attempted in this investigation and hence the reliability of the numerical solutions can only be shown on the basis of known solutions found by the theorems of limit analysis or by other types of analysis. This comparison was made whenever possible and the solutions found by the present approach are strongly supported by solutions derived from the theorems of limit analysis. All problems chosen in this investigation were analyzed using a relatively rough discretization. Improved results would be obtained if the mesh size is reduced or the number of layers is increased. This is demonstrated in Figs. 8, 9 and 13. A tolerance of 5% was usually specified

for the effective stress leading to two or three cycles per iteration for each applied load increment. A smaller value for this tolerance increases the number of cycles needed for convergence; thus, increasing the computer time considerably.

2.7 Summary

A finite element analysis capable of predicting the elastic-plastic behavior of complex shaped plates has been presented in this chapter. The approach is formulated in incremental form and is based on linear geometry. Hence, it is applicable to problems where the structure experiences significant plasticity before the deformations become excessive. A layered model is used to aid in the description of the elastic-plastic behavior of each finite plate element since the process of plastification is mathematically difficult to describe. The approach is based on the tangent stiffness concept and an iterative solution technique is needed to find the new equilibrium configuration corresponding to each applied load increment. For each cycle of iteration, the effective or instantaneous stiffness matrix of the entire structure is recomputed and the governing linear system of equilibrium equations is solved repeatedly. A few example solutions prove the validity of the proposed numerical technique which is applicable to plates of arbitrary geometry and loading and can be extended to more complex material behavior.

3. ELASTIC-PLASTIC ANALYSIS OF STIFFENED PLATES

3.1 Introduction

The behavior of eccentrically stiffened plate structures in the inelastic range is required to assess the effects of overloading and to compute the ultimate load-carrying capacity of such structures as a whole as well as that of its components. The most commonly used methods of elastic analysis for stiffened plate structures were discussed in Refs. 30 and 31, along with their possible extension to include the inelastic behavior of such structures. From an extensive literature survey it was concluded that the classical methods of elastic analysis are not suitable to study the inelastic response of beam-slab type structures and the application of the finite element method was again found to be the best suited. The reliability of the finite element tangent stiffness approach in solving elastic-plastic plate problems was demonstrated in Chapter 2. This approach will be extended to stiffened plates in this chapter making use of a layered beam model which is attached to the layered plate model described in the previous chapter. In-plane behavior must be considered and an incremental analysis is again required to solve this mathematically difficult problem.

3.2 A Finite Element Approach Using a Layered Model

3.2.1 Description of the Layered Beam-Plate Model

The finite element tangent stiffness approach described

in Chapter 2 for the elastic-plastic analysis of plates is extended in this chapter to eccentrically stiffened plates of arbitrary shape and loading. This problem being complex and not amenable to analytic solution, a numerical solution is worked out based on a layered system of beam and plate elements. A layered beam model is attached to layered plate elements in order to be able to describe the process of yielding in the actual beam-plate structure. It is assumed that the structure experiences significant plasticity before the deformations become excessive permitting the formulation of the outlined approach to be based on the first order theory. In-plane deformations and forces must be considered in the present analysis because both quantities are of prime interest in a stiffened plate structure. In view of a future inclusion of nonlinearities due to geometry, the tangent stiffness approach was preferred to the initial stiffness approach. As in the case of the analysis of inelastic plates, the load is applied incrementally, the stiffness matrix of the system must be derived and solved repeatedly for each load increment. The approach allows the tracing of the entire load-deformation relationship for any point of interest in the structure and the study of the process of plastification of complex shaped stiffened plates. The method is developed for an isotropic elastic linearly-strain hardening material; however, it can be easily extended to cope with arbitrary material behavior.

Plate elements are subdivided into a number of layers,

as described in Chapter 2, in order to be able to follow the process of plastification in the plate. Each layer is assumed to be in a state of plane stress and the state of stress at the centroid of a layer is taken as representative for the entire layer. Any layer is considered either elastic or elastic-plastic depending on the magnitude of effective stress present in this layer at a given load level. In the present analysis, the increments of total strain are computed as the sum of strain increments resulting from in-plane and out-of-plane behavior. In-plane strains in any layer k are computed at the centroid of this layer using the basic relationships derived in Appendix IV of Ref. 31:

$$\{\dot{\varepsilon}_i\}^k = [B]\ \{\dot{\delta}_i\}^e \tag{3.1}$$

where [B] is the matrix connecting strains to nodal displacements as derived in Appendix IV of Ref. 31 and $\{\delta_i\}^e$ is the nodal displacement vector made up of the consistent listing of in-plane displacement components. The strains in any layer k associated with out-of-plane deformations of the plate are given by Eq. 2.1 b:

$$\{\dot{\varepsilon}_0\}^k = [H^k]\ \{\dot{\phi}\} \tag{3.2}$$

The curvature terms listed in $\{\dot{\phi}\}$ are again defined at the centroid of a plate element and are computed as shown in Appendix III of Ref. 31. Having found the displacement field by the proposed analysis based on a trial stiffness matrix associated with the previous load

increment, the in-plane displacement components and the curvatures at the centroid of a plate element can be computed. The total strain increments can be evaluated by adding the strain increments resulting from in-plane and out-of-plane action:

$$\{\dot{\epsilon}\}^k = \{\dot{\epsilon}_i\}^k + \{\dot{\epsilon}_0\}^k \qquad (3.3)$$

Depending on the current magnitude of the effective stress in a layer, the stress increments are evaluated using basic relationships: Eq. 2.6 being valid for an elastic layer, and Eq. 2.31 b, if the layer is found to be plastic. It is seen that for the purpose of computing stress increments in an elastic-plastic layer, Eq. 2.31 b is still valid, if the current total stresses resulting from in-plane and out-of-plane action are substituted.

Yielding starts often at the bottom fiber of a stiffener element in an eccentrically stiffened plate and successively spreads across the entire beam cross section. In order to study the process of plastification in a beam, a stiffener element is subdivided into a number of layers as shown in Fig. 23. An approach based on the plastic hinge concept would grossly oversimplify the actual behavior. The interaction of all involved stress resultants acting on a beam element stressed into the plastic range is difficult to describe mathematically if one ceases to accept the yield hinge concept. In the most general case, two shear forces and the bending moment about the y-axis interact with the axial force and the twisting moment in a beam. In order to

avoid obscuring the overall analysis with this interaction problem, it is assumed for the present approach that the beams are slender. It is also assumed that the shear force as well as the twisting moment do not significantly affect yielding in a layer and can be neglected in the yield condition. It is further assumed that GK_T, the torsion constant of the stiffener remains unchanged. The effect of these assumptions could be studied in a more refined analysis. It is assumed in the present analysis that the elastic-plastic behavior of the beams can adequately be described by the proposed layered finite beam model. Due to the above stated assumptions a beam layer is seen to be in a state of uniaxial stress for consideration of yielding and hence the yield condition reduces to its simplest form. The state of stress at the centroid of a layer is taken as representative for the entire beam layer. Stresses in beam layers are computed based on a linear distribution of strain extending to the bottom fiber of the stiffener. Basically, an arbitrary stress-strain relationship could be specified for each stiffener layer. The problems solved in this chapter are confined to isotropic elastic perfectly-plastic behavior of the material. It is expected that this approach can be extended to beams made of reinforced concrete by appropriate consideration of the material behavior of each layer made of concrete or reinforcing steel.

In the present analysis, any layer must be specified by its width, thickness and its distance to the plane of reference,

which is defined to coincide with the middle plane of the plate. As defined in Ref. 31, a beam element is bounded by two nodal points I and K, lying in the middle plane of the plate as shown in Fig. 23. Due to the incremental nature of the analysis proposed, the axial strain increments in any beam layer K due to bending moment and axial force can be evaluated separately using basic relationships. The total strain can then be obtained by adding the two parts. The axial strain component in any layer K is given by:

$$\dot{\epsilon}_s^k = \frac{1}{L}\left[(\dot{u}_k - \dot{u}_i) + Z_k(\dot{\theta}_{yk} - \dot{\theta}_{yi}) \right] \tag{3.4}$$

Using this expression, the strain can be computed at the centroid of any layer K if the displacement components, as defined in Ref. 31, are known. Having determined the strain increment, the associated stress increment is found from the stress-strain relationship specified for the beam layer in consideration. The stress resultants acting on a beam element are defined at the plane of reference and are found by adding up the contribution of each layer:

$$\dot{M}_s = \sum_{k=1}^{\ell} \dot{\sigma}_x^k \, z_k \, t_k \, b_k \tag{3.5}$$

$$\dot{N}_s = \sum_{k=1}^{\ell} \dot{\sigma}_x^k \, t_k \, b_k \tag{3.6}$$

where ℓ is the number of beam layers, t_k is the thickness and b_k is the width of beam layer K.

3.2.2 Elastic-Plastic Stress-Strain Relations

The elastic-plastic response of beam and plate layers must be known in order to be able to formulate the proposed analysis. Plate layers are treated exactly as discussed in Chapter 2, which deals with the inelastic analysis of transversely loaded plates. In the presently discussed incremental elastic-plastic analysis of unsymmetrically stiffened plates, the stresses resisted by a layer due to in-plane and out-of-plane action must be considered. These stress increments are computed from incremental total strains which are found from appropriate strain-displacement relations. The same equations as derived in Sections 2.3.2 and 2.3.3, governing the elastic-plastic behavior of a layer, are applicable if the total stresses resulting from in-plane and out-of-plane action are substituted into these equations. No restrictions must be placed on the loading path, since the plastic stress-strain relations derived from the flow theory are themselves incremental. In the present analysis, Von Mises' yield condition in connection with Prandtl-Reuss' flow rule is adapted and the derivation of the stress-strain relations given in Section 2.3.3 for an elastic linearly-strain hardening material shall apply. If the computed effective stress in a plate layer is less than the specified value, the layer is termed elastic and Eq. 2.6 is applicable. For an elastic-plastic layer in which the total strains are composed of elastic and plastic parts, the incremental stress-strain relations given by Eq. 2.32, are used. Neutral loading and

unloading are treated as discussed in Chapter 2. From these stress-strain relations the increments of stresses for given increments of total strain resulting from in-plane and out-of-plane behavior of the stiffened plate are determined. The elastic-plastic stress matrix found in this manner is required to generate the element stiffness matrices associated with in-plane and out-of-plane behavior of the finite plate element.

Due to the assumption made that the twisting moment as well as the shear forces are small and need not be considered in the yield condition, each beam layer is stressed uniaxially. Furthermore, it is assumed that the beams are made of elastic linearly-strain hardening material of the type shown in Fig. 5. If the total stress is less than the current yield stress, a beam layer K is considered elastic and the increment of stress is found from the increment of strain by:

$$\{\dot{\sigma}_s\}^k = [D_s]\ \{\dot{\epsilon}_s\}^k \tag{3.7}$$

where $[D_s]$ is a matrix consisting of one element of value E_s, the modulus of elasticity of the beam material. If the current total stress is equal to the current yield stress, the layer is considered to be elastic-plastic and the increment of stress is given by:

$$\{\dot{\sigma}_s\}^k = [D_{se}]\ \{\dot{\epsilon}_s\}^k \tag{3.8}$$

where $[D_{se}]$ is identical with the strain-hardening modulus E_{ps}.

3.2.3 Generation of Element Stiffness Matrices

The instantaneous element stiffness matrices are established in a similar manner as described in Refs. 30 and 31, which presents an elastic finite element analysis of eccentrically stiffened plate structures. The elastic-plastic analysis of eccentrically stiffened plates requires again a step-by-step iterative procedure. The fact that first order theory is assumed to be adequate and hence, the structure is assumed to behave linearly elastic for each increment of load allows computing of the in-plane and out-of-plane stiffness matrices separately and to construct the system stiffness matrix from the component stiffness matrices.

The in-plane stiffness matrix for any plate element is found by summing up the in-plane stiffness contributions of each layer of the plate element. Separate consideration is to be given to each layer because the state of stress and hence, the effective stress is different in each layer. The in-plane stiffness matrix for a plate element is given in Ref. 31. The same matrix can be used in the incremental elastic-plastic analysis, if the plate thickness h is replaced by the thickness of the layer in consideration. The elements D_{ij} of the stress matrix [D] depend on the state of stress in a layer and must be computed as outlined in Section 3.2.2.

The assumptions made for the derivation of the stiffness matrix governing the out-of-plane behavior of a plate element were discussed in Section 3.3.2 of Ref. 31. In the present

elastic-plastic analysis each layer must be treated separately, since the state of stress is different in each layer and the distance of the centroid of the layer to the plane of reference must be accounted for. For any plate layer, the same stress matrix [D] as generated for the in-plane stiffness matrix is applicable in evaluating the stiffness matrix governing the out-of-plane behavior of the plate element. As shown in Section 2.4.1, the contribution of each layer is found by applying Eq. 2.34. The stiffness contributions of all layers are then added.

In a similar fashion, the stiffness matrix for the stiffener element is formed by considering a stiffener layer at a time. This stiffness matrix is derived in Section 3.3.6 of Ref. 31 and can be applied in the elastic-plastic analysis if the cross-sectional properties of the stiffener layer in consideration are substituted. For a stiffener layer found to be elastic, the stress matrix $[D_s]$ in Eq. 3.7 reduces to E_s, the modulus of elasticity of the beam layer. In an elastic-plastic layer, the strain-hardening modulus E_{ps} is used instead of E_s.

3.3 The Incremental Elastic-Plastic Solution Procedure

3.3.1 Assembly of the System Stiffness Matrix

The incremental finite element displacement approach derived in Chapter 2 for the solution of elastic-plastic plate problems is extended in this chapter to elastic-plastic eccentrically stiffened plate structures. A step-by-step incremental

procedure which follows closely the procedure discussed in Chapter 2 forms the basis of this inelastic analysis. The tangent stiffness matrix $[K_e]$ of the structure must be reassembled at any stage of loading. This key matrix is a function of the geometry and of the existing state of stress in each plate and beam layer and must be modified for each load increment to account for plastification in the structure. The incremental displacement vector $\{\dot{\delta}\}$ resulting from the applied load increment $\{\dot{F}\}$ is obtained by solving the stiffness relationship:

$$\{\dot{F}\} = [K_e] \{\dot{\delta}\} \tag{3.9}$$

in which $[K_e]$ is the tangent stiffness matrix of the entire structure which is discretized by an assemblage of beam and plate elements. The displacement vector of the structure is a listing of displacement components consistent with the force vector components. Five displacement components are introduced at each nodal point as in the case of the elastic analysis of stiffened plates, presented in Ref. 31. The process of assembling the overall tangent stiffness matrix is done in the computer. The out-of-plane and in-plane stiffness matrices are computed for the plate elements framing into a nodal point by appropriate addition of the component stiffness matrices listed in the appendices. For this purpose, the contributions of all plate layers involved are added. Finally, the stiffness of the stiffener elements framing into the nodal point in consideration are computed and added to the already

accumulated stiffness. A stiffener layer or plate layer at a time must be considered since the state of stress is different in each layer and its stiffness is a function of this state of stress. Depending on the magnitude of effective stress in a plate layer which is computed from total stresses resulting from in-plane and out-of-plane action, it is determined first whether the layer is elastic or elastic-plastic. The appropriate stress matrix must be used in computing the stiffness matrices. Stiffener layers are treated alike and their contribution is added to the present stiffness. No fundamental difficulties are encountered whether one deals with elastic linearly-strain hardening or with a more general material behavior of the beams.

It is seen that the process of assembling the system tangent stiffness matrix follows closely the procedure outlined in Chapter 2. The essential difference lies in the fact that in the present analysis the in-plane behavior must be considered and the effect of the beam elements must properly be accounted for. Appropriate stress-strain relationships must be used depending on the state of stress found in a layer. These relationships were derived in Chapter 2 and are equally valid in the present analysis if the total stresses due to in-plane and out-of-plane action are considered. The evaluation of the coefficients of the stress matrix proceeds as discussed in Section 2.2.1.

3.3.2 The Iterative Solution Technique

The iterative solution technique used in the analysis of elastic-plastic eccentrically stiffened plates is schematically illustrated in Fig. 24. The approach taken in the present analysis follows closely the procedure outlined in Chapter 2 used in the analysis of inelastic plates except that the in-plane behavior of the plate and the behavior of beam elements must be included. A unit load is applied first to the structure. Based on an assumed elastic behavior of every plate and beam layer, the overall stiffness matrix is assembled and the displacement vector corresponding to the applied unit load is found by solving the governing system of simultaneous equations. The applied loads are then scaled to cause initial yielding in the most highly stressed layer. Depending on the dimensions of the beam and plate components yielding will initiate in either a beam or a plate layer. All other field quantities are scaled similarly.

After the initiation of first yielding the behavior of the structure is non-linear and the incremental iterative technique is started. Steps 1 through 11, as discussed in Section 2.4.2 for the i-th cycle of iteration constitute again the iterative procedure taken in the present analysis. The structure is assumed to behave linearly elastic for any given cycle within the iteration designed to find the response of the structure for the load increment applied. Hence, strain and stress increments resulting from in-plane and out-of-plane deformation of the beam and plate

elements can be evaluated separately. The strain increments caused by the in-plane and the out-of-plane behavior of the plate elements are computed using the strain-displacement relations listed in Ref. 31.

The strain increments in beam layers, caused by axial and bending deformation, are evaluated using Eq. 3.4. Depending on the total accumulated stress in a stiffener layer or the total accumulated effective stress in a plate layer, the layer is assumed elastic or elastic-plastic. Appropriate stress-strain relations must be used to find the increment of stress corresponding to the strain increment evaluated. All plate and stiffener layers must be considered when it is checked in cycle i whether the assumed effective stress is within a specified tolerance of the computed value for the effective stress. Improved guesses on total stresses and on effective stresses in elastic-plastic layers are obtained by the procedure outlined in Section 2.4.4. The tolerance specified for the effective stress should not be kept too small since a small value can significantly increase the overall computation time. A value of 5 to 10% was used in the present analysis. If desired, different values could be assigned to beam and plate layers. Unloading and neutral loading are treated as outlined in Section 2.4.3.

3.4 Numerical Results

Two example structures have been chosen to demonstrate

the application of the described incremental finite element approach, which is capable of analyzing complex shaped eccentrically stiffened plate structures in the elastic-plastic range. A general computer program has been written to implement this procedure allowing to trace the entire load-deflection behavior of a transversely loaded stiffened plate structure, to describe the sequence of plastification and the redistribution of stresses in all beam and plate layers. Elastic perfectly-plastic material behavior is assumed for both the plate and the stiffener material.

The two examples chosen to verify the presented approach have purposely been kept simple in order to be able to check the results by some other method. Von Mises yield condition in connection with the Prandtl-Reuss' flow rule are assumed to be valid. For the purpose of this investigation, all example structures are thought to be made of structural steel. The following material properties were assumed in the analysis:

Parameter	Plate Layers	Beam Layers
E	30,000 ksi	30,000 ksi
σ_o	36 ksi	36 ksi
E_p	0	0
ν	0.30	--

The results are presented in a non-dimensionalized form. Other assumptions associated with the discretization and the

geometry of the example structures are shown in the figures, which present some results of this investigation. The computer program provides a complete listing of all important field quantities at any chosen stage of loading and hence, permits a detailed study of the elastic-plastic response of complex shaped eccentrically stiffened plate structures.

3.4.1 Simply Supported Three-Beam Bridge Model

The bridge model investigated to illustrate the application of the proposed finite element stiffness approach capable of finding the elastic-plastic response of eccentrically stiffened plates, is shown in Fig. 25. The uniformly loaded structure is discretized by sixteen plate elements and twelve beam elements. Each plate element is further subdivided into six plate layers, and similarly each beam element into five beam layers. Fig. 26 shows the load-deflection behavior at the center beam at midspan of this structure. As illustrated in this figure, simple plastic theory underestimates the ultimate load by approximately 10%. This can be attributed to the fact that the plate is stressed biaxially. The propagation of yielded regions across the cross section at midspan is shown in Fig. 27. As expected, the lower most layer of the center beam plastifies first, and yielding is restricted to beams up to a load of 1.70 times the yield load. The load-carrying capacity of the structure is reached shortly after yielding in the top most plate layer is initiated. Fig. 28

demonstrates clearly the dependency of the lateral distribution of load on the state of plastification in the structure. At the midspan section, the load is shared equally by all beams when the failure stage is approached. On the other hand, the lateral distribution of load does not change any more at the quarter point section for loads greater than 1.50 times the yield load. Figure 29 depicts the bending moment carried by the center beam in function of the non-dimensionalized center deflection. Similarly, the variation of the axial force in the center beam is shown in Fig. 30. Though yielding in beams occurs at the quarter point section as this would not be expected from a consideration of simple plastic theory, the moment and axial force values corresponding to a fully plastic cross section are nowhere reached. Figure 31 depicts deflection profiles for the cross section located at midspan and at quarter point for different load levels. These figures demonstrate that the deflections remain small up to a load of 1.40 times the yield load. It can also be observed that the deflection curve changes its shape from a concave to a convex form during the load history.

3.4.2 Continuous Three-Beam Bridge Model

A continuous uniformly loaded bridge model of the dimensions shown in Fig. 23 was investigated next. The structure was discretized exactly in the same way as the simply supported model described in Section 3.4.1. The load-deflection behavior at the

center beam at midspan is depicted in Fig. 32. The figure shows clearly the large additional strength available after initiation of yielding which occured at the support, again in the lower most layer of the center beam. Indicated in Fig. 32 is also the collapse load of the structure found by simple plastic theory. It can also be observed that the center deflection associated with the collapse load is only approximately one-sixtieth of the span length; thus the first order theory seems to be adequate for the present analysis. The propagation of yielding through the cross sections located at midspan and at the quarter point is illustrated in Fig. 33. Yielding is restricted to the support cross section up to a load of 1.45 times the yield load. The outermost plate layers at this cross-section plastify at a load of 2.20 times the yield load. At the midspan cross section, the layers close to the center start yielding at 2.42 times the yield load. Such plots are instructive and help in the understanding of the elastic-plastic behavior of stiffened plate structures. The lateral distribution of load for different stages of plastification is depicted in Fig. 34. It is interesting to observe that the lateral distribution of load does not change significantly at both the support and the midspan cross-section up to a load of $\bar{p} = 1.50$. As expected, the load is shared equally by all beams when the state of collapse is approached. Fig. 35 shows the variation of the center beam bending moment at the support and at the midspan cross section as a function of the non-dimensionalized deflection

at midspan. Similarly, the variation of the axial force in the center beam is shown in Fig. 36. The deflected shape of the midspan and the quarter span cross section is shown in Fig. 37 for different load levels. It can be observed that the deflections remain small up to a load $\bar{p} = 2.00$. No change in shape of the transverse deflection profile is recognizable at the midspan section in this example as in the case of the simply supported three-beam bridge model.

3.5 Summary

A finite element analysis capable of determining the elastic-plastic response of complex shaped eccentrically stiffened plate structures is presented in this chapter. The approach is formulated in incremental form and is based on linear geometry and the tangent stiffness concept. A layered beam-plate model is adopted to aid in the desciption of the elastic-plastic behavior of the structure. The iterative solution technique outlined in Chapter 2 for the elastic-plastic analysis of plates is extended to account for the in-plane behavior of the plate elements and the behavior of the stiffener elements. Two example structures were analyzed to demonstrate the validity of the proposed approach. The response of two three-beam bridge models could be closely predicted using the outlined approach. The computer program developed to implement the presented analysis yields the state of stress and deformation in every beam and plate layer used in the discretization

of the structure. The analysis shows clearly that the lateral distribution of load at any section depends on the amount of plastification the structure has undergone. It was found that simple plastic theory considerably underestimates the load-carrying capacity of the continuous three-beam bridge model and hence, a more refined analysis is clearly advisable.

4. SUMMARY AND CONCLUSIONS

4.1 Summary

This report presents two different types of finite element analyses: (1) a finite element analysis of elastic-plastic transversely loaded plates, and (2) a finite element analysis of elastic-plastic eccentrically stiffened plates subjected to transverse loading. The formulations of these methods, which are all based on linear geometry, are described in detail in Chapters 2 and 3. For each type of analysis, a general computer program has been developed and was applied in the analysis of several sample structures.

In Chapter 2, a general finite element displacement analysis capable of determining the complete elastic-plastic behavior of complex shaped plates is presented. The approach is formulated in incremental form and is based on the tangent stiffness concept. A layered plate model is adopted to aid in the description of the elastic-plastic behavior of the plate since the process of plastification in a plate element is mathematically difficult to describe. The analysis is developed for an elastic linearly-strain hardening material and can easily be extended to more general material behavior. A few example solutions demonstrate the validity of the described numerical technique which is applicable to plates of arbitrary loading and geometry. The computer program written to implement the approach computes and lists the entire stress and

displacement field in the structure at any desired stage of loading. Therefore, it allows to study the complete elastic-plastic behavior of complex shaped transversely loaded plates.

In Chapter 3, a method of analysis of eccentrically stiffened plates in the elastic-plastic range is described. An incremental finite element displacement approach is used to find the elastic-plastic response of such structures. Layered beam elements are attached to the described layered plate elements in order to be able to describe the process of plastification. In-plane behavior of the plate as well as the behavior of the stiffeners are considered. The developed approach allows studying of the entire load-deformation behavior of complex shaped eccentrically stiffened plate structures and permits the design of such structures more rationally.

4.2 Conclusions

The methods of analysis presented in this report are of a general nature and can be applied to a variety of plate structures. Each of the methods discussed has been implemented with the aid of a general finite element program.

a. Based on the numerical examples processed to demonstrate the proposed numerical technique for the elastic-plastic analysis of arbitrarily shaped plates, presented in Chapter 2, the following conclusions can be drawn:

1. The analyzed examples prove the validity of the described incremental approach from which approximate solutions to complex elastic-plastic plate problems can be obtained.

2. The chosen layered plate model together with the iterative technique adopted allows the adequate description of the elastic-plastic behavior of transversely loaded plates. The approach allows the study of the entire load-deformation behavior, the process of plastification and the redistribution of stresses in complex shaped plates.

b. The following conclusions can be drawn from the incremental finite element approach developed to determine the elastic-plastic response of eccentrically stiffened plates:

1. The adopted layered beam-plate model used to aid in the description of the elastic-plastic behavior of eccentrically stiffened plates adequately predicts their elastic-plastic behavior.

2. The approach allows the description of the entire load-deformation behavior, the process of plastification and the redistribution of stresses in complex shaped eccentrically stiffened plates.

3. Based on the two examples processed in this investigation, it is evident that the lateral distribution of load is a function of the extent of plastification in the structure and all beams are stressed equally when the ultimate load is approached. The approach allows the study of the behavior of bridges under any given overload.

5. NOMENCLATURE

a) Scalars

a = Half length of plate element

b = Half width of plate element

D_{ij} = Coefficients of stress matrix for anisotropic material

E = Modulus of elasticity of plate

E_p = Strain-hardening modulus

f = Function describing subsequent yielding

f^* = Function describing initial yielding

h = Plate thickness

J_2 = Second invariant of stress deviator tensor

k = Yield stress in simple shear

L = Length of stiffener element; or span length

ℓ = Number of beam layers

M_x, M_y, M_{xy} = Plate bending moments per unit width

M_s = Bending moment in stiffener with respect to plane of reference

m = Strain hardening parameter

N_s = Axial force in stiffener

p = Distributed load per unit area of finite element

S_{ij} = Components of stress deviator tensor

t = Thickness of plate layer

w = Lateral deflection in z-direction

γ_{xy} = Shearing strain

ϵ_x, ϵ_y = Strain in x-direction and y-direction, respectively

ϵ_{ij} = Components of strain tensor

θ_x, θ_y = Slope about x-axis and y-axis, respectively

λ = Positive scalar

ν = Poisson's Ratio

σ_{ij} = Components of stress tensor

σ_x, σ_y = Normal stresses in x-direction and y-direction, respectively

$\bar{\sigma}$ = Current effective stress

σ_o = Initial effective stress

τ_{xy} = Shearing stress

$\phi_x, \phi_y, \phi_{xy}$ = Curvatures of plate surface

ϕ' = Rate of change of angle of twist

b) Vectors and Matrices

$[A]$ = Matrix relating the rate of effective stress to the stress rate vector

$[B]$ = Matrix relating element displacements to generalized strains

$[C]$ = Matrix relating element displacements to generalized coordinates

$[D]$ = Stress matrix relating generalized strains to generalized stresses

$[D_e]$ = Elastic-plastic stress matrix

$\{F\}$ = Overall force vector of system

$[K]$ = Overall structural stiffness matrix

$[K^e]$ = Element stiffness matrix

$[K_e]$ = Instantaneous overall stiffness matrix

$[K_i]$ = Component stiffness matrix

$\{M\}$ = Vector of plate bending moments

$\{\delta\}$ = Overall displacement vector of system

$\{\epsilon\}$ = Vector of total strains

$\{\epsilon^e\}$ = Vector of elastic strains

$\{\epsilon^p\}$ = Vector of plastic strains

$\{\phi\}$ = Vector of curvatures of plate surface

$\{\sigma\}$ = Vector of stresses referred to a cartesian coordinate system

6. TABLES AND FIGURES

TABLE 1: AVAILABLE SOLUTIONS FOR LIMIT LOAD - SIMPLY SUPPORTED SQUARE PLATE

Method	Author	Ref.	Yield Criterion			
			Johansen	Tresca	Von Mises	
Lower Bound	Wolfensberger	33	0.945			Multiplier 24 M_p/L^2
	Ranaweera and Leckie	27		0.920	0.995	
	Shull and Hu	29		0.826		
	Koopman and Lance	14		0.964		
	Hodge and Belytscho	12			1.036	
	Prager	26	1.000			
Upper Bound	Ranaweera and Leckie	27		0.961	1.044	
	Shull and Hu	29		1.000		
	Koopman and Lance	14		1.000		
	Hodge	11			1.106	
	Prager	26	1.000			
Finite Difference	Lopez and Ang	20			1.031	
	Bhaumik and Hanley	7	1.041	0.922	1.000	
Finite Element	Armen et al	3			1.137	
	Present Analysis Mesh: 8 x 8				0.982	

TABLE 2: AVAILABLE SOLUTIONS FOR LIMIT LOAD - CLAMPED SQUARE PLATE

Method	Author	Ref.	Yield Criterion			
			Johansen	Tresca	Von Mises	
Lower Bound	Wolfensberger	33	1.560			Multiplier 24 M_p/L^2
	Ranaweera and Leckie	27		1.553	1.710	
	Koopman and Lance	14		1.596		
	Hodge and Belytscho	12			1.786	
Upper Bound	Ranaweera and Leckie	27		1.682	1.844	
	Koopman and Lance	14		1.712		
	Hodge	11			2.052	
Finite Difference	Lopez and Ang	20			1.901	
	Bhaumik and Hanley	7	1.746	1.560	1.740	
Finite Element	Armen et al.	3			2.590	
	Present Analysis Mesh: 8 x 8 Mesh: 12 x 12				2.220 1.865	

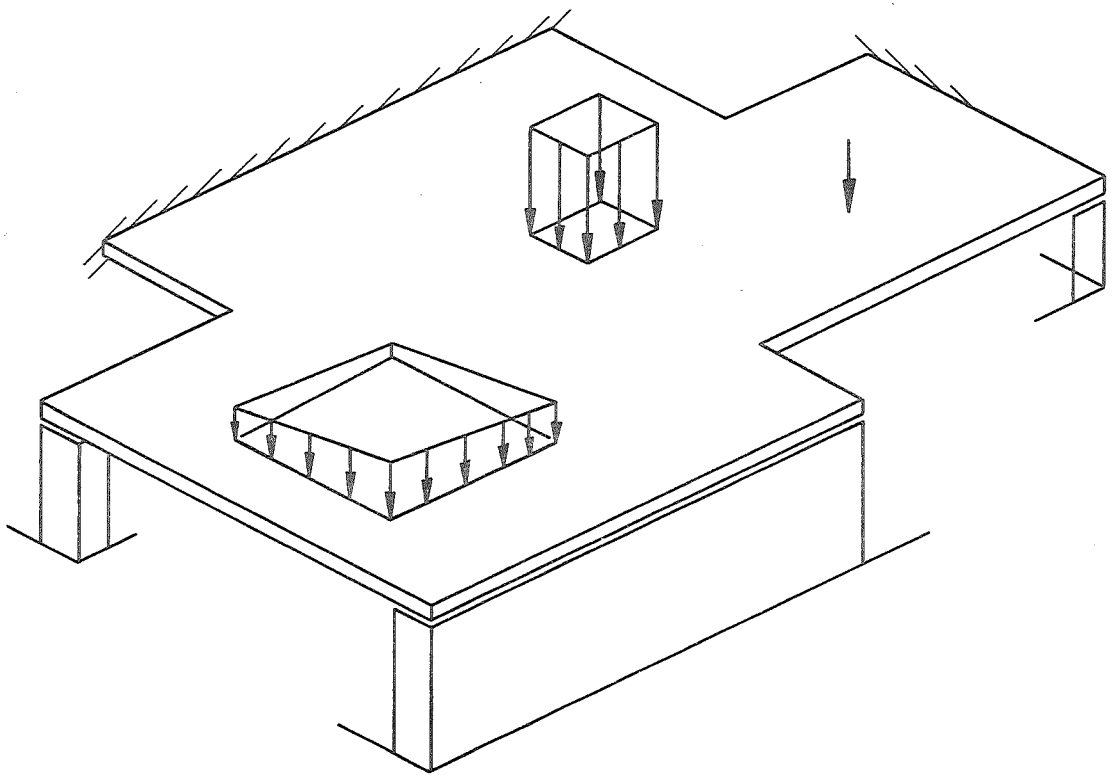

Fig. 1 Plate of Arbitrary Loading and Geometry

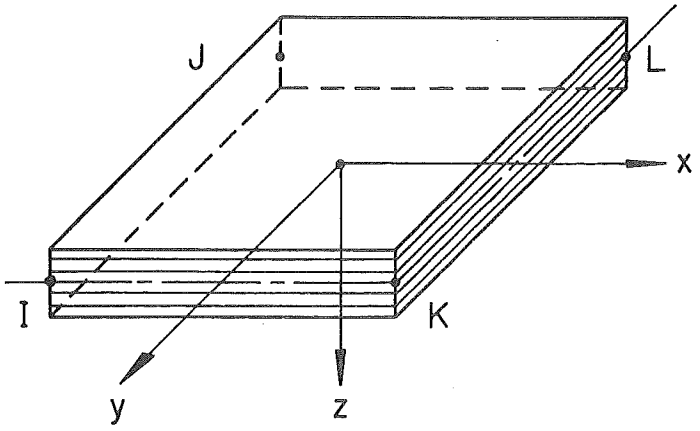

(a.) Layered Finite Plate Element

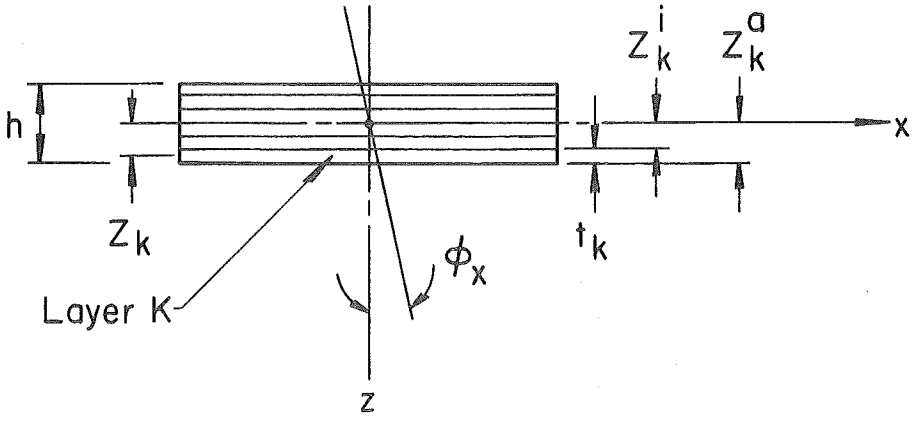

(b.) Cross Section of Layered Model

Fig. 2 Layered Plate Finite Element for Elastic-Plastic Analysis of Plates

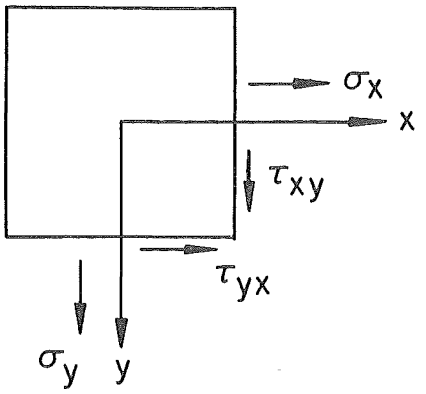

(a.) State of Stress in a Layer

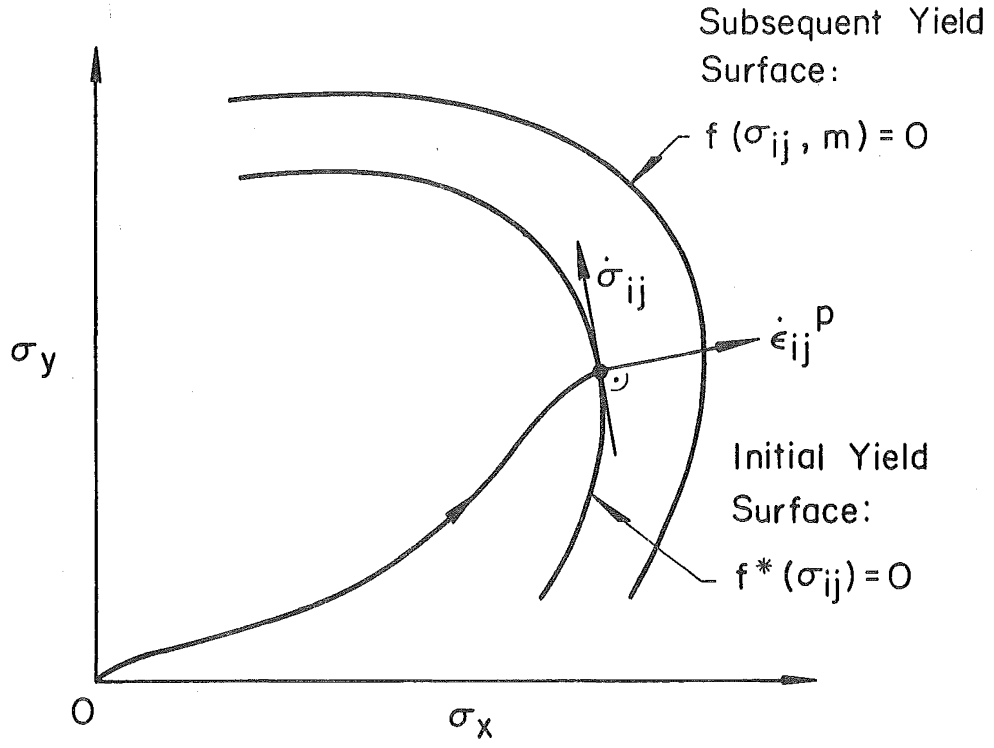

(b) Loading Path and Yield Surfaces

Fig. 3 Loading Path and Yield Surfaces for a Layer of the Finite Plate Element

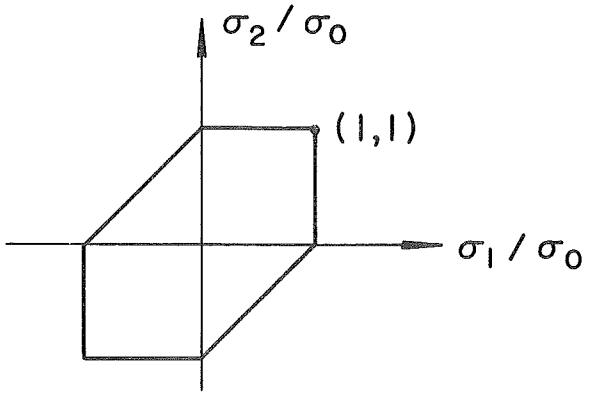

(a.) Tresca's Yield Condition

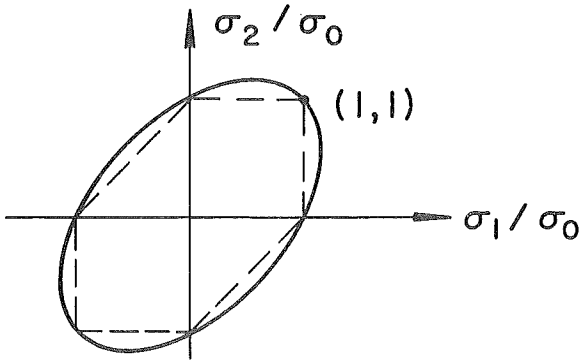

(b.) Von Mises' Yield Condition

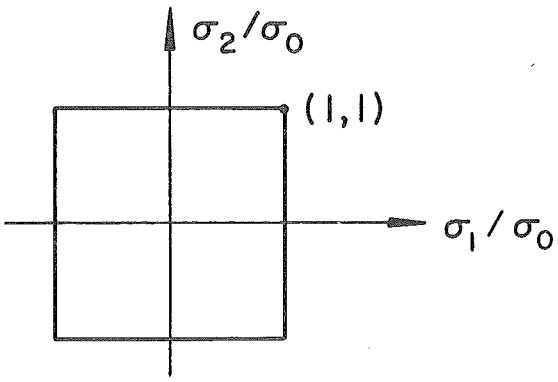

(c.) Johansen's Yield Condition

Fig. 4 Most Commonly Used Yield Criteria

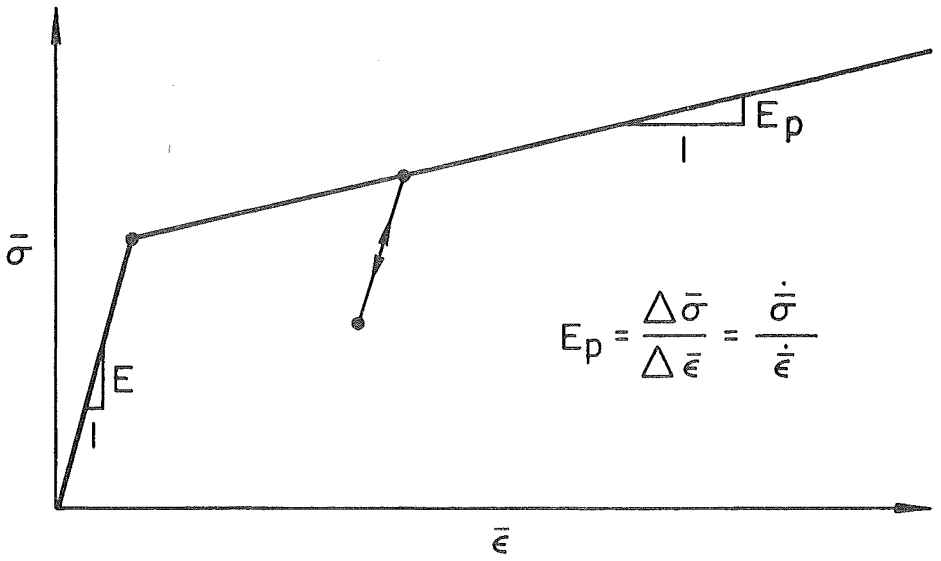

(a.) Effective Stress versus Effective Total Strain Curve

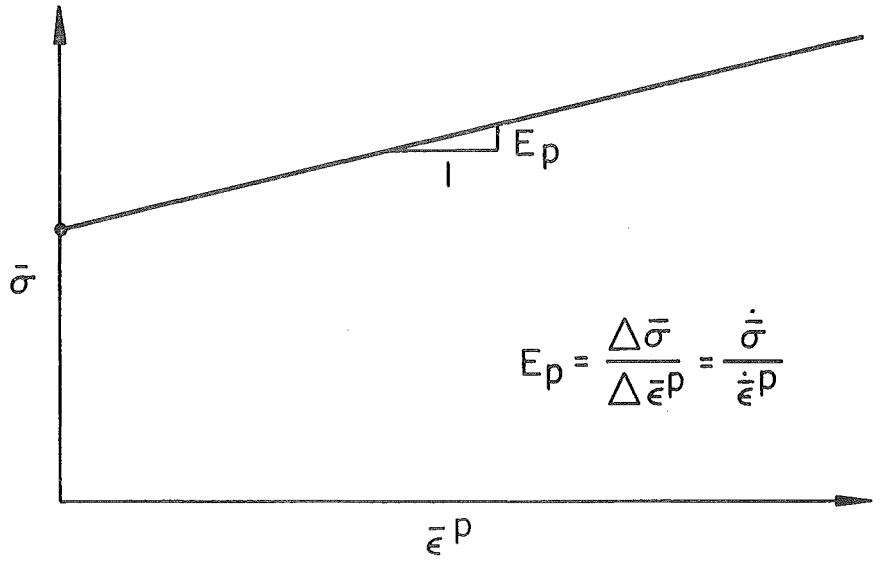

(b.) Effective Stress versus Effective Plastic Strain Curve

Fig. 5 Effective Stress versus Effective Strain Curves

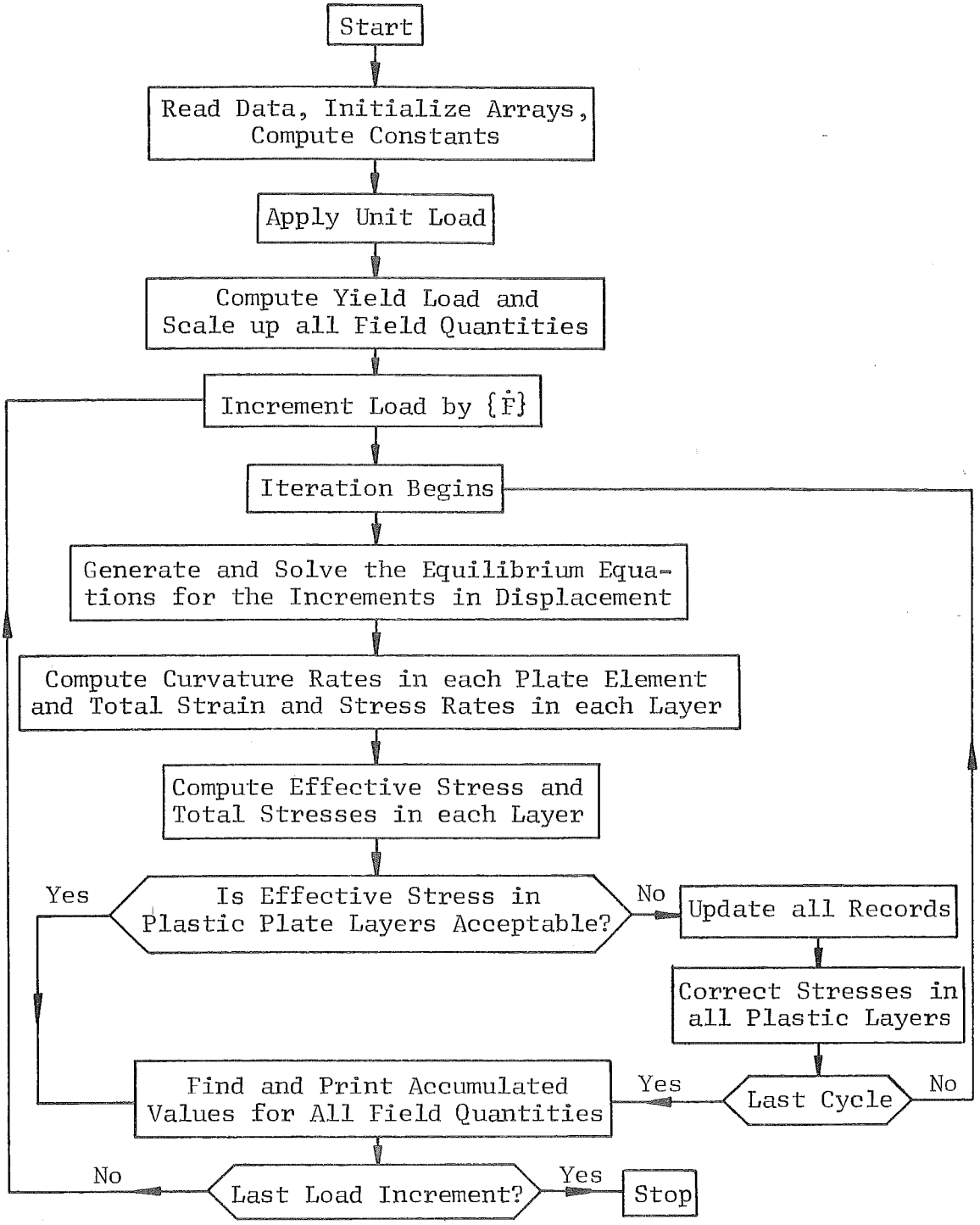

Fig. 6 Flow Diagram for Elastic-Plastic Plate Analysis

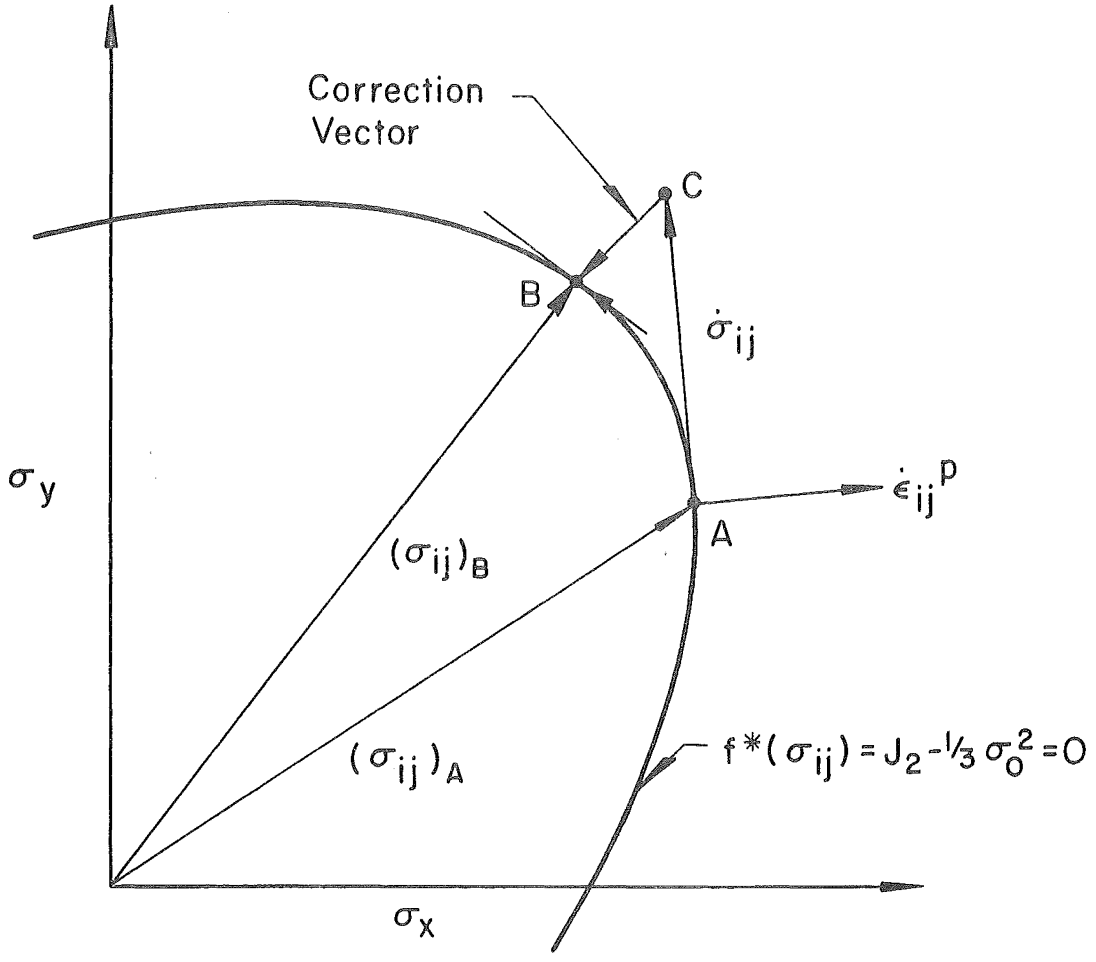

Fig. 7 Yield Surface Correction for Elastic Perfectly-Plastic Material

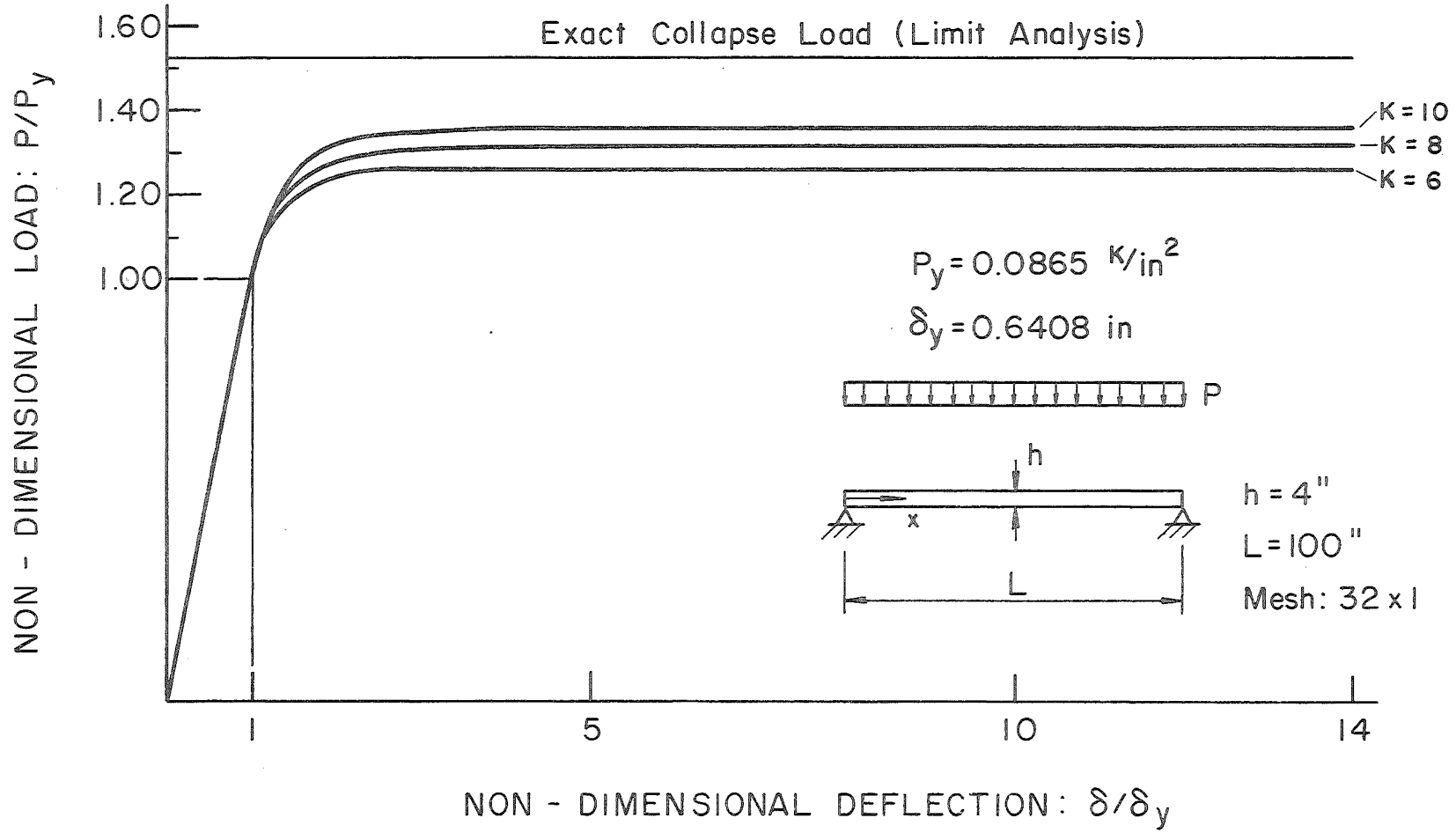

Fig. 8 Load-Deflection Curve at Center of Simply Supported Plate Strip

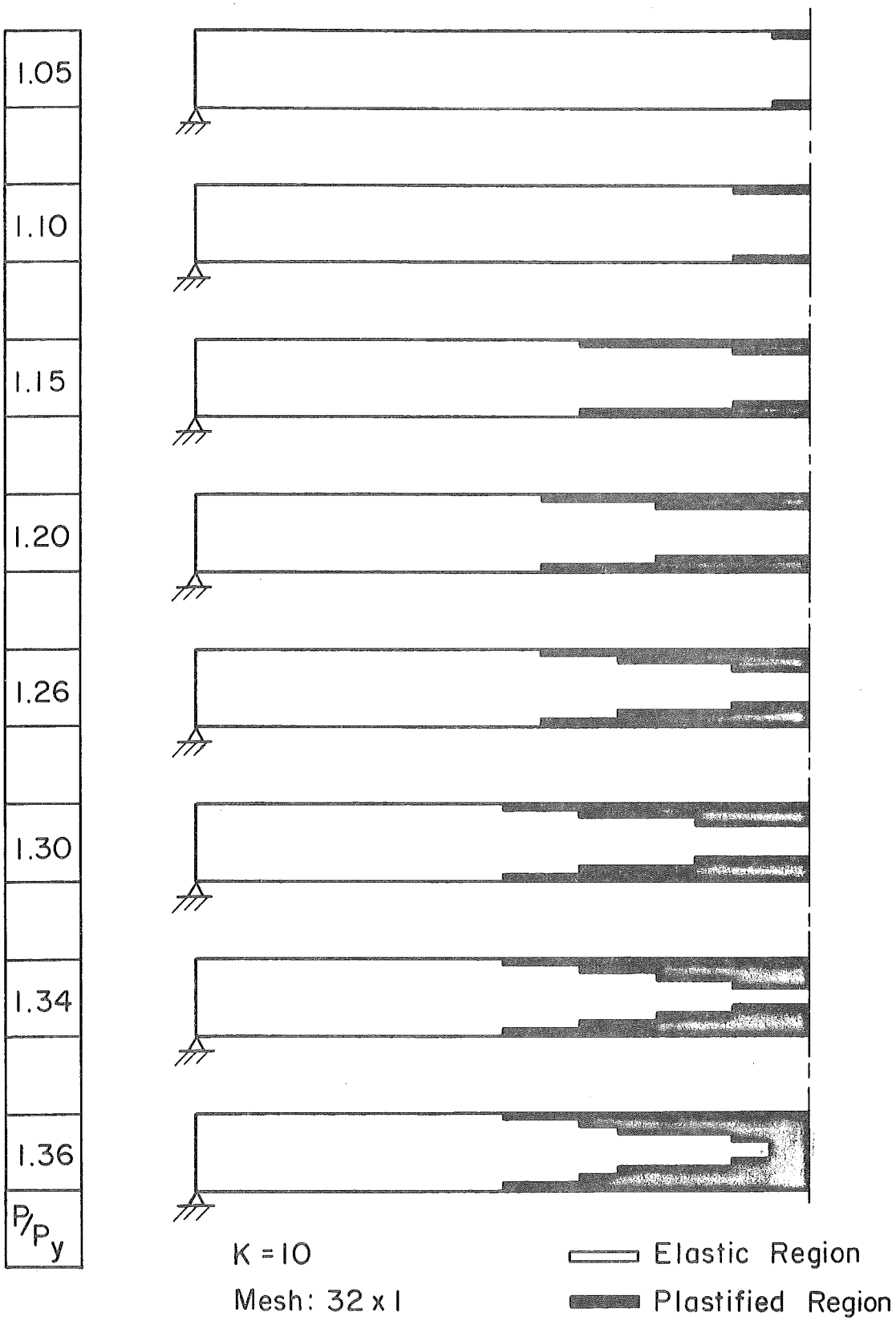

Fig. 9 Progression of Elastic-Plastic Boundary for Simply Supported Plate Strip

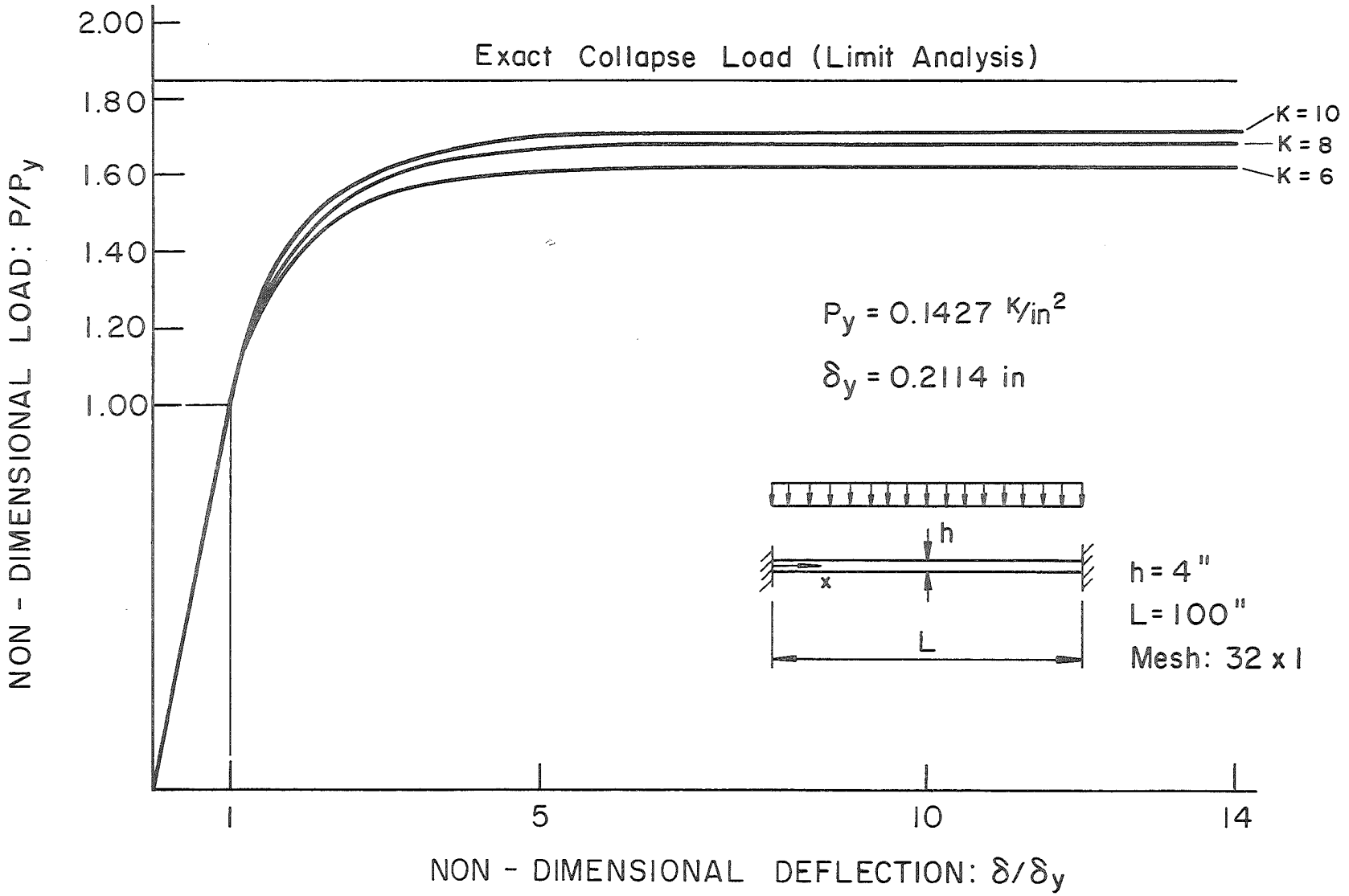

Fig. 10 Load-Deflection Curve at Center of Clamped Plate Strip

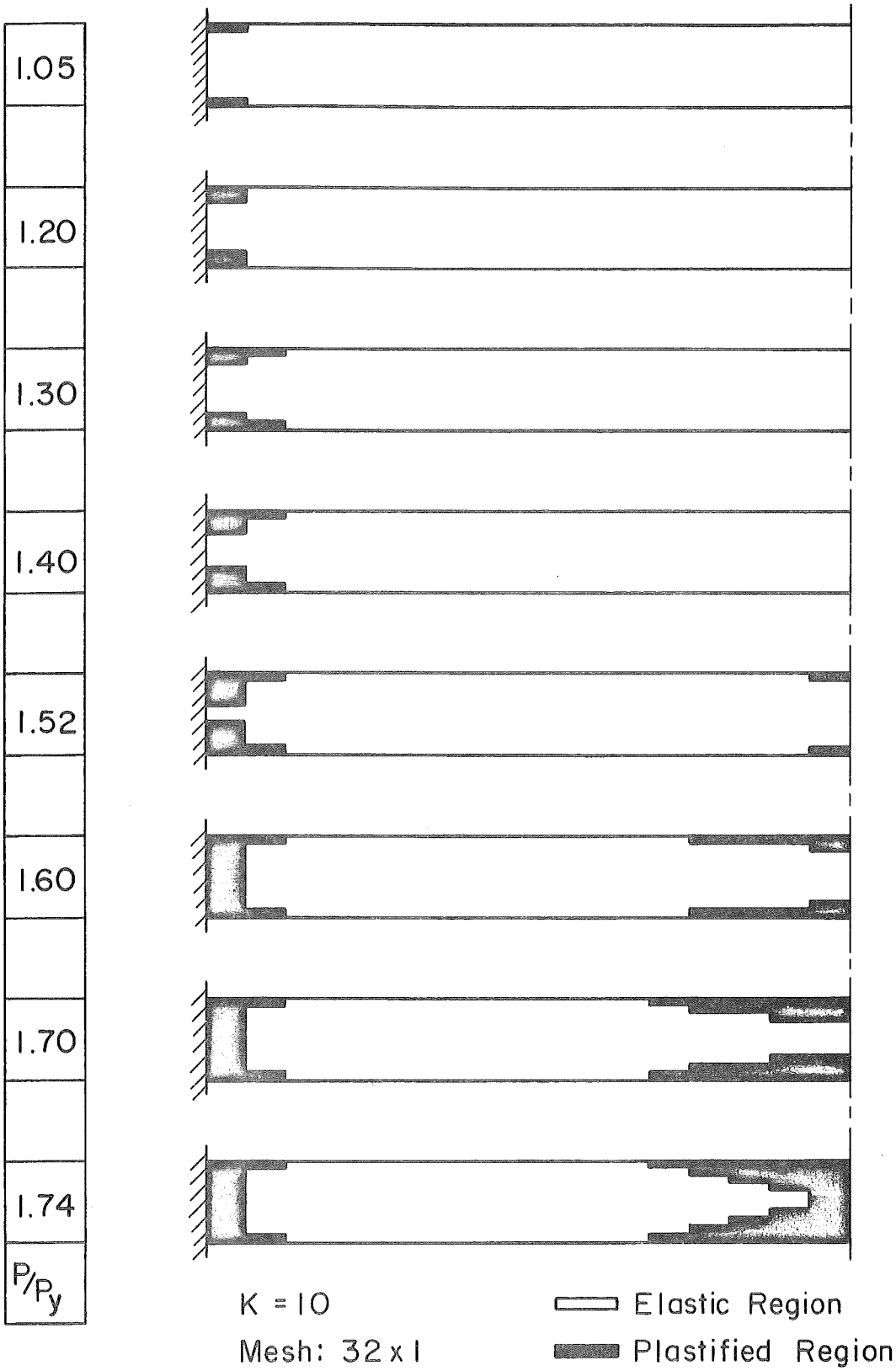

Fig. 11 Progression of Elastic-Plastic Boundary for Clamped Plate Strip

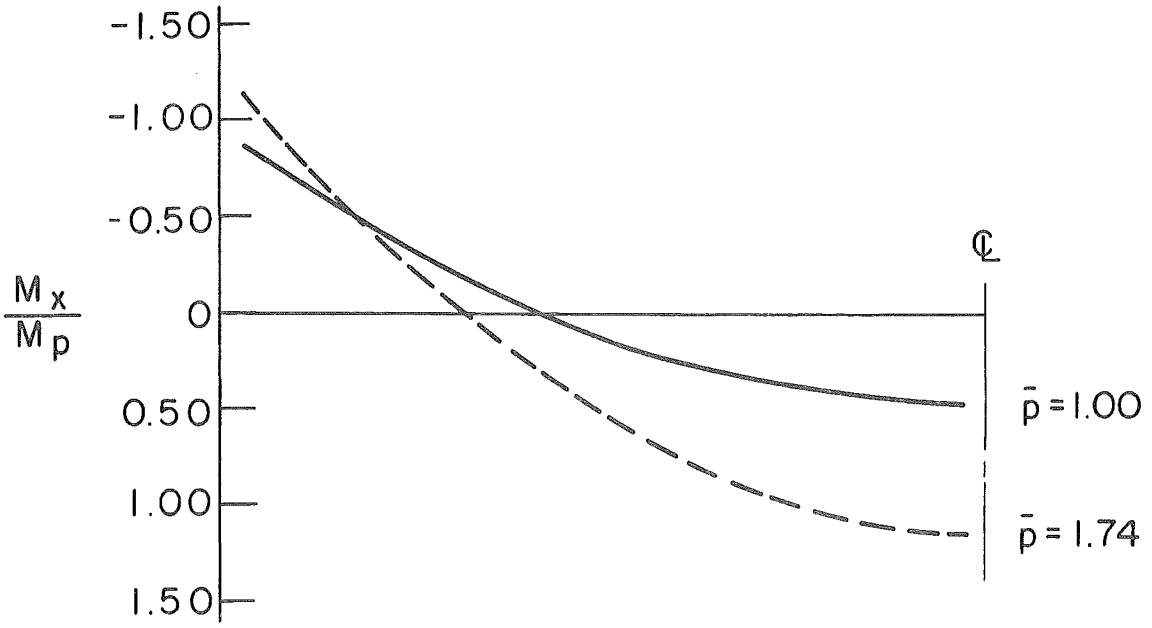

BENDING MOMENT M_x ALONG x-AXIS

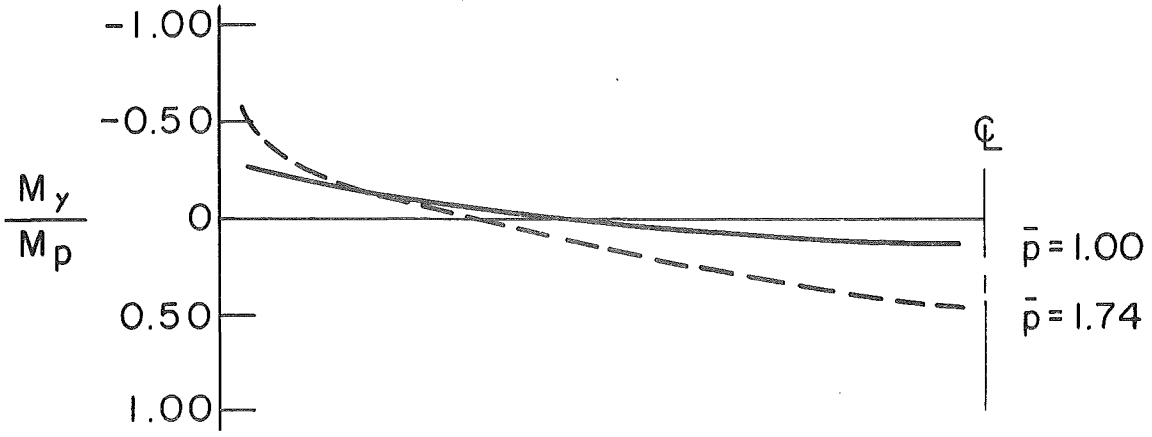

BENDING MOMENT M_y ALONG x-AXIS

Fig. 12 Redistribution of Moments in Clamped Plate Strip

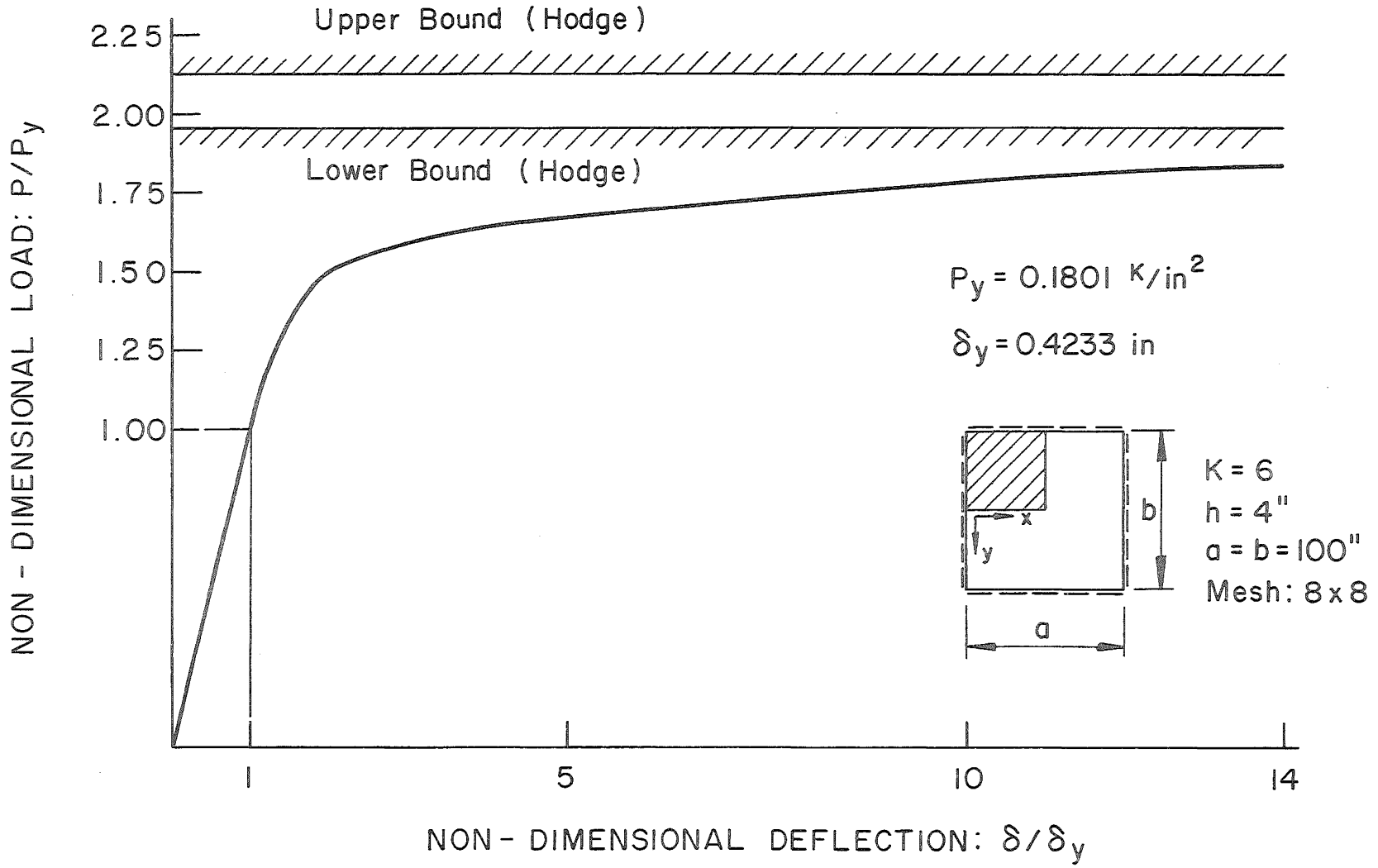

Fig. 13 Load-Deflection Curve at Center of Simply Supported Plate

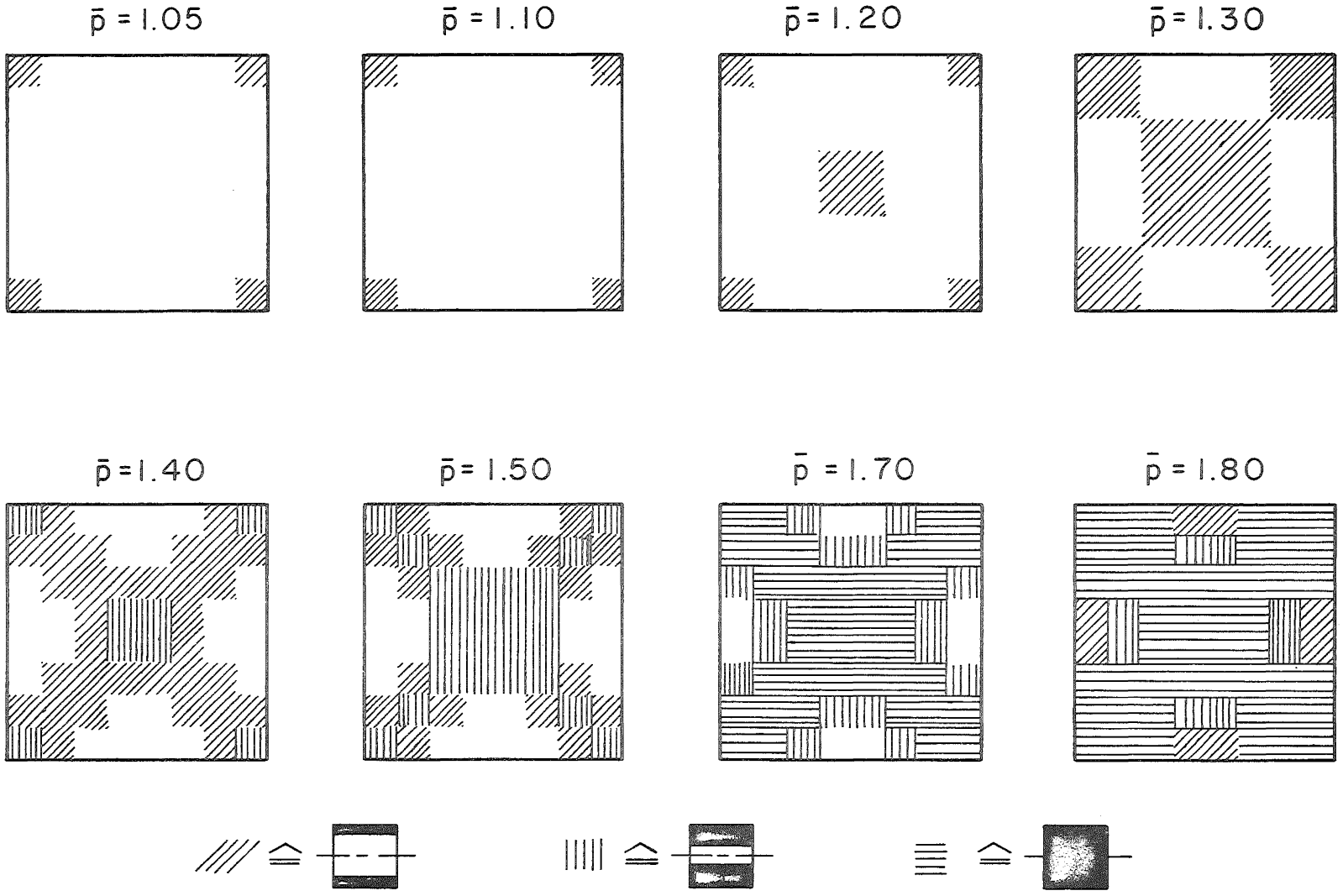

Fig. 14 Progression of Yielded Regions - Simply Supported Square Plate

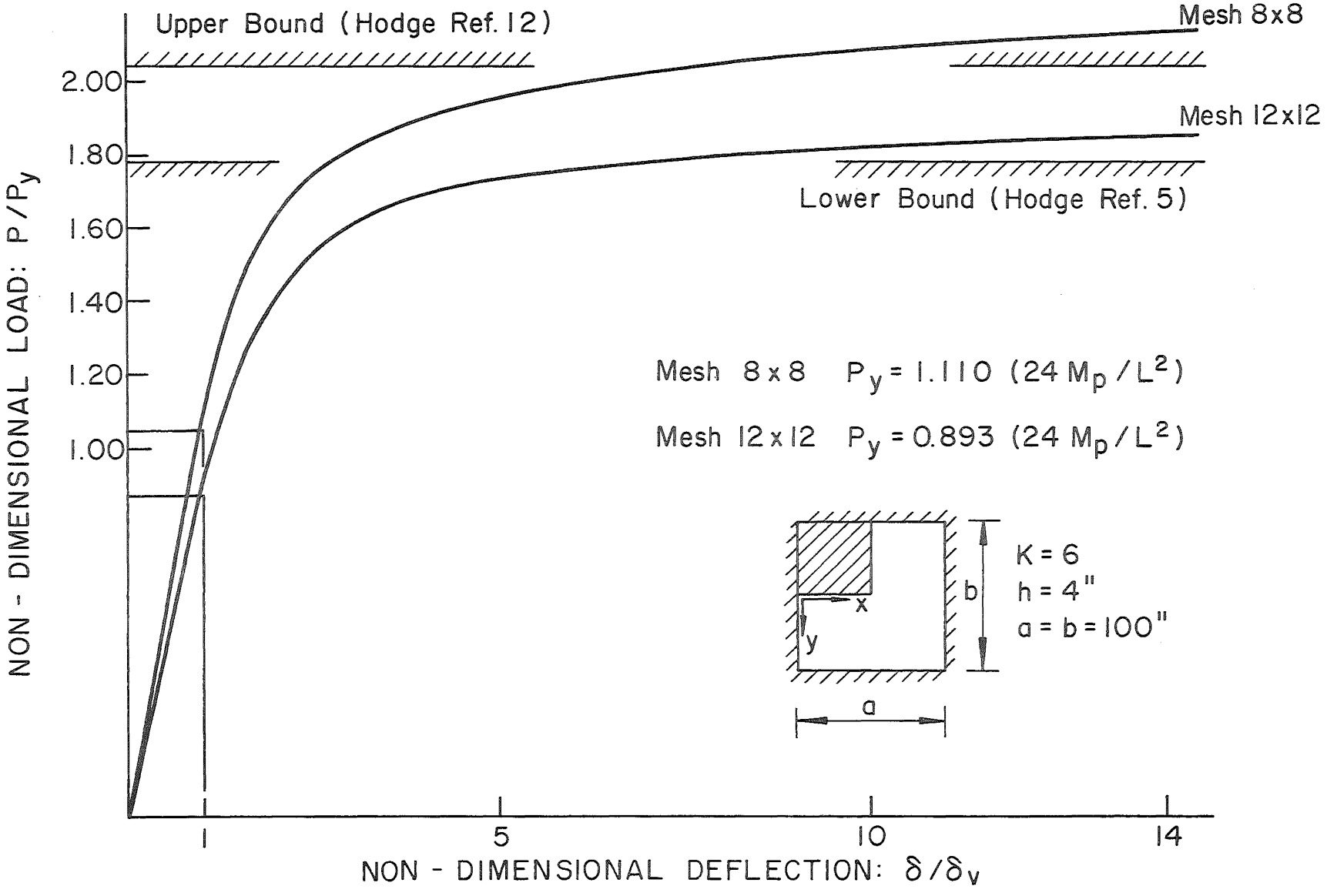

Fig. 15 Load-Deflection Curve at Center of Clamped Square Plate

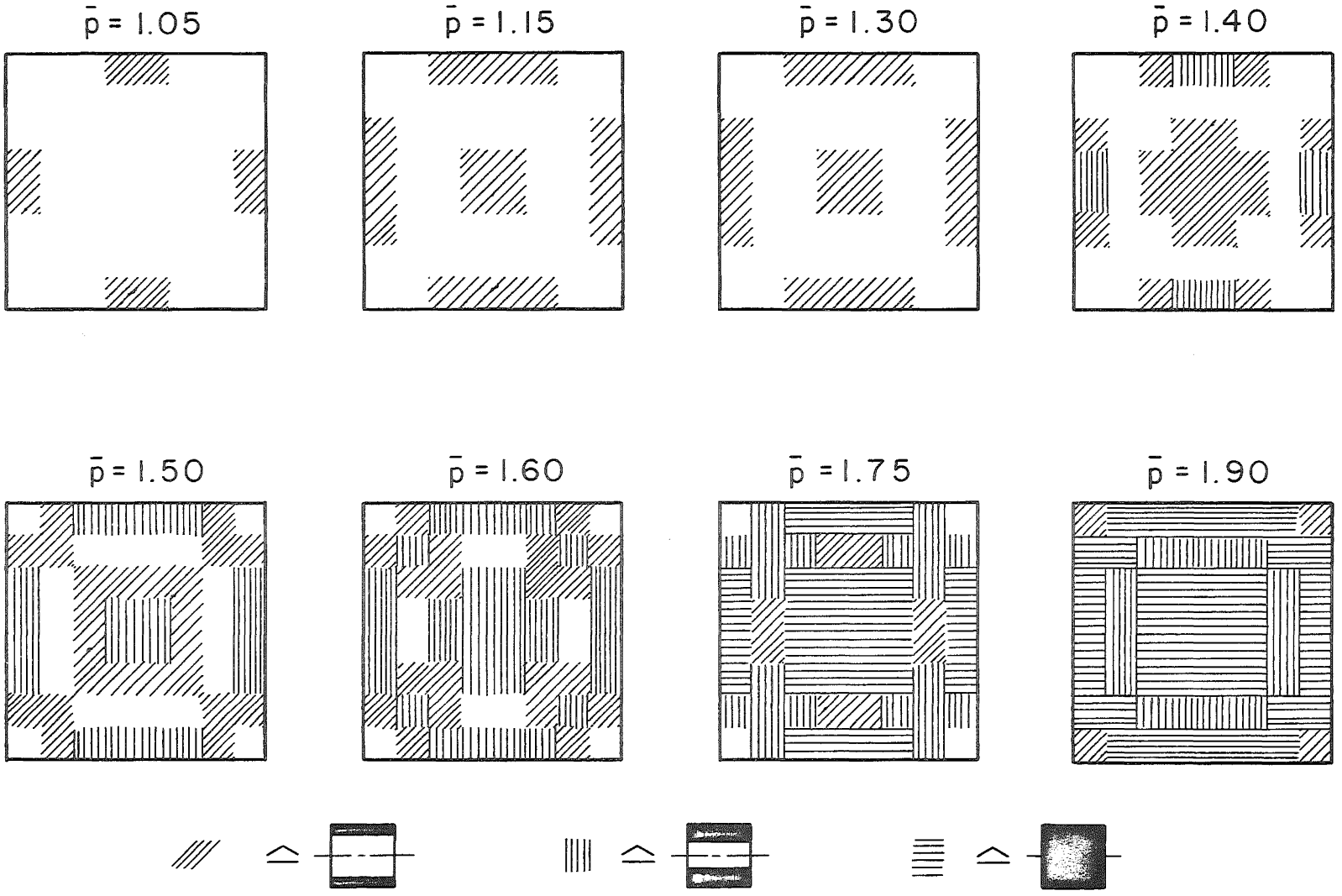

Fig. 16 Progression of Yielded Regions - Clamped Square Plate

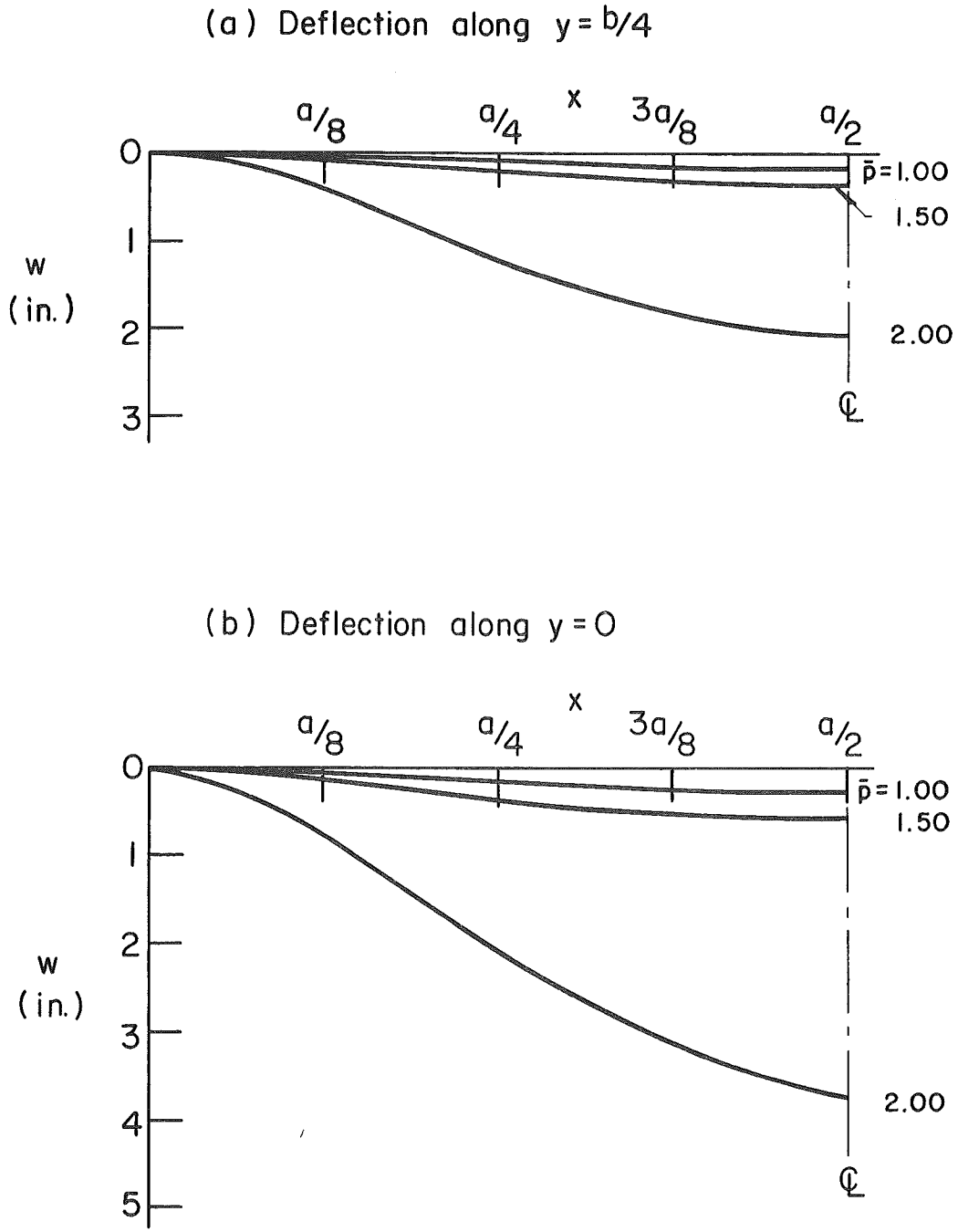

Fig. 17 Typical Displacement Contours - Clamped Plate

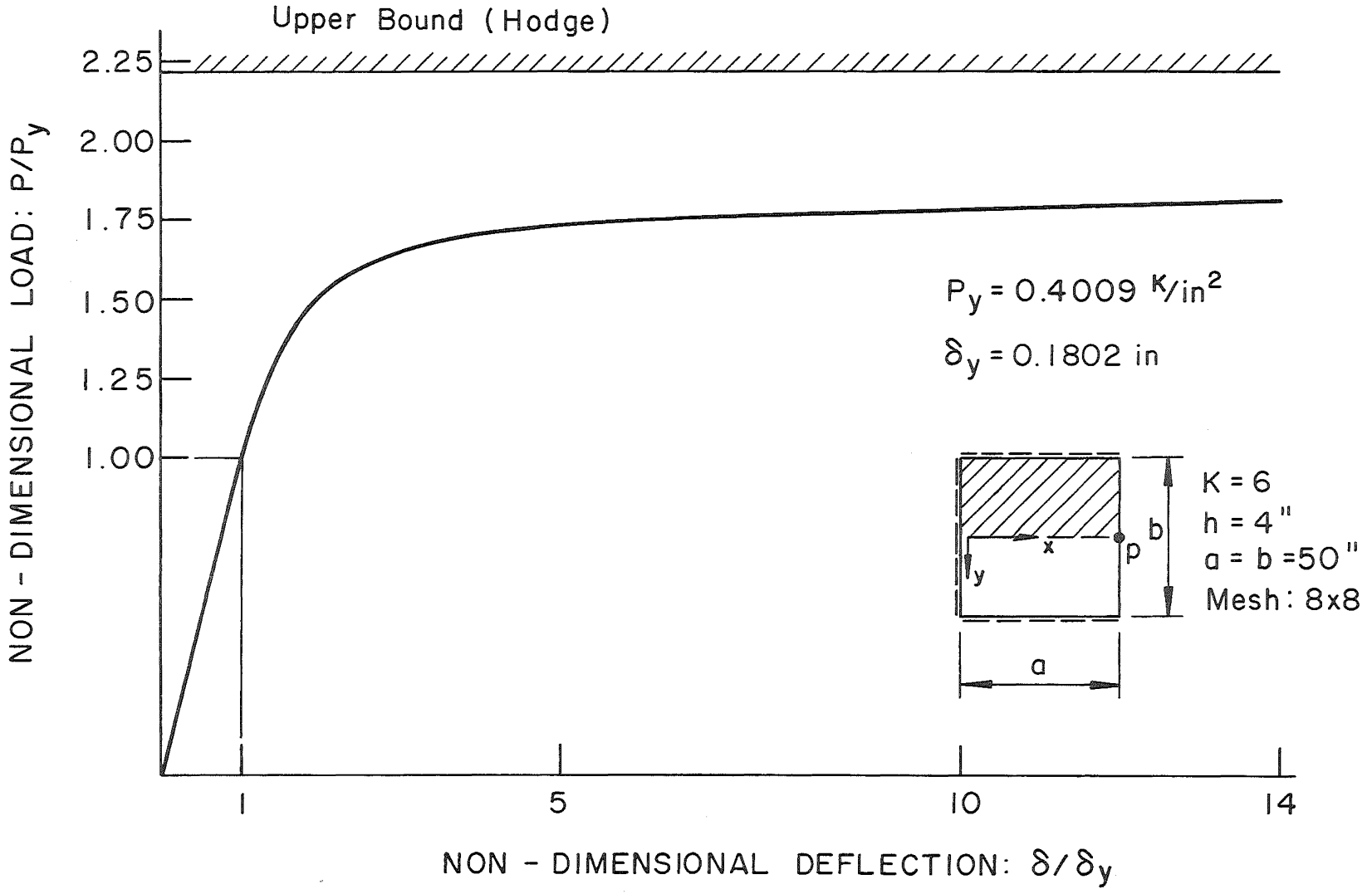

Fig. 18 Load-Deflection Curve at Point P of Plate with Three Simple Supports and One Free Edge

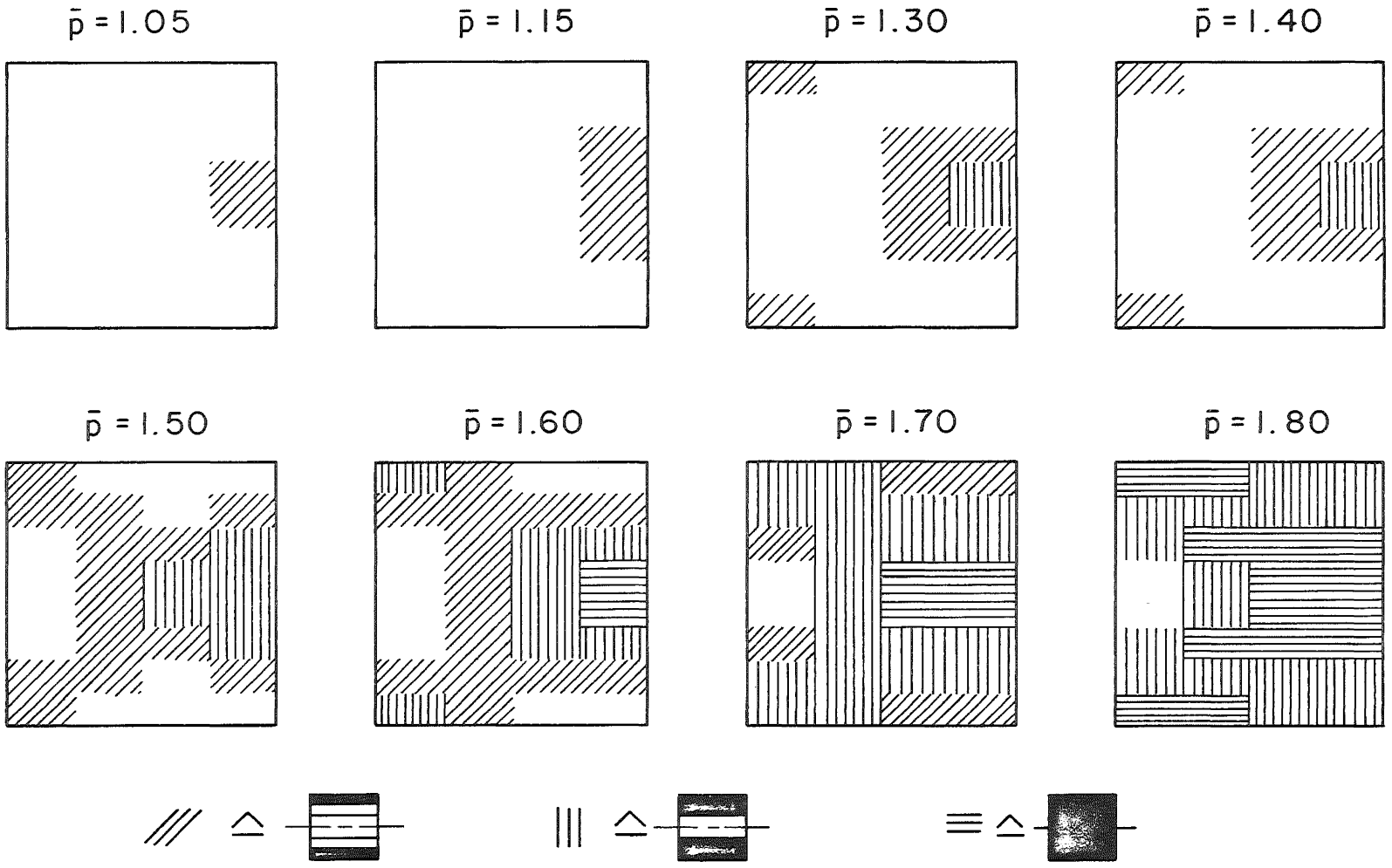

Fig. 19 Progression of Yielded Regions - Plate with Three Simple Supports and One Free Edge

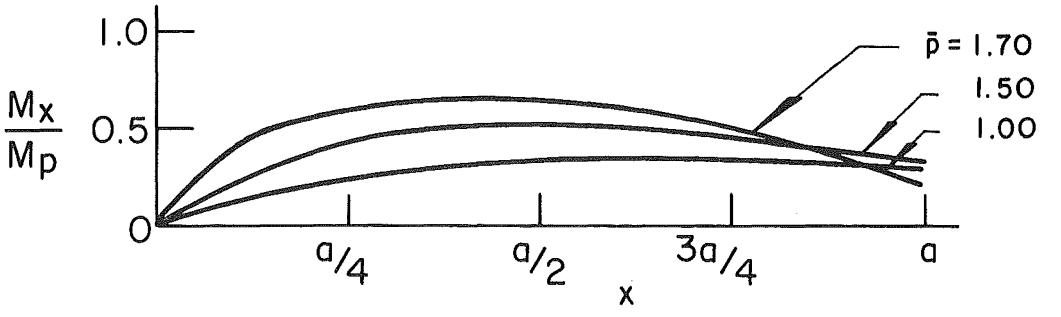

Bending Moment M_x along x-Axis

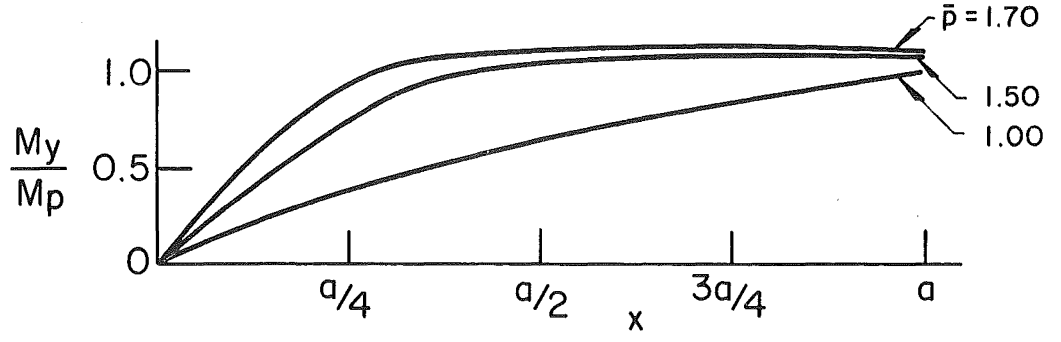

Bending Moment M_y along x-Axis

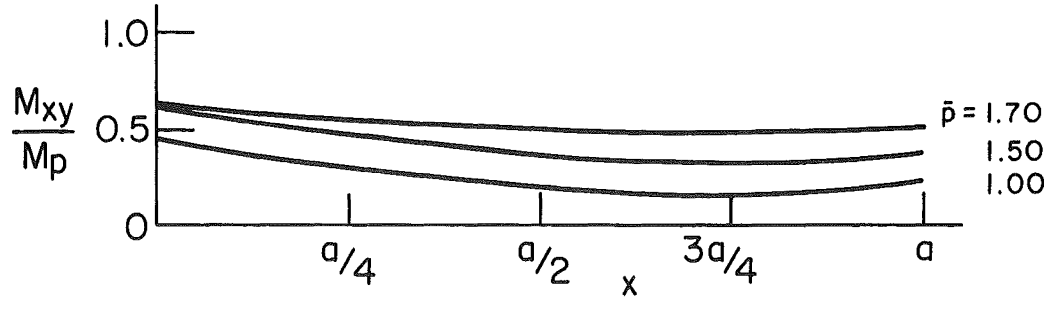

Twisting Moment M_{xy} along $y = 7/16\ b$

Fig. 20 Redistribution of Moments due to Plastic Flow - Plate with Three Simple Supports and One Free Edge

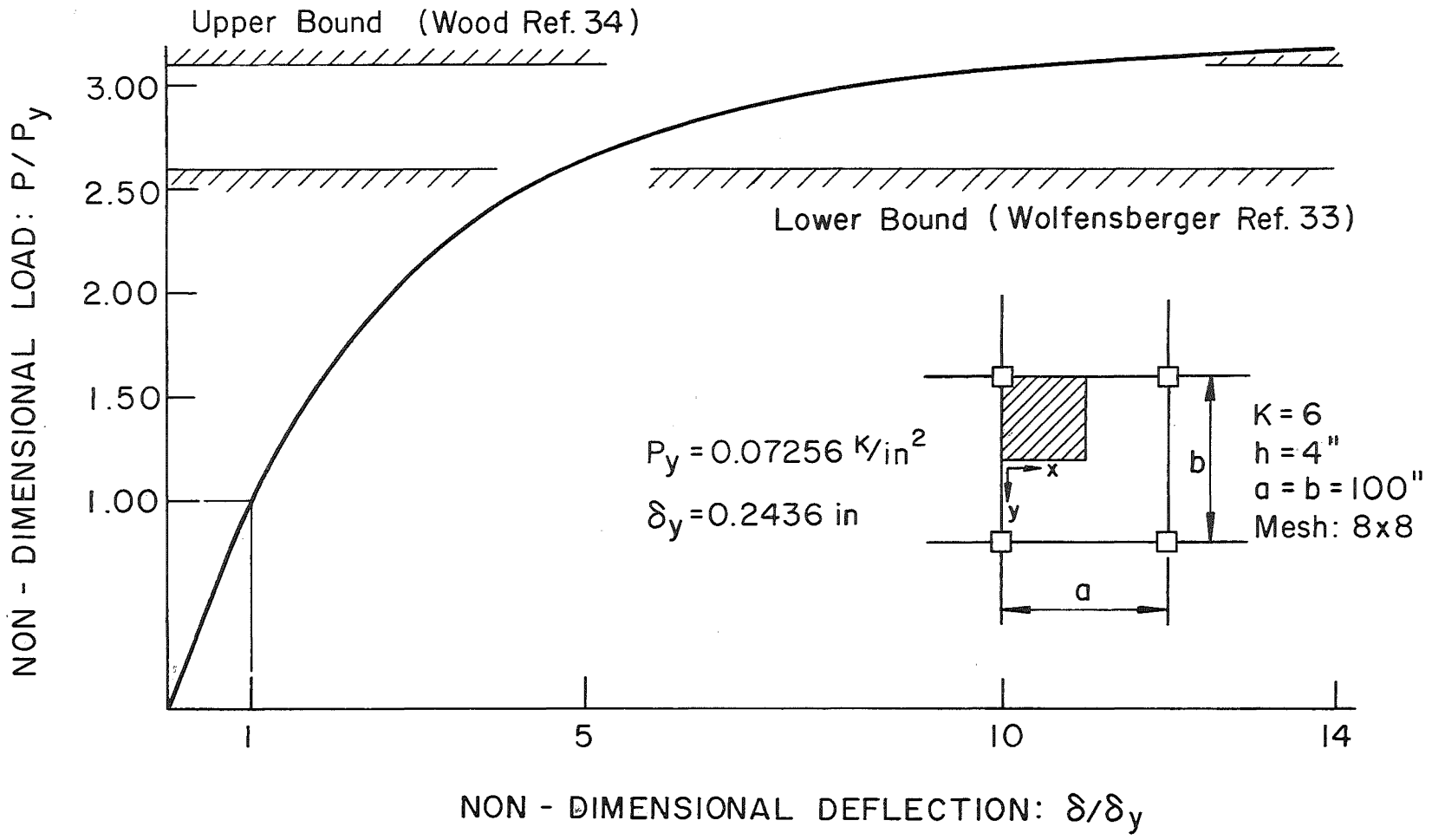

Fig. 21 Load-Deflection Curve at Center of Flat Slab Panel

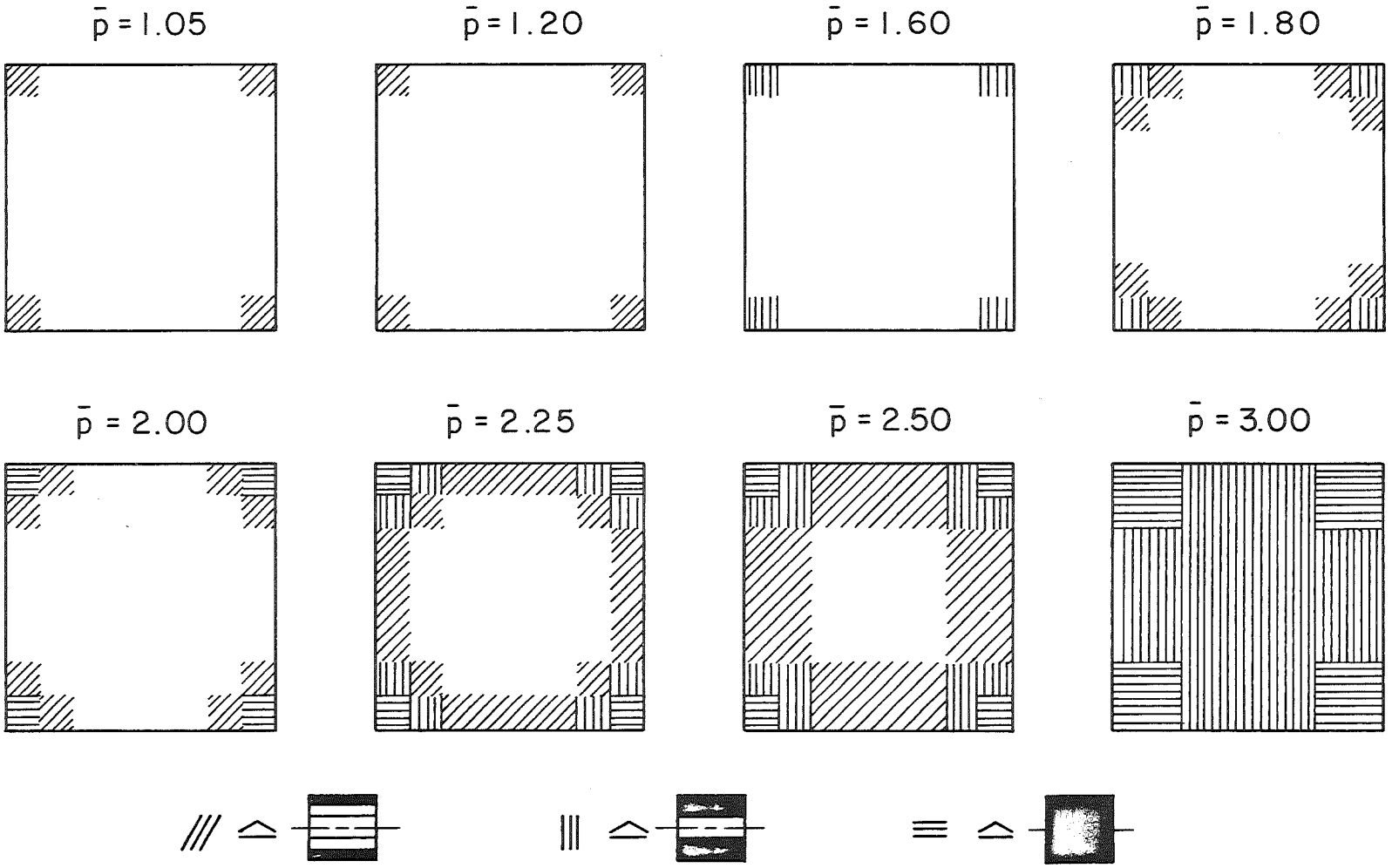

Fig. 22 Progression of Yielded Regions - Flat Slab Panel

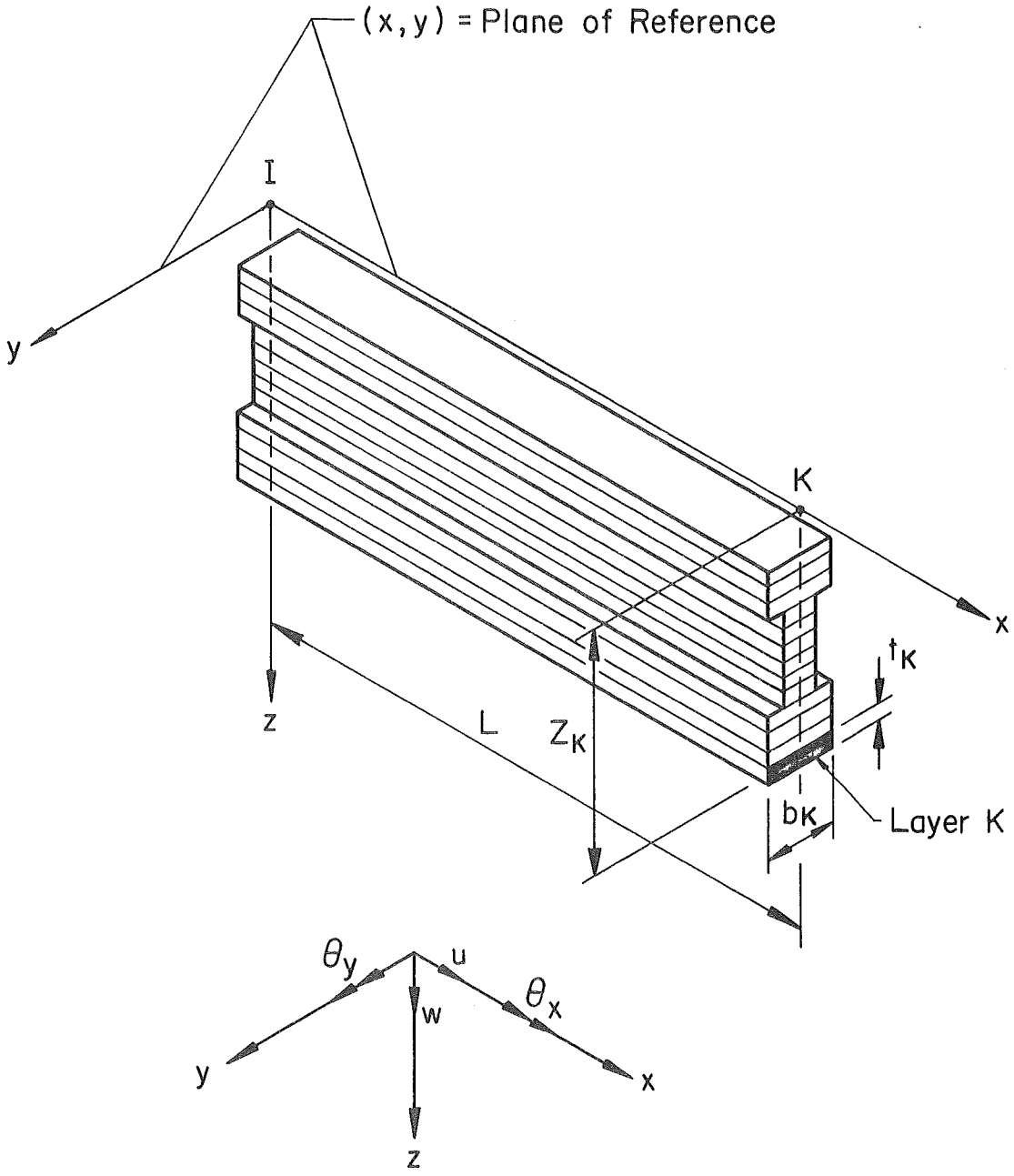

Fig. 23 Layered Finite Beam Element for Elastic-Plastic Analysis of Stiffened Plates

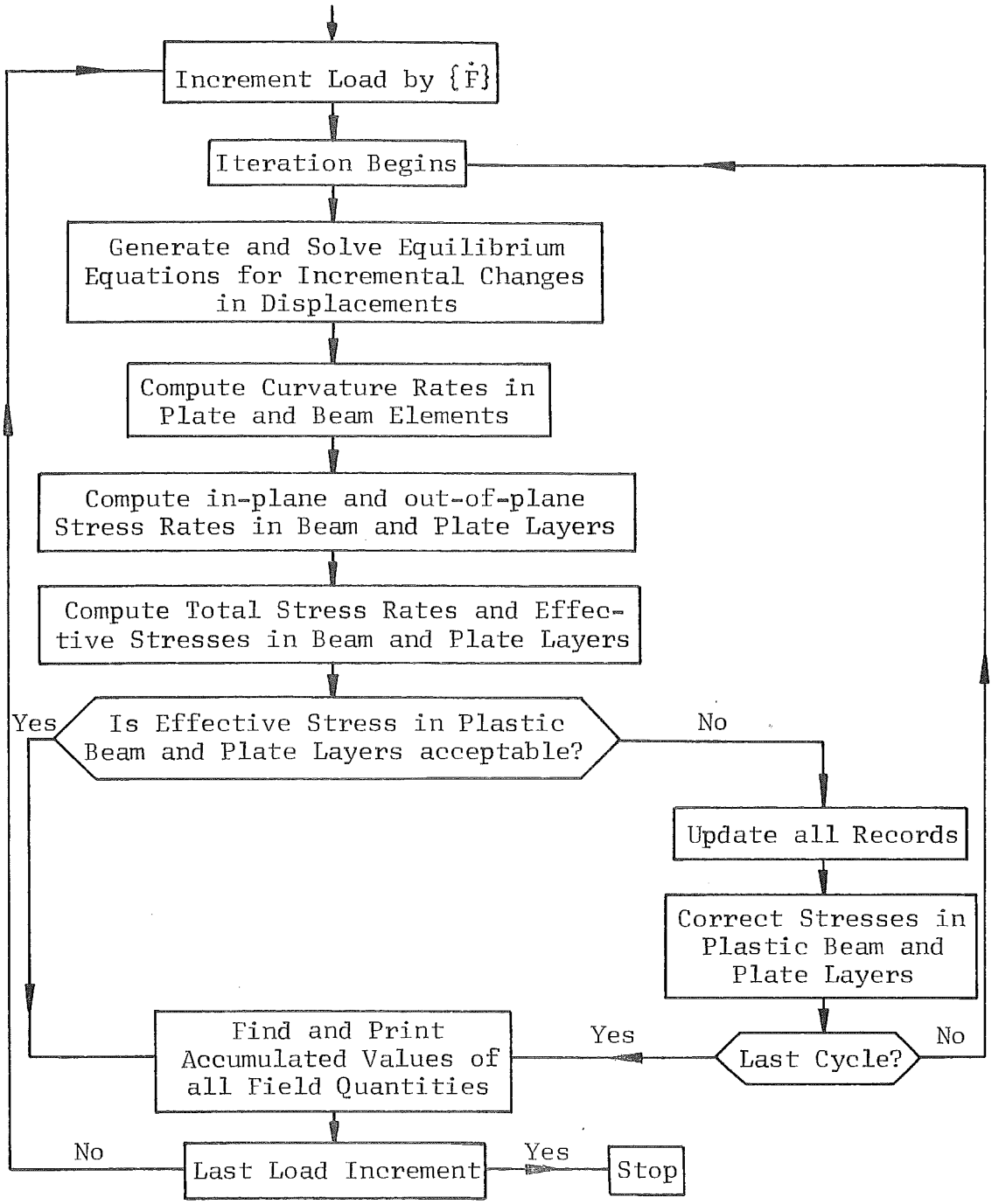

Fig. 24 Flow Diagram for Elastic-Plastic Eccentrically Stiffened Plate Analysis

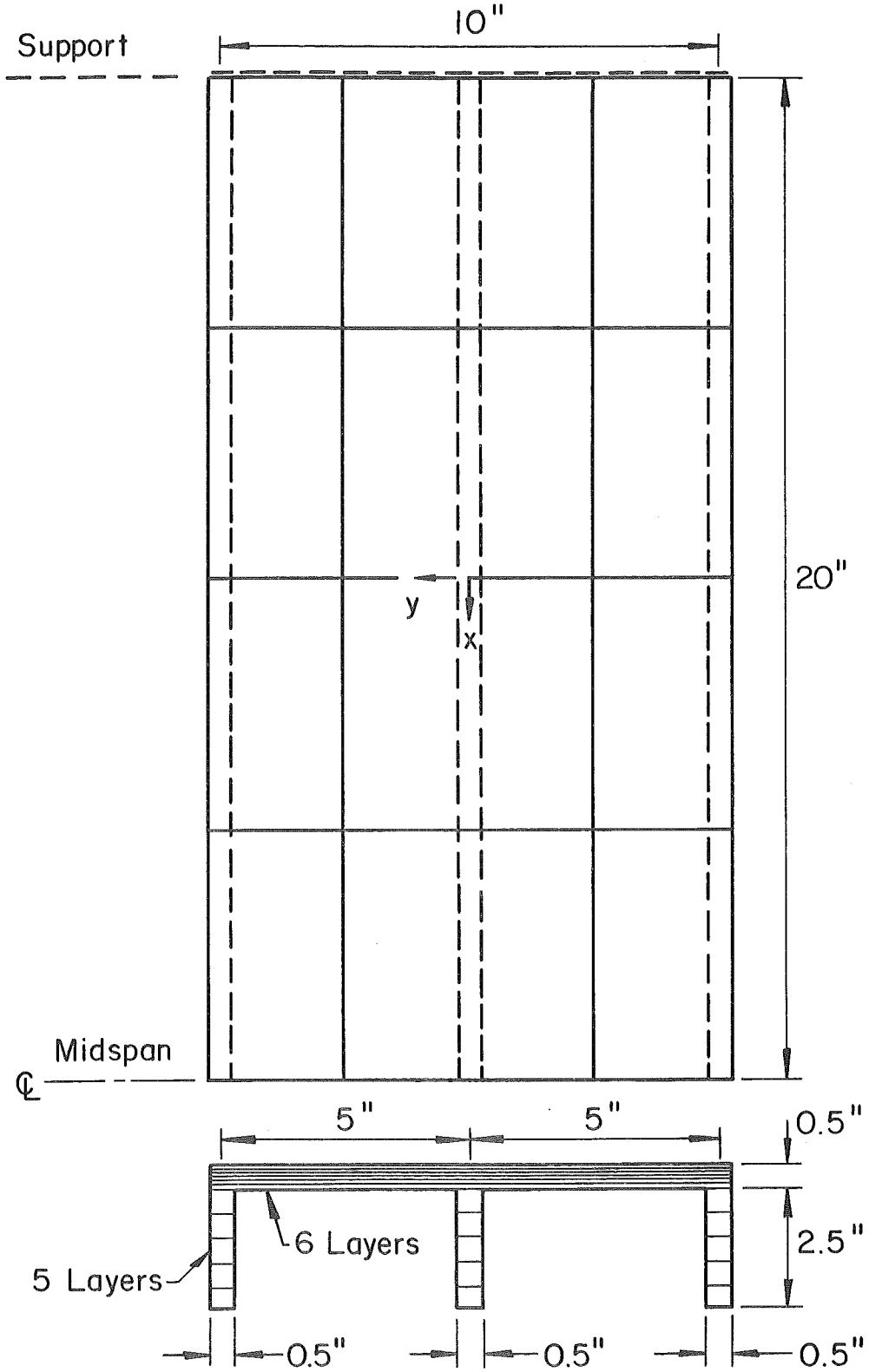

Fig. 25 Dimensions of Three-Beam Bridge Model

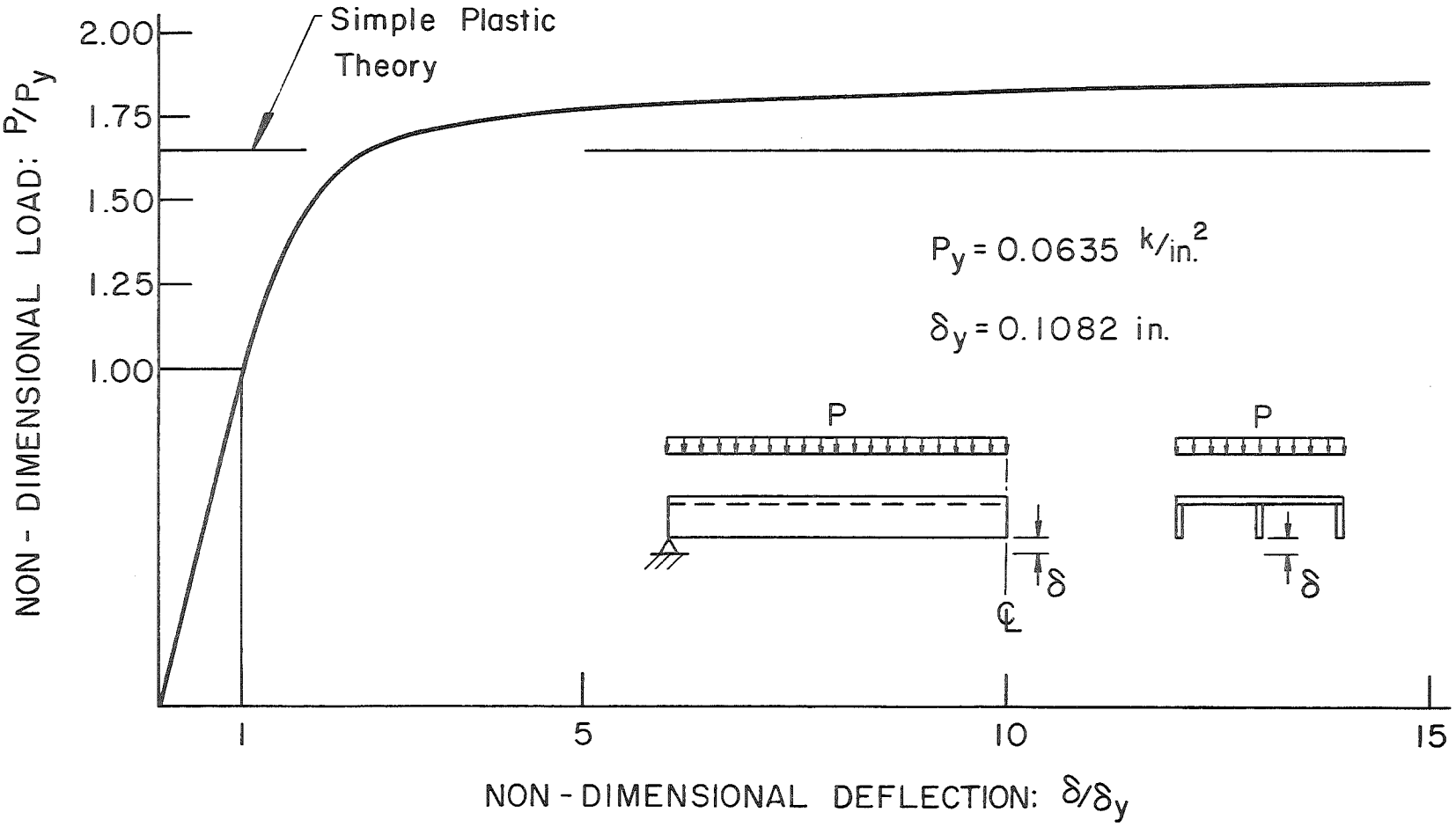

Fig. 26 Load-Deflection Curve at Center Point of Simply Supported Three-Beam Bridge Model

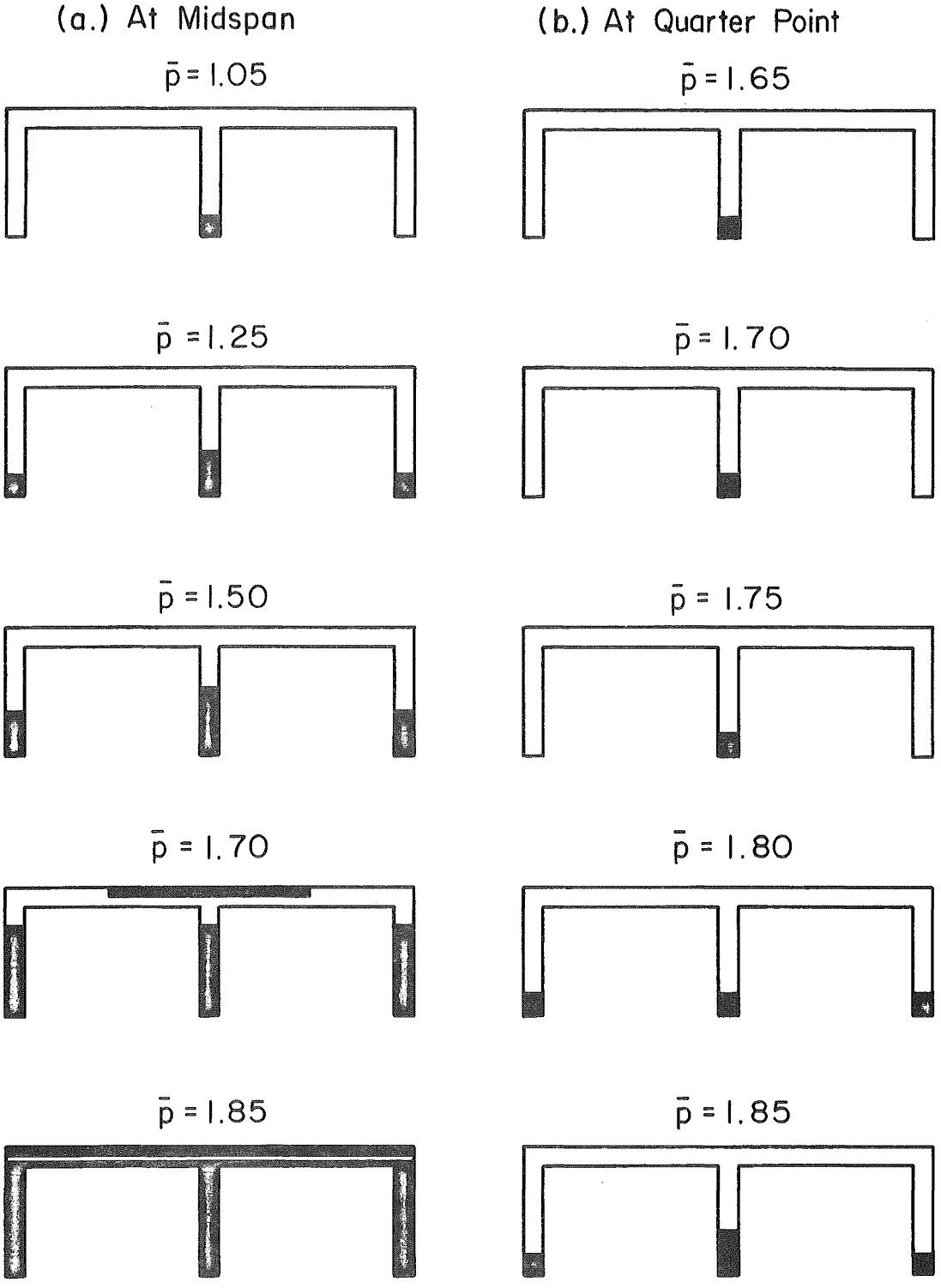

Fig. 27 Progression of Yielded Regions through Cross Section - Simply Supported Three-Beam Bridge Model

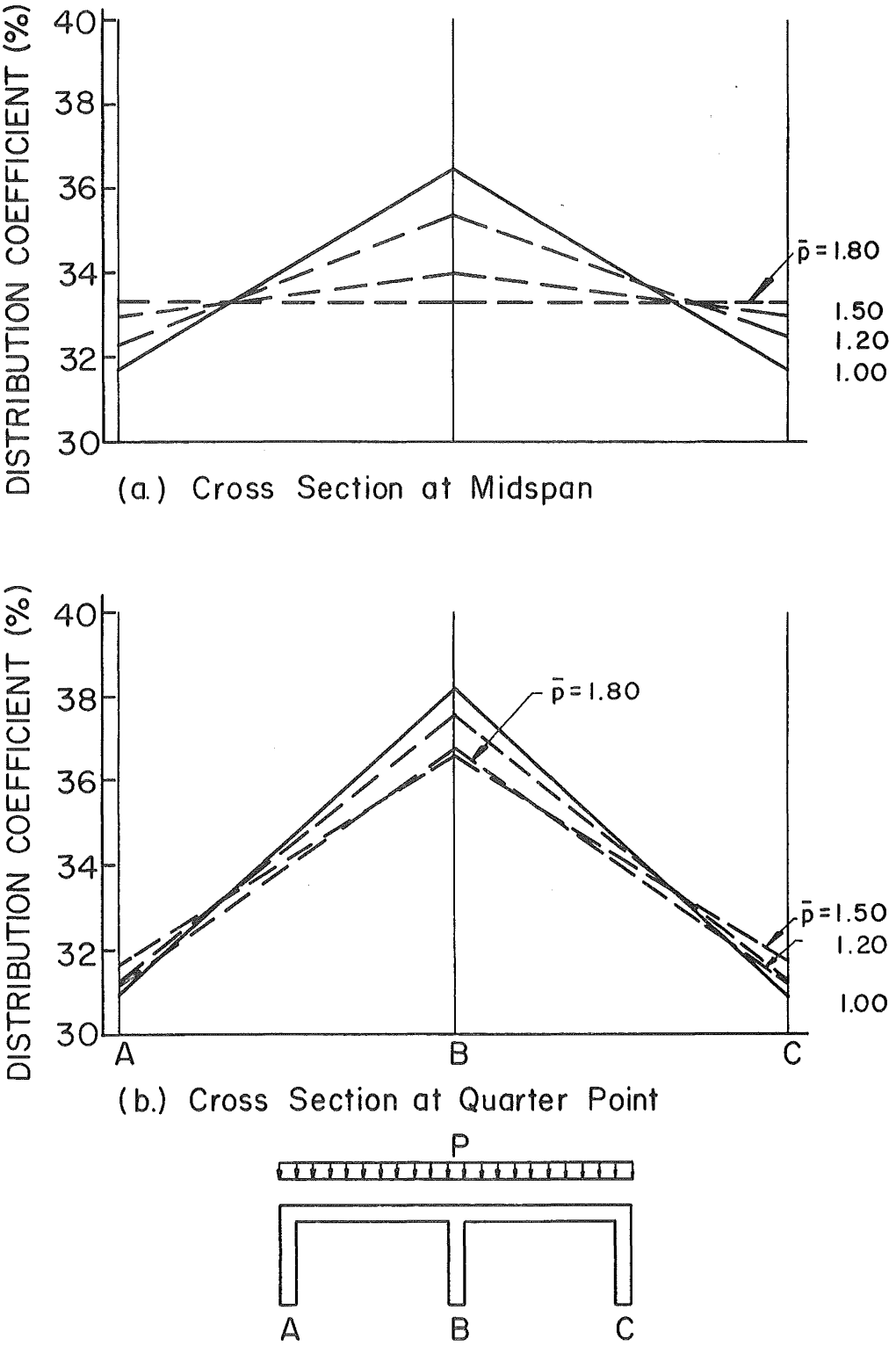

Fig. 28 Inelastic Lateral Distribution of Load - Simply Supported Three-Beam Bridge Model

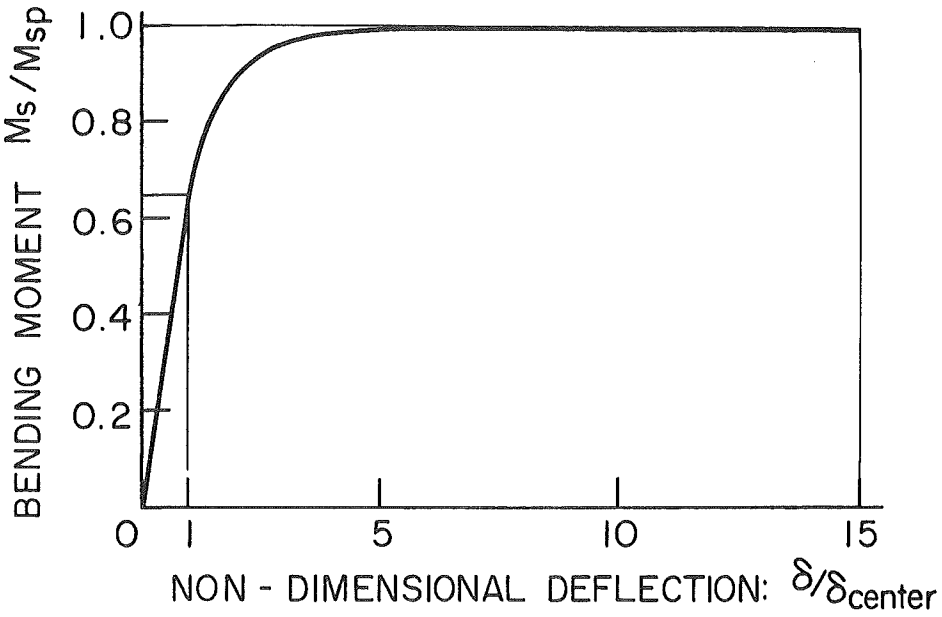

(a.) Center Beam - Midspan

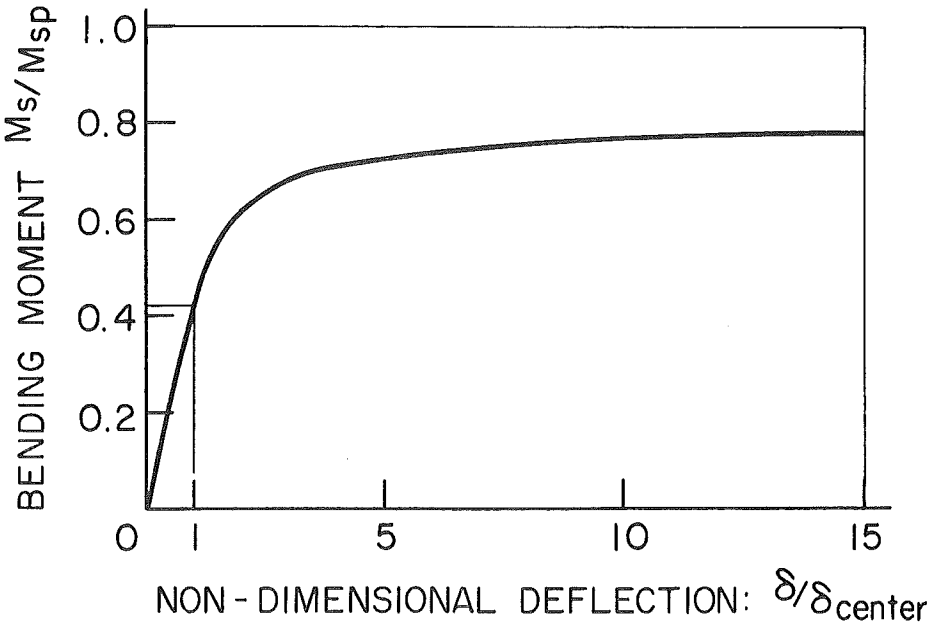

(b.) Center Beam - Quarter Point

Fig. 29 Bending Moment in Center Beam versus Deflection - Simply Supported Three-Beam Bridge Model

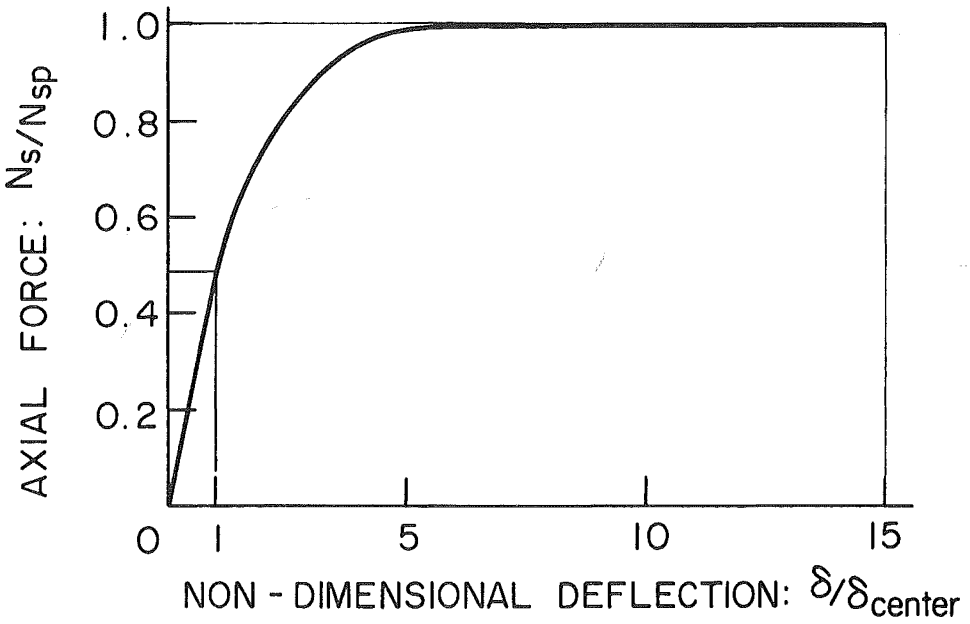

(a.) Center Beam - Midspan

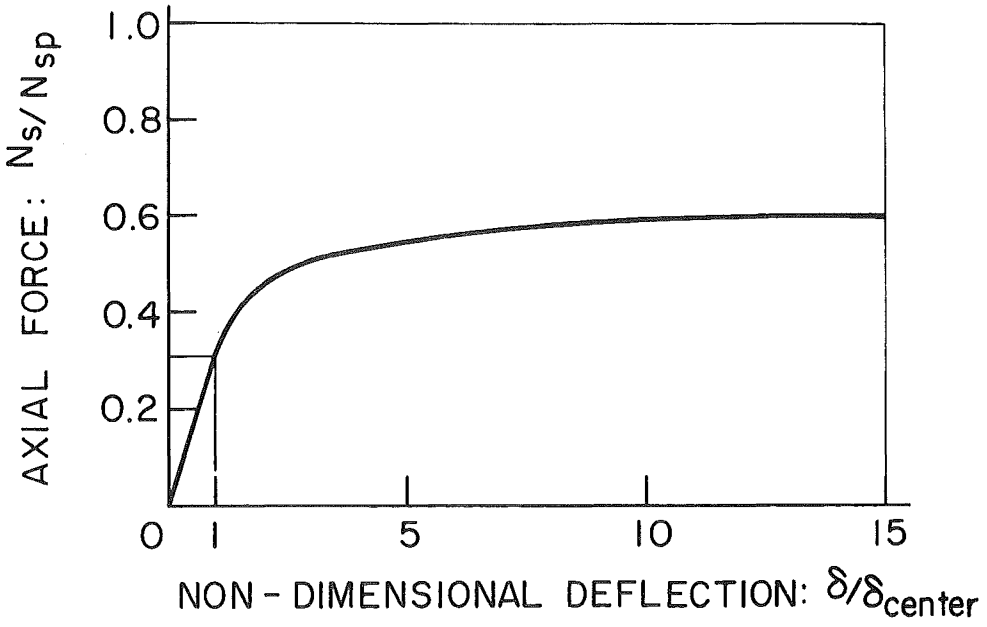

(b.) Center Beam - Quarter Point

Fig. 30 Axial Force in Center Beam versus Deflection - Simply Supported Three-Beam Bridge Model

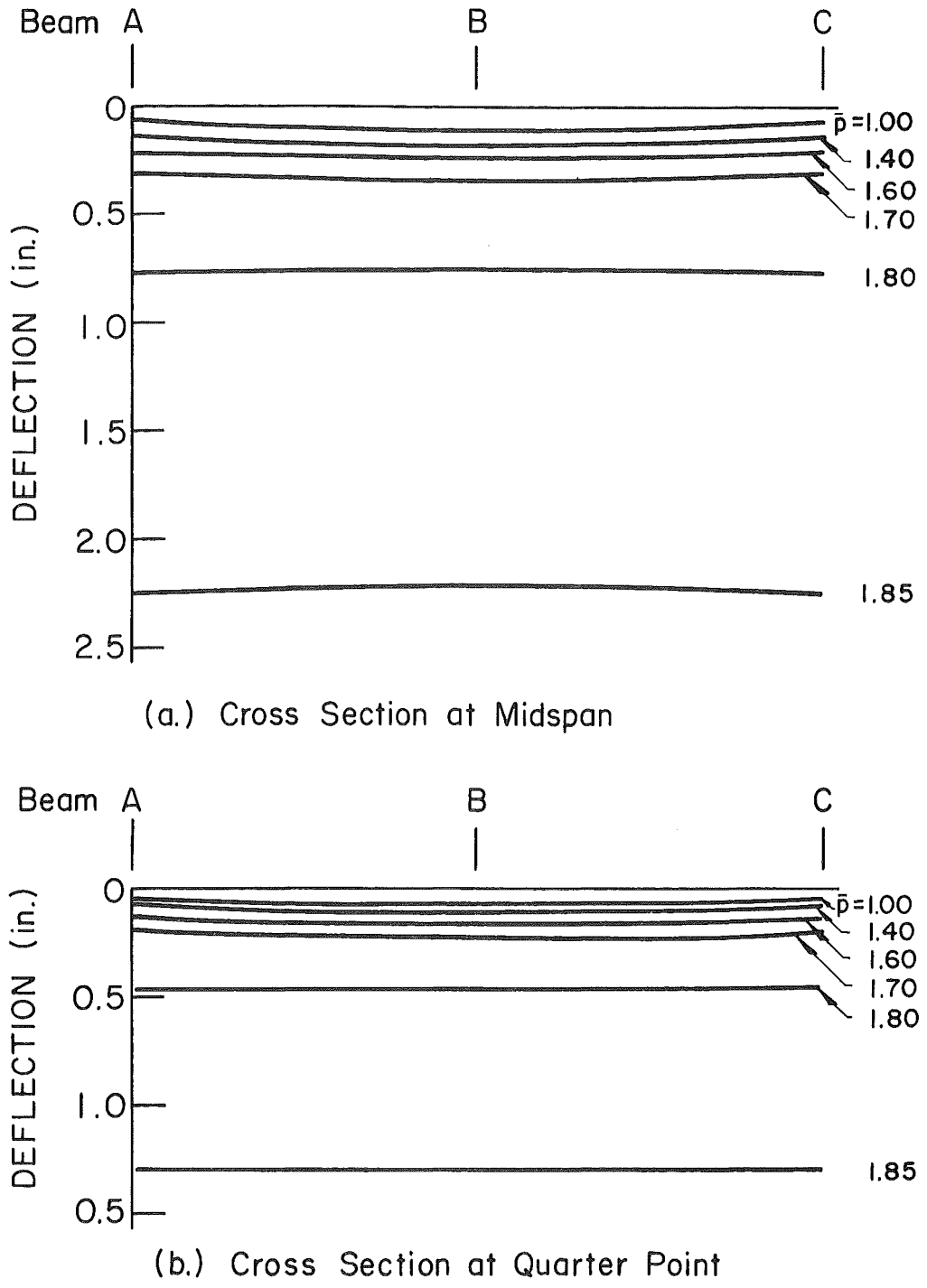

Fig. 31 Transverse Deflection Profiles - Simply Supported Three-Beam Bridge Model

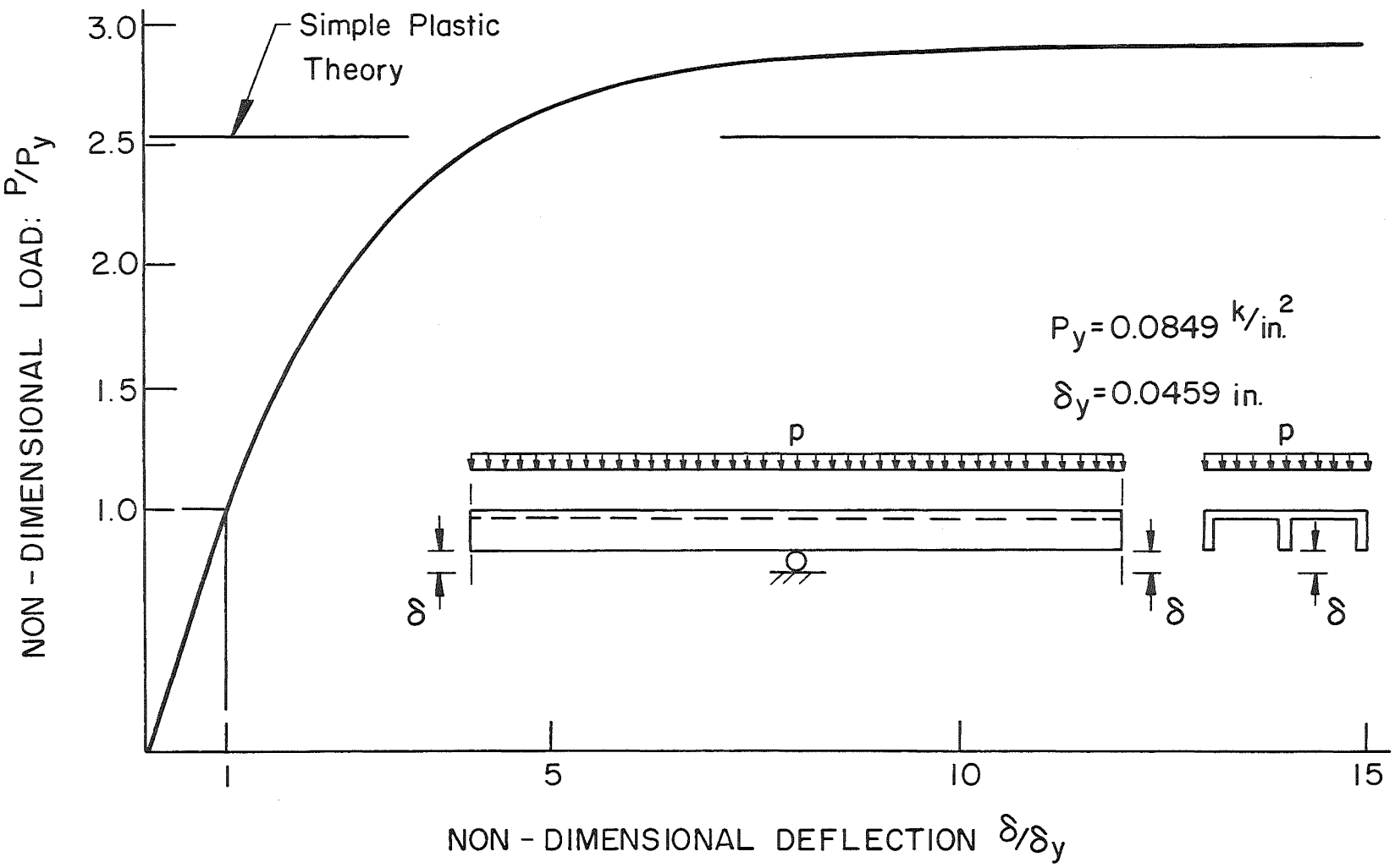

Fig. 32 Load-Deflection Curve at Center Point of Continuous Three-Beam Bridge Model

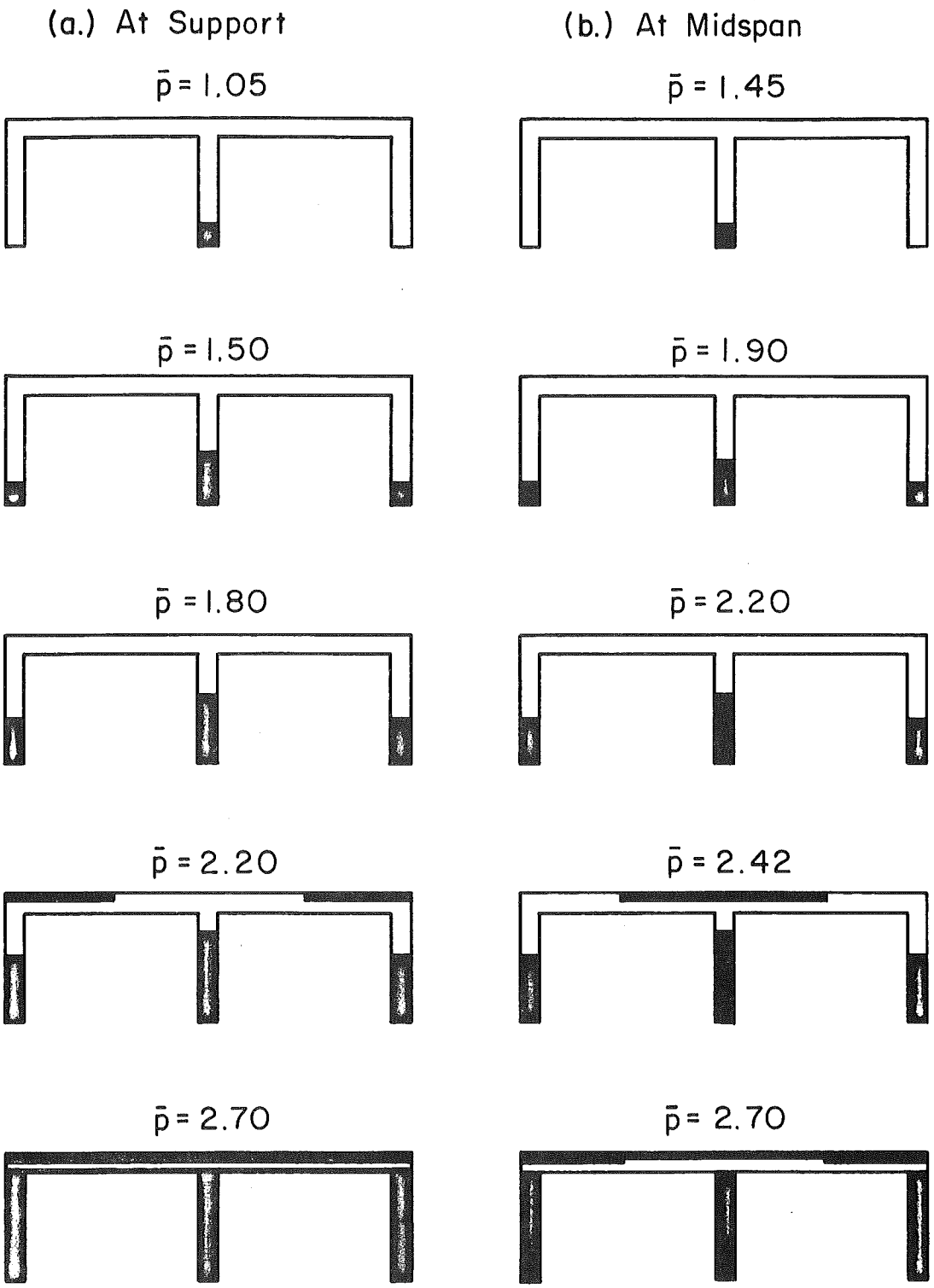

Fig. 33 Progression of Yielded Regions through Cross Section - Continuous Three-Beam Bridge Model

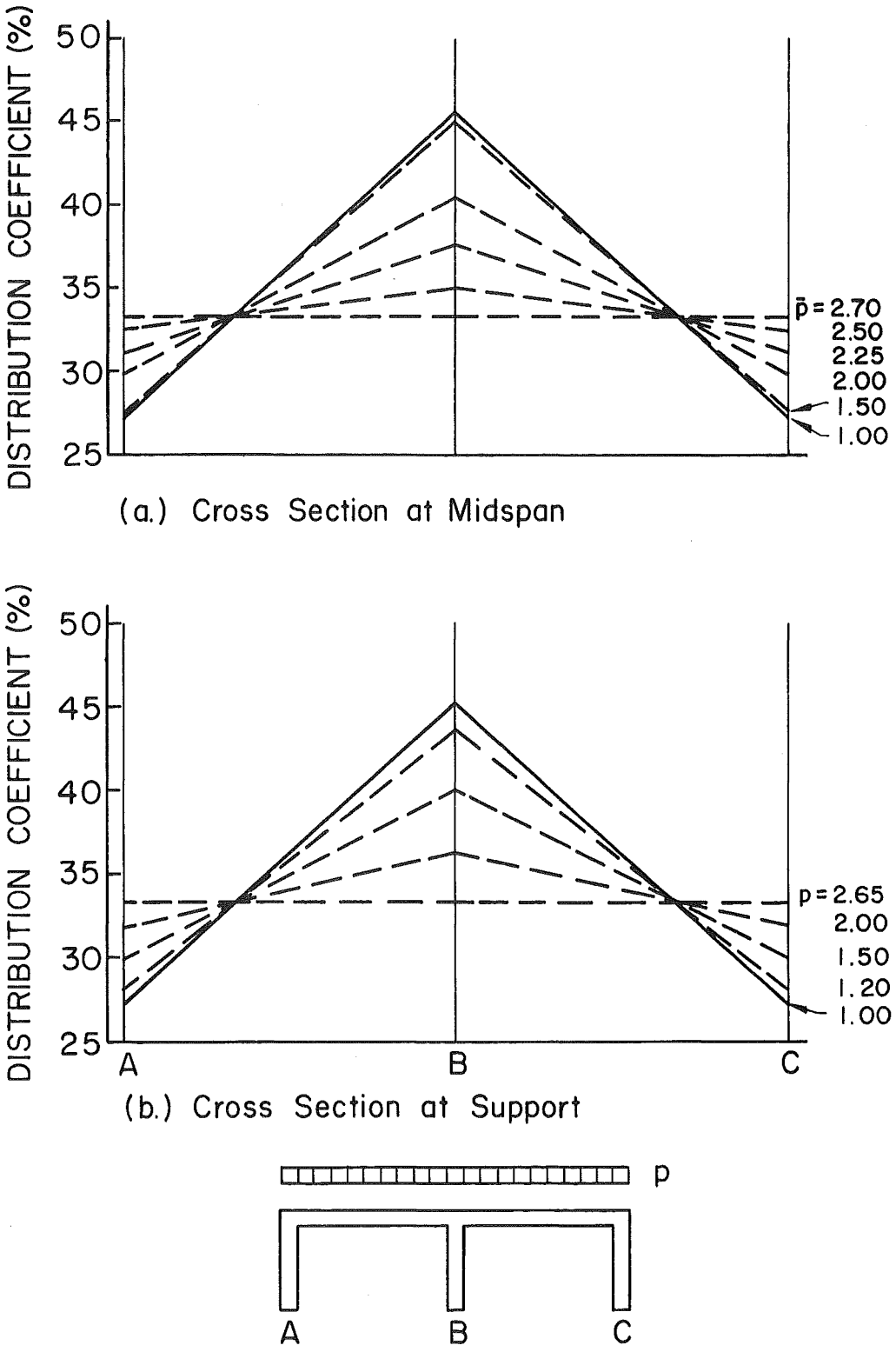

Fig. 34 Inelastic Lateral Distribution of Load - Continuous Three-Beam Bridge Model

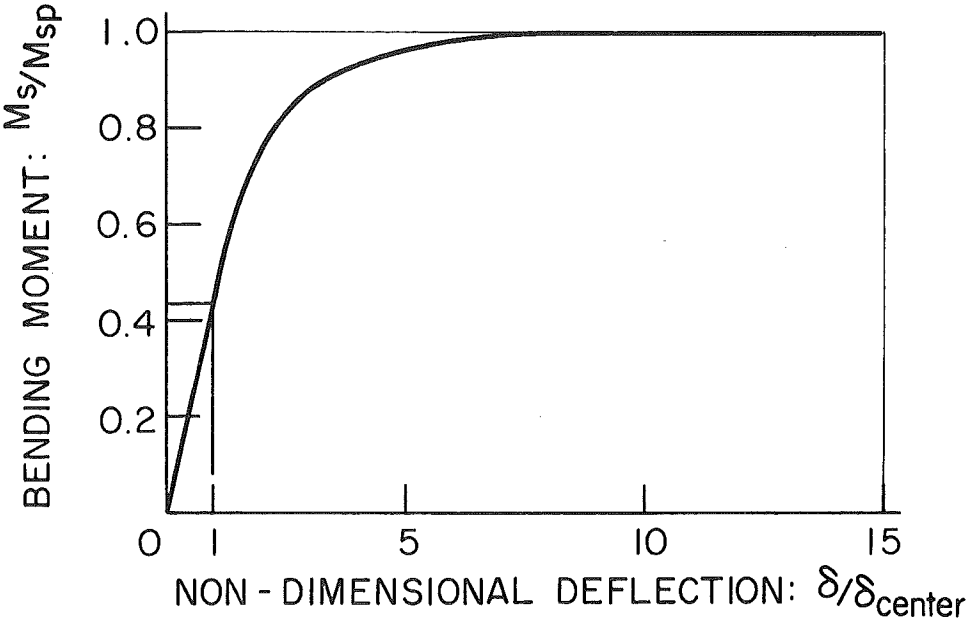

(a.) Center Beam - Midspan

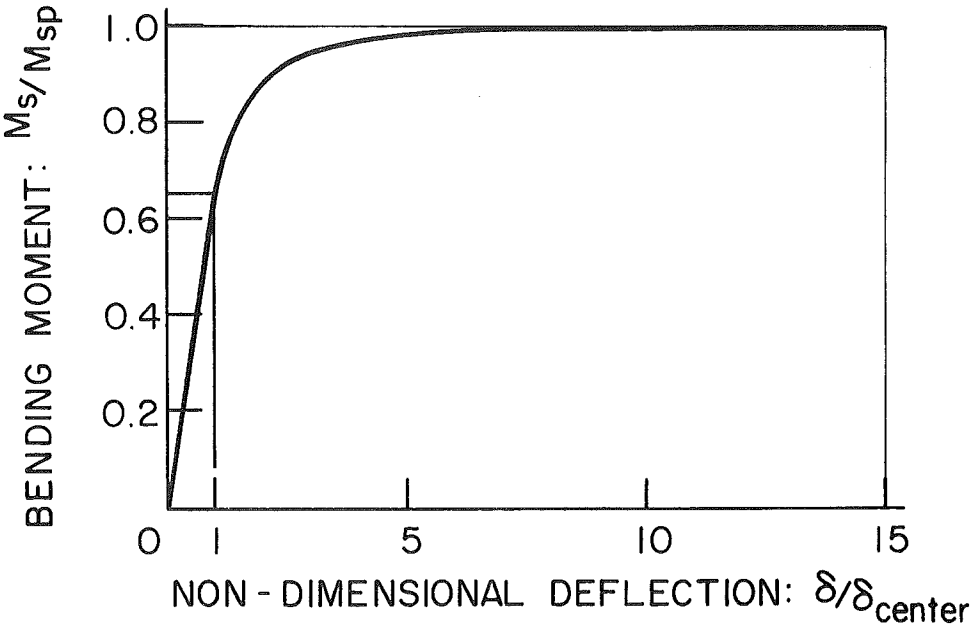

(b.) Center Beam - Support

Fig. 35 Bending Moment in Center Beam versus Deflection - Continuous Three-Beam Bridge Model

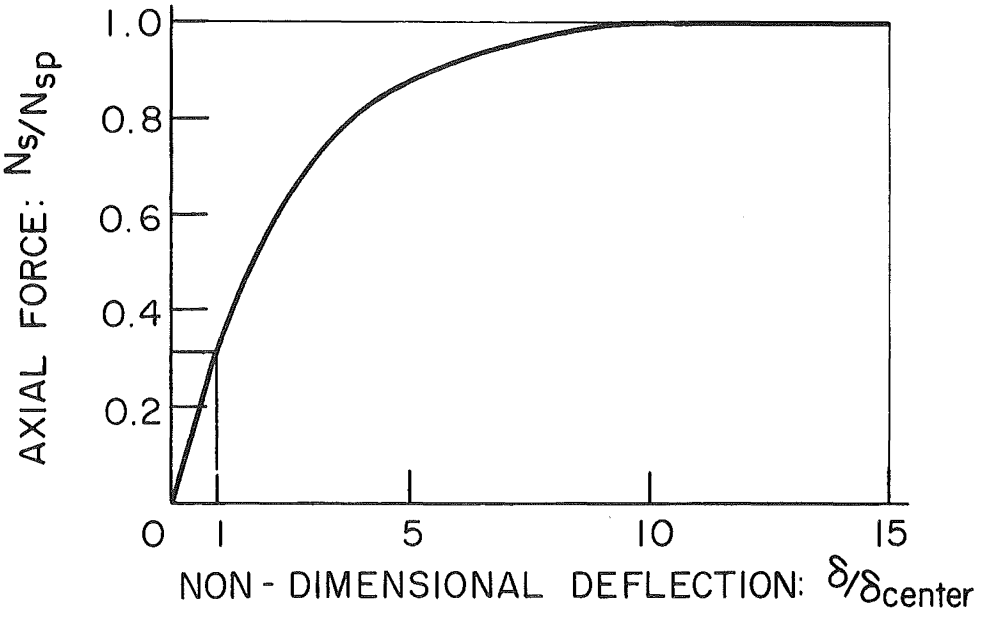

(a.) Center Beam - Midspan

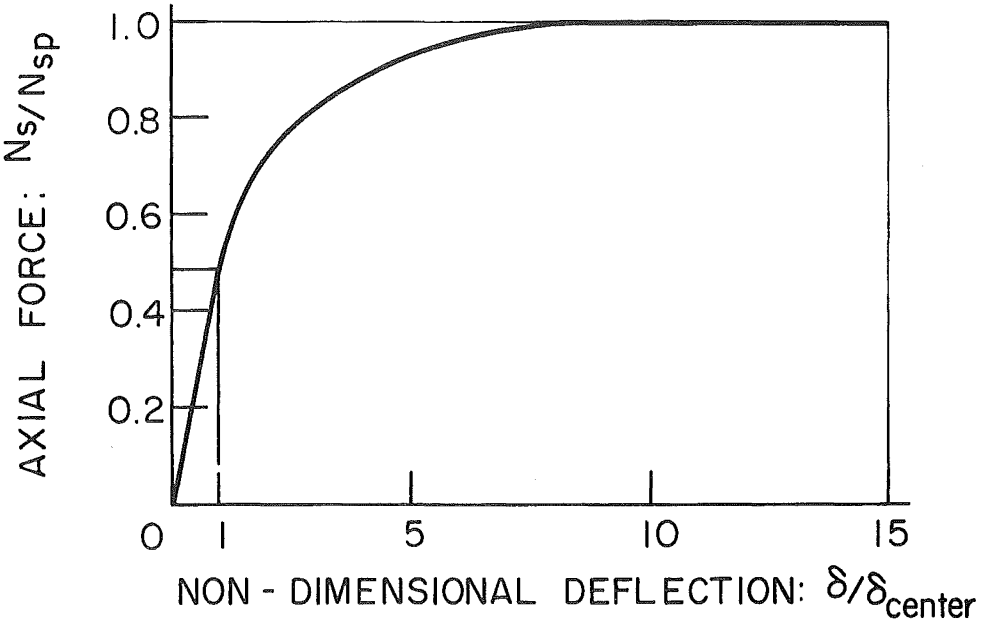

(b.) Center Beam - Support

Fig. 36 Axial Force in Center Beam versus Deflection - Continuous Three-Beam Bridge Model

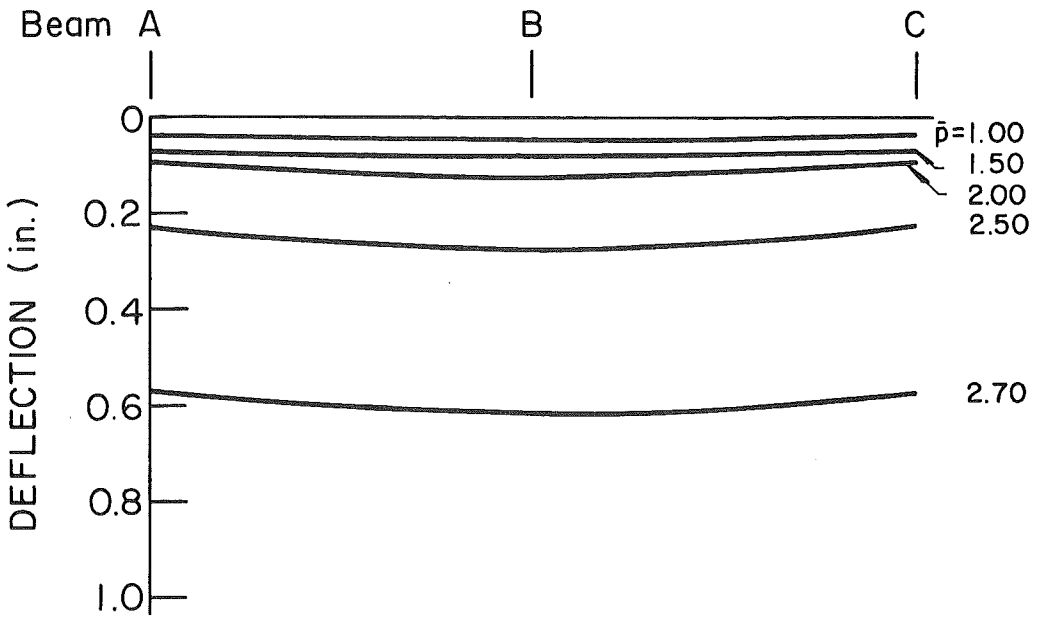

(a.) Cross Section at Midspan

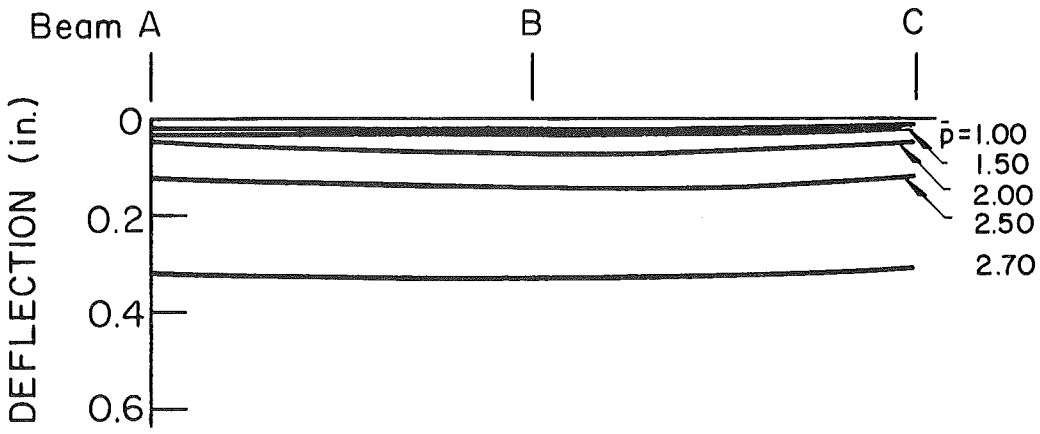

(b.) Cross Section at Quarter Point

Fig. 37 Transverse Deflection Profiles - Continuous Three-Beam Bridge Model

7. REFERENCES

1. American Concrete Institute
   BUILDING CODE REQUIREMENTS FOR REINFORCED CONCRETE, (ACI 318-63), Detroit, Michigan, 1963.

2. Anand, S. C., Lee, S. L., and Rossow, E. C.
   FINITE ELEMENT ANALYSIS OF ELASTIC-PLASTIC PLANE STRESS PROBLEMS BASED UPON TRESCA YIELD CONDITION, Ingenieur-Archiv, 39. Band, Zweites Heft, 1970.

3. Armen, H., Pifko, A. B., Levine, H. S., and Isakson, G.
   PLASTICITY, Chapter 8 of the Conference on Finite Element Techniques, University of Southampton, April 1970.

4. Armen, H., Pifko, A. B., and Levine, H. S.
   FINITE ELEMENT ANALYSIS OF STRUCTURES IN THE PLASTIC RANGE, NASA Report CR1649, Washington, D.C., February 1971.

5. Bach, C.
   ELASTIZITAT UND FESTIGKEIT, Third Edition, Julius Springer, Berlin, 1898.

6. Beedle, L. S.
   PLASTIC DESIGN OF STEEL FRAMES, John Wiley & Sons, New York, 1958.

7. Bhaumik, A. K. and Hanley, J. T.
   ELASTO-PLASTIC PLATE ANALYSIS BY FINITE DIFFERENCES, Journal of the Structural Division, ASCE, Vol. 93, ST5, October 1967.

8. Drucker, D. C., Greenberg, H. J., and Prager, W.
   THE SAFETY FACTOR FOR AN ELASTIC-PLASTIC BODY IN PLANE STRAIN, Journal of Applied Mechanics, 18, 1951.

9. Drucker, D. C.
A MORE FUNDAMENTAL APPROACH TO PLASTIC STRESS-STRAIN RELATIONS, Proceedings, First U. S. National Congress of Applied Mechanics, New York, 1952.

10. Felippa, C. A.
REFINED FINITE ELEMENT ANALYSIS OF LINEAR AND NONLINEAR TWO-DIMENSIONAL STRUCTURES, Report No. SESM 66-22, University of California, October 1966.

11. Hodge, P. G.
PLASTIC ANALYSIS OF STRUCTURES, McGraw-Hill, New York, 1959.

12. Hodge, P. G. and Belytscho, T.
NUMERICAL METHODS FOR THE LIMIT ANALYSIS OF PLATES, Journal of Applied Mechanics, Vol. 35, December 1968.

13. Johansen, K. W.
THE ULTIMATE STRENGTH OF REINFORCED CONCRETE SLABS, Final Report, Third Congress, IVBH, Liege, Belgium, 1948.

14. Koopman, D. C. and Lance, R. H.
ON LINEAR PROGRAMMING AND PLASTIC LIMIT ANALYSIS, Journal of the Mechanics and Physics of Solids, Vol. 12, London, 1964.

15. Kulicki, J. M. and Kostem, C. N.
NONLINEAR ANALYSIS OF CONCRETE FLEXURAL MEMBERS, Preprints of the International Conference on the Planning and Design of Tall Buildings, Vol. DS, Lehigh University, August 1972.

16. Kulicki, J. M. and Kostem, C. N.
THE INELEASTIC ANALYSIS OF REINFORCED AND PRESTRESSED CONCRETE BEAMS, Fritz Engineering Laboratory Report No. 378B.1, Lehigh University, November 1972.

17. Kulicki, J. M. and Kostem, C. N.
USER'S MANUAL FOR PROGRAM BEAM, Fritz Engineering Laboratory Report No. 378B.2, Lehigh University, February 1973.

18. Kulicki, J. M. and Kostem, C. N.
APPLICATIONS OF THE FINITE ELEMENT METHOD TO INELASTIC BEAM-COLUMN PROBLEMS, Fritz Engineering Laboratory Report No. 400.11, Lehigh University, March 1973.

19. Kulicki, J. M. and Kostem, C. N.
FURTHER STUDIES ON THE NONLINEAR FINITE ELEMENT ANALYSIS OF BEAMS, Fritz Engineering Laboratory Report No. 378A.5, Lehigh University, April 1973.

20. Lopez, L. A. and Ang, A. H. S.
FLEXURAL ANALYSIS OF ELASTIC-PLASTIC RECTANGULAR PLATES, Civil Engineering Studies, Structural Research Series No. 305, University of Illinois, Urbana, Illinois, May 1966.

21. Mendelson, A.
PLASTICITY: THEORY AND APPLICATION, The MacMillan Co., New York, 1968.

22. Neal, B. G.
THE PLASTIC METHODS OF STRUCTURAL ANALYSIS, John Wiley & Sons, New York, 1956.

23. Oden, T. J.
FINITE ELEMENT APPLICATIONS IN NONLINEAR STRUCTURAL ANALYSIS, Proceedings of the Symposium on Application of Finite Element Methods in Civil Engineering, Vanderbilt University, Nashville, Tennessee, November 1969.

24. Pope, G. G.
THE APPLICATION OF THE MATRIX DISPLACEMENT METHOD IN PLANE ELASTO-PLASTIC PROBLEMS, Proceedings of Conference on Matrix Methods in Structural Mechanics, Wright-Patterson Air Force Base, Ohio, 1965.

25. Popov, E. P., Khojasteh-Bakht, M. and Yaghami, S.
ANALYSIS OF ELASTIC-PLASTIC CIRCULAR PLATES, Journal of the Engineering Mechanics Division, ASCE, Vol. 93, No. EM6, December 1967.

26. Prager, W.
THE GENERAL THEORY OF LIMIT DESIGN, Proceedings, Eighth International Congress on Theory and Applied Mechanics, Istanbul, Vol. 2, 1952.

27. Ranaweera, M. P. and Leckie, F. A.
BOUND METHODS IN LIMIT ANALYSIS, Chapter 9 of the Conference on Finite Element Techniques, University of Southampton, April 1970.

28. Sawzuk, A. and Jaeger, T.
GRENZTRAGFAEHIGKEITS - THEORIE DER PLATTEN, Springer, Berlin, 1963.

29. Shull, H. E. and Hu, L. W.
LOAD CARRYING CAPACITIES OF SIMPLY SUPPORTED RECTANGULAR PLATES, Journal of Applied Mechanics, ASME, December 1963.

30. Wegmuller, A. W.
FINITE ELEMENT ANALYSIS OF ELASTIC-PLASTIC PLATES AND ECCENTRICALLY STIFFENED PLATES, Ph.D. Dissertation, Department of Civil Engineering, Lehigh University, 1971.

31. Wegmuller, A. W. and Kostem, C. N.
FINITE ELEMENT ANALYSIS OF PLATES AND ECCENTRICALLY STIFFENED PLATES, Fritz Engineering Laboratory Report No. 378A.3, Lehigh University, February 1973.

32. Whang, B.
ELASTO-PLASTIC ORTHOTROPIC PLATES AND SHELLS, Proceedings of the Symposium on Application of Finite Element Methods in Civil Engineering, Vanderbilt University, Nashville, Tennessee, November 1969.

33. Wolfensberger, R.
TRAGLAST UND OPTIMALE BEMESSUNG VON PLATTEN, Doctoral Dissertation, ETH Zurich, 1964.

34. Wood, R. H.
ELASTIC AND PLASTIC DESIGN OF SLABS AND PLATES, Thames and Hudson, London, 1961.

35. Ziegler, H.
A MODIFICATION OF PRAGER'S HARDENING RULE, Quarterly of Applied Mathematics, Vol. 17, No. 1, 1959.

8. ACKNOWLEDGMENTS

The authors would like to express their appreciation to Dr. D. A. VanHorn for his comments and to Dr. Suresh Desai for his continuing interest and encouragement. Acknowledgments are also due to Mrs. Ruth Grimes, who typed the manuscript, Mr. John Gera and Mrs. Sharon Balogh, who prepared the drawings included in this report, and to Lehigh University Computing Center for providing its facilities for the extensive computer work.

Special thanks are due to the National Science Foundation for sponsoring the research project Overloading Behavior of Beam-Slab Highway Bridges (Grant No. GK-23589). The reported investigation was carried out within the framework of this project.